Università degli Studi della Tuscia di Viterbo

Dipartimento di Scienze Agrarie e Forestali (DAFNE)

Corso di Dottorato di Ricerca
in

Scienze delle Produzioni Vegetali e Animali

XXXVII ciclo

APPROACHES TO IMPROVE FIRMNESS IN TOMATO BY BIOTECHNOLOGICAL AND CONVENTIONAL BREEDING STRATEGIES

(s.s.d. AGRI-06/A)

Tesi di dottorato di

Dott.ssa Ludovica Fumelli

Coordinatore del corso

Prof.ssa Roberta Bernini

Tutore

Prof. Andrea Mazzucato

A.A. 2024/25

Summary

Abstract

Tomato (*Solanum lycopersicum* L.) is one of the most important vegetable crops cultivated worldwide. However, post-harvest losses due to fruit deterioration, premature softening and mechanical damage represent a major challenge for its commercialization, with a significant impact on both food waste and food safety. To address a critical need in the agri-food supply chain, different strategies to improve tomato fruit firmness and shelf-life have been investigated in the present work.

The thesis explores both conventional and innovative breeding approaches to enhance fruit firmness and improve fruit quality, while also contributing to achieving a better understanding of mechanisms underlying tomato fruit ripening and softening.

In vitro regeneration capacity of three landraces from the Lazio region characterized by poor fruit firmness and reduced shelf-life, was explored with the aim of finding genotypes suitable for genetic transformation. The potential of the CRISPR/Cas9-mediated gene editing in precisely manipulating target genes without compromising other desirable fruit qualities was highlighted by targeting the cell wall-remodeling-enzyme encoding gene *SlPL*, obtaining Micro-Tom mutants with increased fruit firmness and pathogen resistance. The insights gained from this experiment will help to clarify the complexity of the cell wall disassembly process while opening the possibility to develop resilient and competitive varieties that meet both agronomic and quality needs.

In the frame of the HARNESSTOM (H2020) European project, by a genome wide association study performed on the repository collection of the project, QTLs and candidate genes possibly involved in fruit ripening and softening have been identified. Additionally, two composite populations with yellow and orange fruits, derived by crossing parental lines with different allelic composition, were selected by a participatory pedigree breeding scheme that involved farmers, consumers and researchers and led to the selection of more productive and qualitatively improved lines. Moreover, the participatory breeding allowed to positively select plants with improved fruit firmness.

Thus, the outcomes of this research will contribute to deeper our understanding of the genetic control of tomato fruit softening and provide insights for developing improved tomato varieties with enhanced firmness, ultimately benefiting breeders, producers and consumers.

Riassunto

Il pomodoro (*Solanum lycopersicum* L.) è una delle colture orticole maggiormente coltivate al mondo. Tuttavia, le perdite dovute al deterioramento, al rammollimento e a danni meccanici che si verificano nel post-raccolta rappresentano un'importante sfida per la sua commercializzazione, con impatti negativi sia in termini di spreco che di sicurezza alimentare. Per affrontare questo aspetto critico che si ripercuote su tutte le fasi della filiera, nel presente lavoro sono state esaminate diverse strategie per il miglioramento della consistenza e della serbevolezza della bacca di pomodoro. La tesi esplora approcci di selezione convenzionali e innovativi per l'incremento della *firmness* e della qualità del frutto, ponendo le basi per una migliore comprensione dei meccanismi coinvolti nella maturazione e nel rammollimento del pomodoro.

La capacità di rigenerazione *in vitro* di tre varietà locali del Lazio, con scarsa consistenza dei frutti e ridotta *shelf-life*, è stata valutata al fine di individuare genotipi idonei alla trasformazione genetica. Il potenziale del sistema CRISPR/Cas9 nella manipolazione mirata di geni bersaglio, senza la compromissione di aspetti legati alla qualità organolettica del frutto, è stato evidenziato dal *targeting* del gene *SlPL*, codificante per un enzima coinvolto nel rimodellamento della parte cellulare, grazie all'ottenimento di mutanti del genotipo Micro-Tom con maggiore consistenza della bacca e ridotta suscettibilità a diversi agenti patogeni. Le conoscenze acquisite grazie a questo esperimento contribuiranno a chiarire la complessità del processo di rimodellamento della parete cellulare e al tempo stesso apriranno alla possibilità di sviluppare varietà resilienti e competitive che soddisfino sia esigenze agronomiche che qualitative della coltura.

Nell'ambito del progetto europeo HARNESSTOM (H2020), è stato condotto uno studio di associazione *genome-wide* sulla collezione di genotipi del progetto, identificando possibili QTLs e geni candidati coinvolti nei processi di maturazione e rammollimento del frutto. Infine, due popolazioni composite a bacca gialla e arancione, derivate dall'incrocio di linee parentali a diversa composizione allelica, sono state valutate in un programma di selezione partecipativa, seguendo uno schema *pedigree* che ha visto coinvolte diverse figure, come agricoltori, consumatori e ricercatori, e che ha portato all'ottenimento di linee più produttive e migliori da un punto di vista qualitativo. Inoltre, queste attività di selezione partecipativa hanno permesso di operare una selezione positiva per piante caratterizzate da una maggiore consistenza del frutto.

Pertanto, i risultati ottenuti in questo lavoro potranno contribuire ad una più profonda comprensione del controllo genetico del *softening* del pomodoro e fornire spunti per lo sviluppo di varietà migliorate, a beneficio dei *breeder*, degli agricoltori e dei consumatori.

Chapter 1

Introduction

1.1 The tomato crop

Tomato (*Solanum lycopersicum* L.) is one of the most important vegetable crops worldwide. Excluding tubers, it is first in terms of both production, with 192 Mt produced in 2023, and cultivated area (5.4 Mha). Most of tomatoes are produced in China and India, followed by Turkey, USA, Egypt and Italy (FAOSTAT, 2023; last consultation 01 December 2024). Its diffusion and economic relevance is due to its wide use in the human diet both as fresh fruits and in processed product, like juice, sauce, soups, paste and puree (Krauss et al., 2006; Atanasova and Gatseva, 2019), being indispensable for a lot of traditional dished all around the world. Tomato is also a nutritious food, being an important source of beneficial compounds for human health, such as minerals and antioxidant molecules, like carotenoids, particularly lycopene and β-carotene, ascorbic acid, vitamin E and phenolic compounds (Frusciante et al., 2007). Indeed, its regular consumption has been correlated with a reduced susceptibility to different types of cancers and cardiovascular diseases (Giovannucci et al., 1995; Clinton, 1998; Borguini and Ferraz Da Silva Torres, 2009).

Cultivated tomato, probably derived from the wild cherry tomato *S. lycopersicum* var. *cerasiforme*, originated in the Andean region of South America, from Ecuador, through Peru and Chile (Peralta and Spooner, 2007), though its domestication may have been completed in Mexico and Central America, from where it was exported to the rest of the globe (Rick, 1991; Blanca et al., 2022).

1.1.1 Tomato as model species for research on fleshy fruit

To propagate the species, seed dispersal is a key factor for a broad range of angiosperm plants which reproduce sexually. Fruits are specialized organs for the protection and development of seeds, and most of the literature on fleshy fruits evolution suppose that they have been adapted to attract frugivores (angiosperm–frugivore coevolution), who act as seed disperser (Eriksson, 2016; Giovannoni et al., 2017). So that fruits can appeal to these animals, they must undergo the ripening process. Ripening is a complex chain of events leading to deep changes in fruit metabolism, altering its physiology and biochemical composition: pigments, like carotenoids and anthocyanins, accumulate and chlorophyll degrades; softening, caused by cell wall remodeling, occurs; acids, sugars and volatile compounds increase, participating in flavor formation (Li et al., 2021; Ling et al., 2021; Li et al., 2022a).

Fleshy fruits can be classified as climacteric and non-climacteric, according to their respiration rate and ethylene production during the ripening process. Climacteric fruits, like tomato, apple and banana, show a peak in respiration and a burst of ethylene production, while non-climacteric fruits, such as strawberry and grape, do not show an increase in respiration and ethylene biosynthesis (Figure 1.1) (Giovannoni, 2001; Ji et al., 2021).

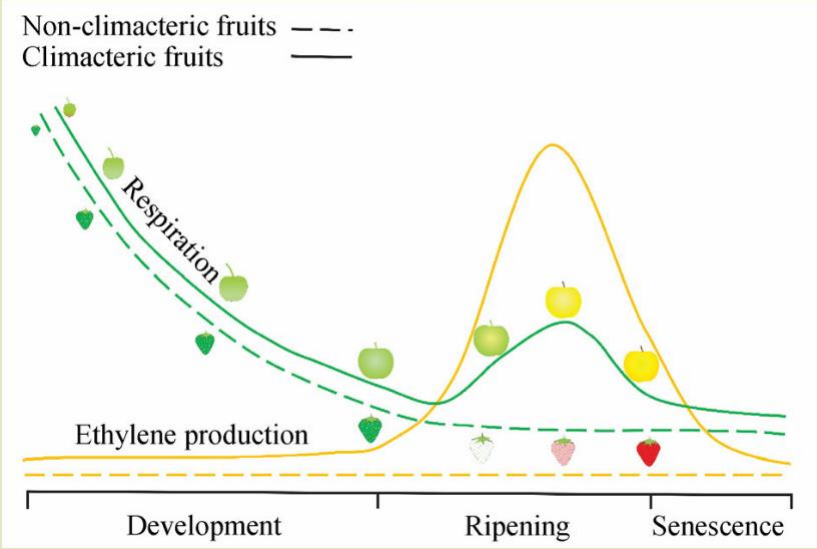

Figure 1.1 Changes in respiration rate and ethylene production in climacteric or non-climacteric fruits during development, ripening and senescence (*Ji et al., 2021*)

Thanks to its diploidy, the autogamous mating system, its short life cycle, the accessibility to germplasm resources including mutant lines and the availability of a high-quality reference genome, tomato has been widely used as model system for fleshy fruit biology research (Yu et al., 2017; Brumos, 2021; Xia et al., 2021). Numerous studies in tomato have brought ripening mechanisms to light, helping to unveil the molecular basis of fruit softening.

1.1.2 Fruit ripening and softening processes in tomato

Ripening-related events are finely regulated by genetic processes, followed by biochemical and physiological changes leading to modifications in fruit size, color, aroma, flavor and texture (Ji et al., 2021). Ripening of fleshy fruit is also strongly influenced by the balance of different phytohormones, with ethylene being mainly involved in climacteric fruit ripening (Alexander and Grierson, 2002; Kevany et al., 2007), and abscisic acid (ABA) and auxin regulating ripening in non-climacteric fruit (Castellarin et al., 2011; Pérez-Llorca et al., 2019). Furthermore, epigenetic mechanisms, like DNA and histone methylation/demethylation, are known to affect the ripening process (Giovannoni et al., 2017).

The genetic control of ripening relies on a broad range of Transcription Factors (TFs), which interact with ethylene and mostly belong to four classes: MADS-box, NAC, ERF and MYB (Ji et al, 2021; Peng et al., 2022). MADS-box TFs are master regulators of many developmental processes, spanning from organ development to flower differentiation and fruit ripening (Becker and Theißen, 2003). The *SlMADS-RIN* (*ripening inhibitor*) is considered a master regulator of ripening, since in the tomato *rin* mutant, ripening is strongly compromised by a deletion between *MADS-RIN* and its neighboring gene *MACROCALYX (MC)*, another MADS-domain TF regulating sepal development, which leads to the formation of a fuse protein RIN-MC which affects and alter both genes' function (Vrebalov et al., 2002; Wang et al., 2020a). Other proteins of this gene family involved in fruit ripening and interacting with RIN are TAGL1 (Itkin et al., 2009; Vrebalov et al., 2009), FUL1, FUL2 (Bemer et al., 2012*)*, MADS1 (Dong et al., 2013), FYFL (Xie et al., 2014) and CMB1 (Zhang et al., 2018a).

The NAC domain- protein family is one of the largest plant-specific TFs classes (Aida et al., 1997). In tomato, *NAC- NON-RIPENING (NAC-NOR)* was shown to play a crucial role in ripening; the *nor* mutant, which produce a truncated protein, fails to produce autocatalytic ethylene (Ji et al., 2021) and *nor* fruits do not manage to fully ripen (Juan-Cabot et al., 2022).

Three NAC TFs, SINAC1(Ma et al., 2014), SINAC4 (Zhu et al., 2014), and NOR-like1 (Gao et al., 2018) have also been identified and suggested to participate in tomato fruit ripening.

Lastly, among the ERF (ethylene response factor) and MYB TFs encoding genes, *SlERF.B3*, *SlERF.F12*, *SlMYB70*, and *SlMYB75* regulate ethylene metabolism and signaling (Peng et al., 2022).

Other important mechanisms involved in the ripening process have an epigenetic basis; modifications like DNA and histone methylation/demethylation and acetylation play an important role in the transcriptional activation and regulation of genes involved in tomato fruit development and ripening (Peng et al., 2022). *SlSPL-CNR*, a SQUAMOSA PROMOTER BINDING–LIKE PROTEIN (SPL) gene that resides at the *Colorless non-ripening* (*Cnr*) locus, is necessary for the manifestation of ripening (Manning et al., 2006). The *cnr* mutant has a hypermethylated region in the promoter which results in drastically reduced transcriptional activity and in an unripen fruit phenotype.

In Figure 2.1, it is shown a gene and protein overview of master regulators of ripening in tomato, in Wild type and mutant variants.

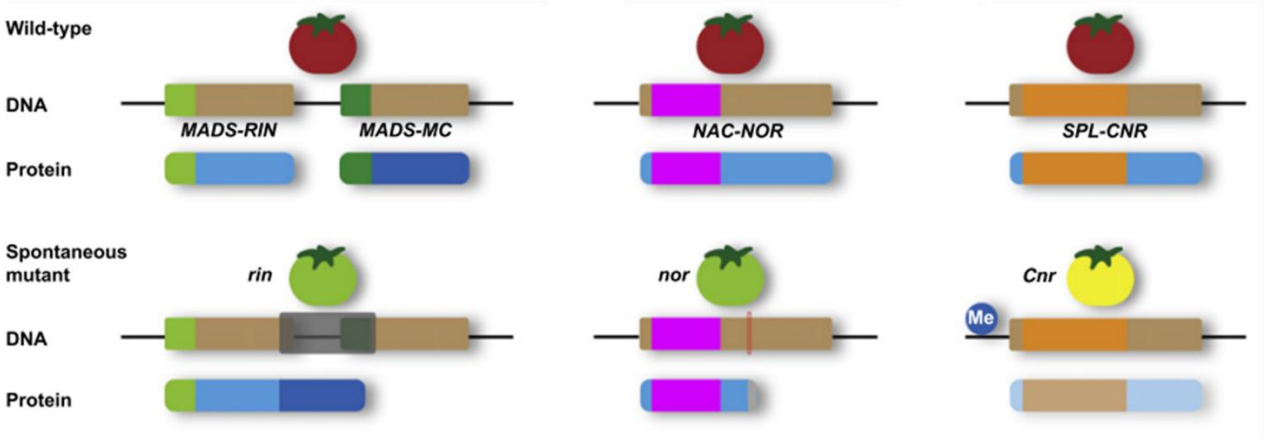

Figure 2.1. Tomato fruit ripening and the effects of mutations in three "master regulator of ripening" genes: MADS-ripening inhibitor (MADS-RIN), NAC-non-ripening (NAC-NOR) and SPL-colorless non-ripening (SPL-CNR) (*Wang. et al., 2020b*).

Once the fruit has received appropriate stimuli to start the ripening cascade, catabolic and anabolic pathways are activated and profound changes start to shape its new appearance. One of the fundamental events that occurs with ripening is softening. Softening takes place through a modification of texture, that is due to changes in cell wall and cuticles structure (Giovannoni

et al., 2017). Primary cell walls principally comprise three classes of polysaccharides: cellulose, hemicelluloses, and pectins. Pectins undergo the most relevant changes during softening, being remodeled, disassembled and solubilized by the action of a variety of enzymes, like polygalacturonases (PGs), pectate lyases (PLs), pectin-methylesterases (PMEs), β-galactosidase and expansins (EXPs) (Wang et al., 2018). Similar to pectins, changes in cuticle composition have also an impact on the fruit softening process, reducing water loss and delaying softening (Lara et al., 2019).

1.1.2.1 Tomato ripening mutants

Several spontaneous monogenic mutations leading to different degrees of ripening impairment have been described, like *Never-ripe* (*Nr*) (Rick and Butler, 1956), *Green ripe* (*Gr*) (Kerr, 1958), *rin* (Robinson and Tomes, 1968), *nor* (Tigchelaar et al., 1973), *alcobaça* (*alc*) (Almeida, 1961; Kopeliovitch et al., 1981) and *Cnr* (Thompson et al., 1999) (Figure 3.1). Their discovery opened up to important studies that were the starting point for understanding the key mechanisms of tomato ripening. These mutations mostly affect ethylene biosynthesis/response and fruits from these mutants are characterized either by ethylene insensitivity (failing to ripen even with its exogenous application) or by the absence of ethylene burst (Lanahan et al., 1994; Osei et al., 2017).

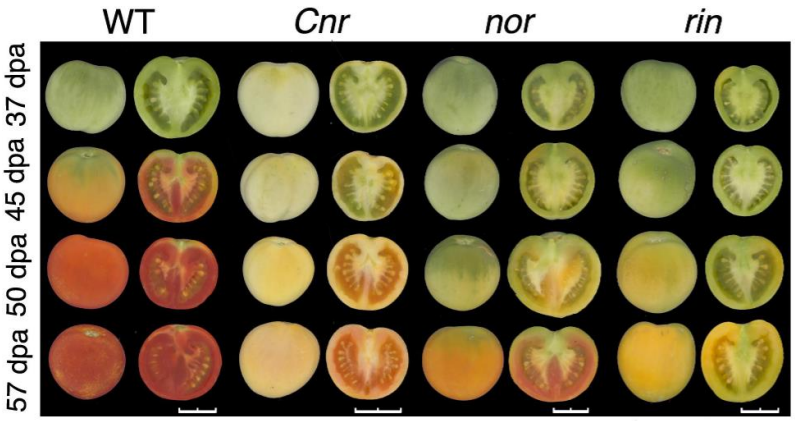

Figure 3.1. Fruit phenotype at different ripening stages of *Cnr*, *nor* and *rin* mutants (Adaskaveg et al., 2021)

Nr carries a non-synonymous mutation in the *ETR3* encoding gene, responsible for a proline to leucine substitution (Wilkinson et al., 1995; Schubert et al., 2019), leading to an incomplete and delayed ripening phenotype (Lanahan et al., 1994), with fruits that remain orange-colored and only slightly soften (Rick and Butler, 1956; Hobson, 1967). At the *Gr* locus, a 334 bp deletion, identified in a gene involved in ethylene response (Barry and Giovannoni, 2006), causes lower lycopene accumulation and reduced softening of the fruit (Barry et al., 2005). Fruits of the *rin* mutant, comprising a deletion between the *MADS-RIN* TF and its adjacent gene *MADS-MC*, do not turn red at ripening but only show a late occurrence of a yellow color, sign of carotenoid synthesis inhibition (Robinson, 1968; Vrebalov et al., 2002). *Nor* and *alc* mutations, both occurring in the *NAC-NOR* gene, in the third and second exon respectively, are responsible for different fruit phenotypes. In *nor*, the biosynthesis of ethylene and carotenoids is significantly inhibited, causing the fruits to remain firm and orange-ish (Giovannoni et al., 1995; 2004); while in *alc* the fruit reaches an almost normal pigmentation, exhibiting a climacteric rise and showing a lower negative impact on fruit quality, while still maintaining a long shelf-life (Kopeliovitch et al., 1980; Yu et al., 2017). Lastly, *cnr* fruits maintain a yellow skin and a non-pigmented pericarp, have a mealy texture and do not show a climacteric peak of ethylene production (Thompson et al., 1999).

1.1.3 Breeding to improve firmness and shelf-life

Preventing post-harvest losses, caused by fruit deterioration, premature softening, microbial decay or mechanical damage, is a major concern that all the stakeholders of the agri-food supply chain are facing. Spanning from harvesting to consumption, losses up to 50% have been estimated in the tomato market (Arah et al., 2016). To meet this challenge, tomato breeders have long concentrated on enhancing fruit firmness to improve harvesting, storage and transport, extend shelf-life (even tough fruit firmness is not necessarily correlated to the shelf-life, it may be a valid indicator of how a product can perform “on the shelf” (Brouwer et al., 2019)) and guarantee food security, to better preserve the product quality and minimize food waste (Nie et al., 2024). Different strategies have been adopted over the years and breeders and researchers teamed up to reach this goal.

1.1.3.1 Conventional breeding strategies

To improve crop quality, breeding companies rely on crosses to exploit naturally occurring mutations and transfer desirable traits into their elite material. The development of F_1 hybrids has long been, and still is, the mainstay of conventional tomato breeding. To slow down the ripening process and avoid excessive softening, the *rin* and *nor* mutations have widely been used to develop commercial varieties with extended shelf-life (Wang and Seymour, 2022). The "Red Centre" (HRAS 87-70 x *rin*-HRAS 81-85) and "Juliette" (79T-I x *rin*-795054-1) hybrids, carrying the *rin* mutation, showing a 40 days shelf-life, have been released by Nguyen (1991; 1994) in Australia. "Vasilisa" (Gavrish and Bogdanov, 1992), 'Chang-line' (Lu et al., 1994) and "Rafal' (Seroczyńska et al., 1998) are *nor*-carrying hybrids with extraordinary storage features. The use of *alc* mutation in fresh-market tomato breeding has been proposed as well (Mutschler et al., 1992).

But because of their strong effect on the ripening process, they must be used in heterozygous form; this, together with the pleiotropic effects that their use cause at the expense of organoleptic quality (Juan-Cabot et al., 2022), lead the way to new approaches to better face the tomato softening issue.

1.1.3.2 New Breeding Technologies

The main objective of breeding is controlling specific traits while maintaining other features unchanged. Especially for tomato, the goal is to reduce softening while keeping other aspects of ripening normal. Thus, the focal point of modern tomato breeding is increasing fruit firmness and storage-life preserving other desirable qualities (Wang and Seymour, 2022). Acting upstream of ethylene biosynthesis (Thompson et al., 1999), mutations like *Cnr*, *nor* and *rin* can have detrimental effects on fruit color and flavor (Wang and Seymour, 2022). For this reason, researchers have been looking for alternative ways to control fruit softening, by studying genes that act downstream of the ethylene pathway or do not interfere with it. Through biotechnologies and genome editing techniques, especially CRISPR/Cas9, different genes have been targeted, showing fewer negative effects on the ripening process and being proposed as valid candidates for breeding programs.

Genes encoding for cell wall-remodeling enzymes have long been the target of genetic transformation for the reduction of fruit softening, especially in strawberry (Brummell et al.,

2022). In tomato, polygalacturonase (*SlPG2a*), pectate lyase (*SlPL*), β-galactanase (*SlTBG4*) and xyloglucan endotransglucosylase/hydrolase (*SlXTH5*) (Wang et al., 2023) have been studied to achieve this objective. The most famous case is undoubtedly the first commercialized GM tomato FLAVR SAVR^{TM}, obtained by antisense RNA technology on a PG-encoding gene (Kramer and Redenbaugh, 1994). More recently, the knocking out the polygalacturonase-encoding gene *SlPG2a* did not show any significant firmness increase in the Wang et al. (2019) experiment, while in 2022 Nie et al. could obtain delayed softening and higher firmness in CRISPR/Cas *PG* mutants. Different authors showed that the silencing of *SlPL* (*Solyc03g111690*) in Ailsa Craig through CRISPR/Cas9 system, and in Micro-Tom by RNAi, can have a positive impact on delaying fruit softening (Uluisik et al., 2016; Yang et al., 2017; Wang et al., 2019). Noteworthy, when combining mutated *SlPG2a* and *SlPL*, Ortega-Salazar et al. (2024) could increase firmness and reduce water-loss to a higher extent than in single mutants. Smith et al. (2002) reported firmer fruits in a *SlTBG4*-silenced line obtained by antisense-RNA, even though Wang et al. (2019) could not match such results in CRISPR edited plants. Controlling cuticle permeability can also be an effective way to regulate water loss and increase fruit firmness (Brummell et al., 2022). The overexpression of the lipid transfer protein SlLTPG3, involved in cuticular wax and cutin biosynthesis, reduced fruit softening and water loss and extended tomato shelf-life (Wang et al., 2022). Similar results were achieved by knocking out the GA2-oxidase-encoding gene *SlFIS1* by CRISPR/Cas9 (Li et al., 2020) and by silencing through RNAi the transcription factor SlFSR, which regulate the expression of *SlPG2a*, *SlPL*, *SlCEL2*, *TBG4*, *SlEXP1* and *SlXYL (β-D-xylosidase),* among others (Zhang et al., 2018b). Worth mentioning is also the LATERAL ORGAN BOUNDARIES1 (SlLOB1) TF silencing, which reduced cell wall swelling, considerably decreased postharvest fruit softening, and downregulated *SlEXP1*, *SlCEL2*, *SlXYL* and *SlPL* expression, with no negative effects on ethylene production (Shi et al., 2021).

1.1.3.3 GWAS for quality improvement

Starting back in the early 2000s with human genetics (Hirschhorn et al., 2005; Wang et al., 2005) and followed ten years later by their application in crops genetic (Huang et al., 2010; Pasam et al., 2012; Ranc et al., 2012), the genome wide association studies (GWAS) have become a popular tool for crop breeding and biotechnological research. The GWAS great potential resides in the possibility of combining phenotypic data with genotypic information to identify genetic variants associated with key traits, dissecting QTLs, and suggesting candidate genes for

mutagenesis and new breeding techniques applications (Korte and Farlow, 2013; Liu et al., 2023). The basics behind the method comprise a wide collection of individuals to be phenotyped and a dense set of markers that cover the entire genome of interest to be used in genotyping . For the analysis, copy-number variants or sequence variation can be drawn on, yet the single-nucleotide polymorphisms (SNPs) are the most commonly used markers (Uffelmann et al., 2021), also because of breakthroughs in the next-generation sequencing (NGS) technology (Kim et al., 2021).

Over the past decades, several statistical models have been implemented as well, leading to a better accuracy and efficiency of GWAS (Kim et al., 2021), and allowing successful identification of genes responsible for many economically significant traits of crops, mostly related to agronomic performances (like yield, diseases resistance, plant vigor etc.) and fruit quality (content of nutritional and functional metabolites, firmness, soluble solids content and so on) (Ruggieri et al., 2014; Bauchet et la., 2017; Liu et al, 2023). Thus, GWAS have been widely used in tomato, opening to new possibilities in deciphering complex trait and to look for useful alleles in tomato improvement.

1.2 Aim of the work

In the present work, different strategies have been adopted to address the post-harvest quality-improvement issue in tomato.

Chapter 2 focuses on phenotyping for fruit firmness and shelf-life of traditional tomato varieties from Lazio region. In order to identify possible target genotypes for genetic transformation, an *in vitro* regeneration trial was set up.

In Chapter 3 a CRISPR/Cas9 editing approach was implemented to target two genes responsible for cell wall-remodeling and consequently fruit softening. New insights were gained on cell wall-disassembly metabolism, which affects fruit firmness and enhances resistance to pathogens.

In Chapter 4 the core collection of the HARNESSTOM European project was characterized for fruit traits, including firmness, and a GWAS analysis was carried out to find new QTLs and possibly candidate genes that control the fruit softening process.

In Chapter 5 a breeding strategy, based on a participative selection scheme, was set up for the creation of composite populations with yellow and orange fruits. F_2 to F_5 progenies were evaluated for different qualitative and quantitative traits (i.e. fruit firmness) over a period of four years, allowing the selection of promising material.

Chapter 2

Phenotyping and regeneration of tomato landraces from Lazio region

2.1 Introduction

Camacho-Villa et al. (2005) defined landraces as "Dynamic populations of a cultivated plant with a historical origin, distinct identity, often genetically diverse and locally adapted, and associated with a set of farmers' practices of seed selection and field management as well as with a farmers' knowledge base". Traditional varieties are genotypes of territorial importance, linked to traditions and to the cultural heritage of local communities, that play a fundamental role in preserving agrobiodiversity. Italy is one of the richest countries for tomato landraces (Posadinu et al., 2022), however, most of them lack those aspects required by modern agricultural and market needs, making it necessary to find ways to improve this material without compromising their genetic background and unique features. Biotechnological approaches, like CRISPR/Cas9 system, can be useful tools to combine innovation and tradition to enhance the features of local genotypes.

For this reason, in the context of the regional project "Nuove varietà tipiche di pomodoro con migliorate caratteristiche agronomiche e di qualità (NOVIPOM)", three traditional tomato varieties from Lazio have been addressed to improve their fruit firmness and shelf-life by editing cell wall remodeling genes. Firstly, a field trial was set up to characterize the chosen material for the traits to be improved. Moreover, an *in-vitro* experiment to check the regeneration capacity of the selected material, in order to identify the genotypes more suitable for the genetic transformation, was performed for the first time.

2.2 Materials and methods

2.2.1 Plant material

Three tomato landraces from the Lazio region (Scatolone di Bolsena -SCA, Spagnoletta di Gaeta e Formia -SPA and Pantano di Ardea -PAN) (Figure 2.1) and one commercial F_1 hybrid used as control (CTR), all characterized by flattened-ribbed fruits, were analyzed for fruit firmness and shelf-life. Cotyledons from SCA, SPA and PAN, plus the model variety Micro-Tom (MTO) as control, were used as explants for the regeneration experiment.

Figure 2.1. Fruits from the Lazio landraces Scatolone di Bolsena, Spagnoletta di Gaeta e Formia and Pantano di Ardea.

2.2.2 Growth conditions and fruit phenotyping

During summer of 2023, plants from SCA, SPA, PAN and CTR varieties were grown at the experimental farm of the University of Tuscia "Nello Lupori", in Viterbo. The firmness of 20 fruits per accession was measured at five different ripening stages (mature green (MG), breaker (BR), turning (TUR), light red (LR) and red ripe (RR)) on two different sides on the equatorial region of the fruit using a portable digital durometer (T.R. Turoni srl, Forlì, Italy). Weight loss assessment, to evaluate fruit shelf-life, was performed starting from fruit collected at the RR stage. Eight fruits per genotype (two replicates of four fruits each) were collected, stored at room temperature and weighed every five days (d), until no more fruits were available for the measurement after the rotten ones were removed. Weight loss percentage was calculated as follows:

$$\frac{W_0 - W_{1,\,2,\,\ldots,\,n}}{W_0} \times 100$$

where W_0 was the weight recorded at harvest, W_1 the weight recorded after five d, W_2 the weight after 10 d, and so on. Before all analyses, fruits were rinsed with distilled water and cleaned with ethanol.

2.2.3 Regeneration experiment

Regeneration was carried out according to Olimpieri et al. (2011), with slight modifications. Sterile seeds from the SCA, SPA, PAN and MTO genotypes were germinated in Petri dishes at 25°C, transferred onto a growing medium containing 1 X Murashige and Skoog (MS) salts, 3% sucrose and 7 g/L plant agar (pH 5.8) and kept in a growth chamber under standard growing conditions (16 h light/8 h dark at 25°C). Once the cotyledons emerged, they were cut and placed on an induction medium supplemented with 0.1 mg/L 2,4-dichlorophenoxyacetic acid (2,4D), 0.35 mg/L indole-acetic-acid (IAA) and 0.7 mg/L trans-zeatin (T-zea). After 72 h, cotyledons were kept on a regeneration medium containing 0.35 mg/L IAA and 0.7 mg/L T-zea, for one week and finally transferred onto fresh medium every 20 d. Shoots of approximately 1 cm were eventually placed in the rooting medium containing 0.35 mg/L IAA and 0.1 mg/L indole-butyric-acid (IBA) (Supplementary Table S1). Regeneration efficiency was calculated as the number of produced shoots/number of explants * 100. Rooted explants were then transferred in pots to monitor the *in-vivo* transfer survival rate.

2.2.4 Data analysis

Data were analyzed by one-way analysis of variance (ANOVA), and statistical differences were determined by Dunnett's Multiple Comparison *post hoc* test, implemented on DescTools R package (Signorell, 2024) and performed by RStudio v4.3.3 (Posit team, 2022). The same statistical analysis was performed on fruit firmness and weight loss assays. Results were expressed as mean ± standard error and differences were considered significant at $p \leq 0.05$.

2.3 Results and discussion

2.3.1 Fruit phenotyping

Traditional varieties marketability is generally reduced, as they usually lack commercial attributes that make them suitable for large retailers. Since it is *common knowledge* in the field that big flattened-fruited landraces tend to soften easily, fruit firmness decay occurring during ripening was assessed on SCA, SPA, PAN and CTR varieties at five ripening stages spanning from MG to RR (Figure 2.2).

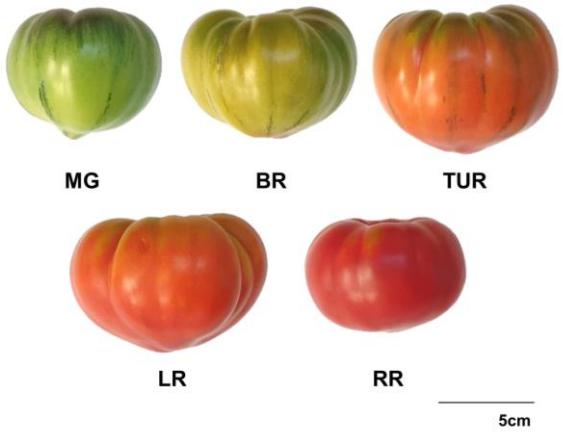

Figure 2.2. Image of representative fruits harvested at five ripening stages: mature green (MG), breaker (BR), turning (TUR), light red (LR) and red ripe (RR).

At the MG stage, only PAN, with an average value of the durometer index (*di*) of 95.5, showed a significantly lower firmness in comparison to CTR (*di* = 97.9). At the BR stage, no differences were found between CTR and any of the landraces, while at the TUR stage, SPA displayed lower values than CTR, with a *di* of 73.6 and 82.0, respectively. At the LP and RR stages, all varieties showed a significant decrease in fruit hardness when compared to CTR (Figure 2.3).

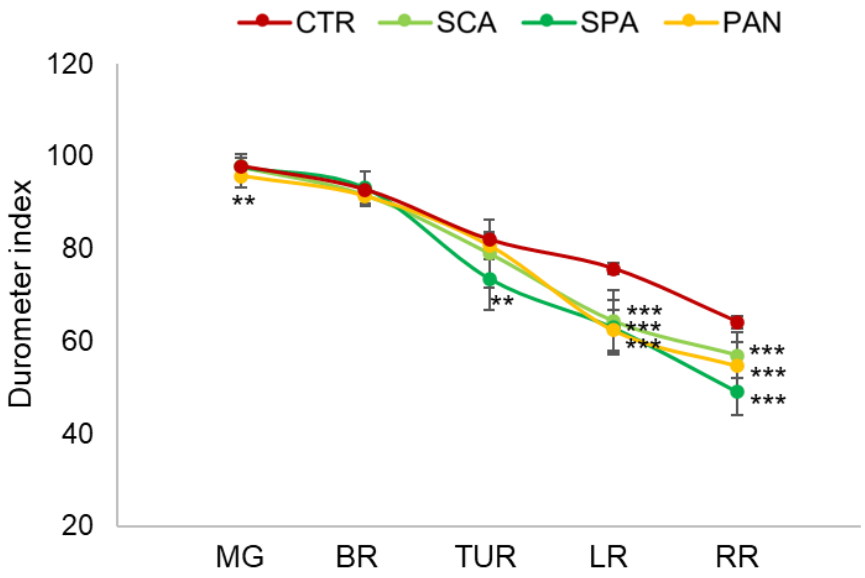

Figure 2.3. Firmness decay during different ripening stages (mature green (MG), breaker (BR), turning (TUR), light red (LR) and red ripe (RR)) of a control hybrid (CTR) and the landraces Scatolone di Bolsena (SCA), Spagnoletta di Gaeta e Formia (SPA) and Pantano di Ardea (PAN)). Asterisks indicate significant differences, determined by Dunnett's test, between each landrace and CTR (** $p \leq 0.01$, *** $p \leq 0.001$).

To evaluate the weight loss and assess the shelf-life, fruits at RR ripening stages were stored at room temperature and weighed every 5 d. Rotten fruits were gradually discarded and only the undamaged ones were kept for the analysis. As shown in Figure 2.4, SCA and SPA fruits could not be stored longer than 5 days post-harvest (dph); half of the PAN fruits could be stored up to 10 dph and three out of four of the CTR fruits did not exhibit signs of rotting until 20 dph, with one fruit kept until the 25th day.

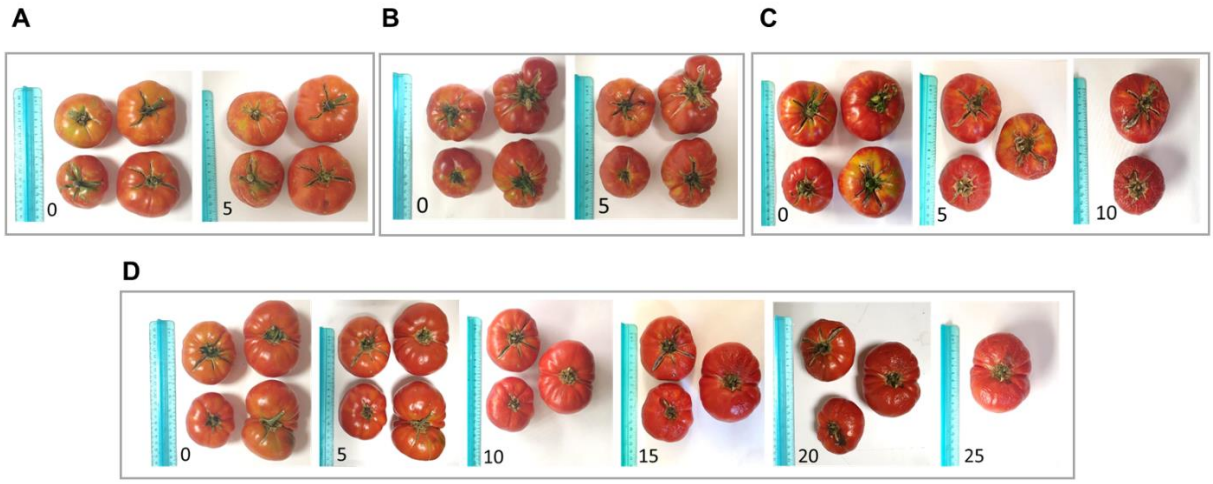

Figure 2.4. Representative fruits of **(A)** Scatolone di Bolsena, **(B)** Spagnoletta di Gaeta e Formia, **(C)** Pantano di Ardea and **(D)** control hybrid, stored at room temperature. Numbers from 0 to 25 indicate the days of storage period.

To compare the weight loss of the local varieties to the hybrid having a representative number of fruits, weight values at 5 dph were used for the statistical analysis, and all three landraces showed a higher significant weight loss percentage in comparison to CTR (Figure 2.5).

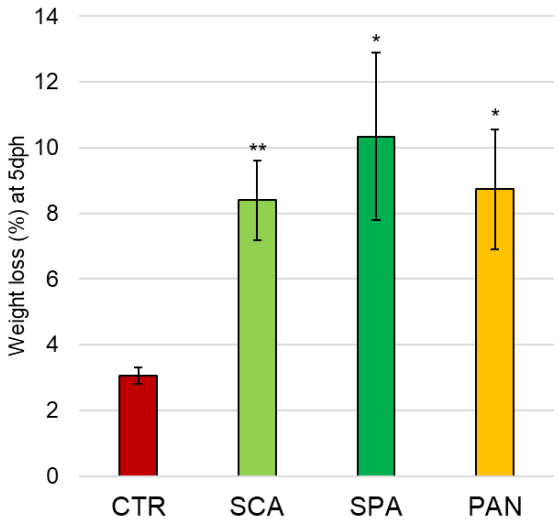

Figure 2.5. Weight loss percentage at 5 days post-harvest (dph) of the control hybrid (CTR), and of the Scatolone di Bolsena (SCA), Spagnoletta di Gaeta e Formia (SPA) and Pantano di Ardea (PAN)) landraces. Asterisks indicate significant differences, determined by Dunnett's test, between each landrace and CTR (* $p \leq 0.05$, ** $p \leq 0.01$).

Landraces are genotypes that have not been subjected to a voluntary improvement but evolved in narrow geographical areas driven by the actions of farmers. This process may lead to the selection of traits related to the organoleptic quality or the agronomic performance of the varieties, while leaving un-improved those traits more strictly related to commercial aspects, like fruit firmness and shelf life. Being these genotypes consumed locally and cultivated in small territories, it is not necessary to have a product that can be stored for prolonged periods of time and that must resist intense handling, like the one destined to large-scale distribution. Additionally, flattened-ribbed accessions are characterized by multilocular fruits and the number of locules has been negatively associated with firmness (Aurand et al., 2012; Solieman et al., 2013).

The significantly lower values of fruit firmness in comparison to a commercial hybrid, and a higher weight loss occurred during the storage period (similarly to what was reported in Sardinian landraces by Posadinu et al., 2023), which is reduced to 5 dph for all the landraces, make the three tested traditional varieties suitable targets for the improvement of post-harvest quality traits.

2.3.2 Regeneration experiment

Regeneration protocols are highly dependent on genotype. Some traditional Italian varieties, like San Marzano and Cuore di bue, have been successfully *in-vitro* regenerated for genetic transformation (Gianoglio et al., 2022; Li et al., 2022b), but no information in the literature could be found for the niche varieties SCA, SPA and PAN. To evaluate the *in-vitro* response of our genotypes, a regeneration experiment was conducted using cotyledonary explants as starting material. The model variety Micro-Tom (MTO), known for its high regeneration efficiency (Sun et al., 2006), was used as control (Figure 2.6).

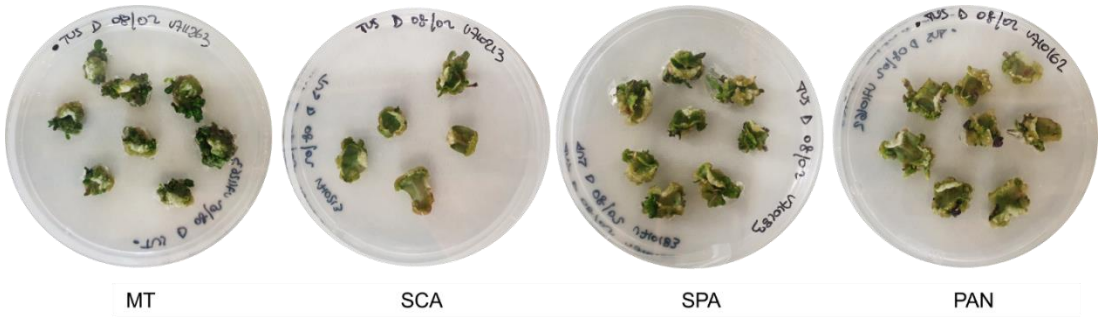

Figure 2.6. Cotyledonary explants of Micro-Tom (MTO), Scatolone di Bolsena (SCA), Spagnoletta di Gaeta e Formia (SPA) and Pantano di Ardea (PAN) on regeneration medium.

All the tested varieties showed a good response to *in-vitro* regeneration (Figure 2.7): SPA was the most responsive genotype, with a regeneration efficiency of 312.5%, followed by PAN, with a value of 262.5%, and SCA and MTO, with 200% and 56.3% regeneration efficiency, respectively. Even showing the lowest data, and considering that a few contamination issues occurred, MTO regeneration percentage was still in line with the 40% value previously reported by Sun et al. (2006).

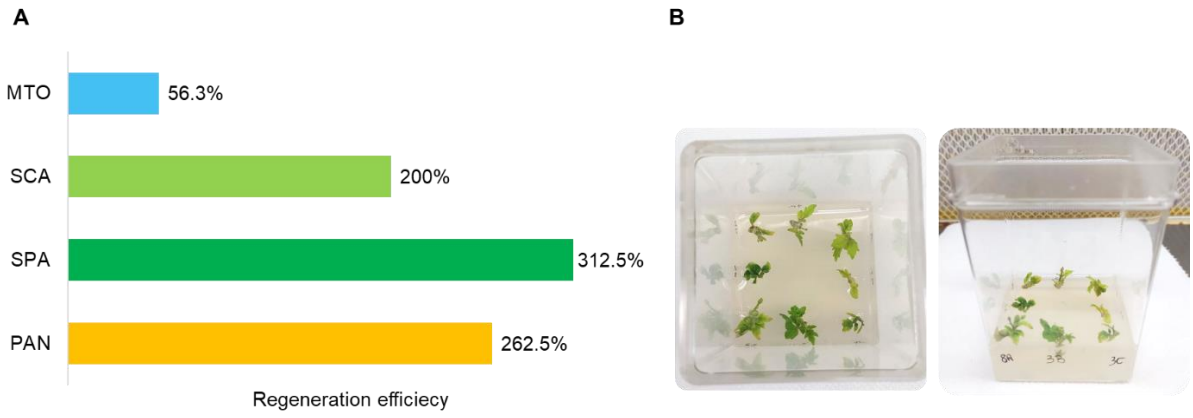

Figure 2.7. Response to *in-vitro* regeneration of Micro-Tom (MTO), Scatolone di Bolsena (SCA), Spagnoletta di Gaeta e Formia (SPA) and Pantano di Ardea (PAN). **(A)** Regeneration efficiency, **(B)** representative regenerated shoots.

Once transferred onto the rooting medium, the totality of the shoots was able to root (Figure 2.8 A) and 90% of the plantlets successfully acclimatized to *ex-vitro* condition (Figure 2.8 B).

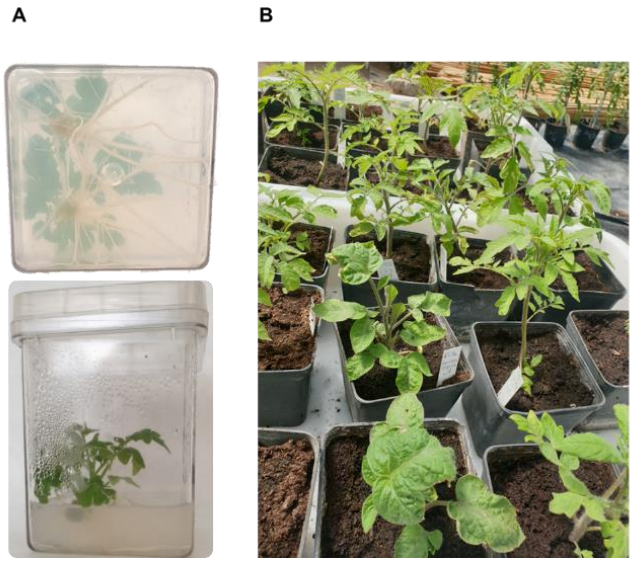

Figure 2.8. (A) *In-vitro* rooting of shoots and **(B)** *ex-vitro* transfer of the plantlets.

Given that all the local genotypes showed a high regeneration efficiency and an almost total acclimatation capacity, and that all of them were lacking post-harvest quality attributes like fruit firmness and shelf-life, one more criterion was added to choose the varieties to proceed with genetic transformation. Because of PAN low yield and big plant size, which would make it difficult to grow it in a growth chamber, this genotype was eventually excluded from further experiment.

2.4 Conclusions

Traditional varieties can be valuable material to preserve the agrobiodiversity and act as source of genetic variability. As their commercialization is limited to local markets and they are grown in restricted areas because of the lack of qualitative and agronomic features required by large-scale distribution, the improvement of landraces guided by innovative technologies can lead to a wider frame of consumers and growers that can use and value these materials. The Scatolone di Bolsena, Spagnoletta di Gaeta e Formia and Pantano di Ardea landraces, as the majority of local varieties, are at risk of genetic erosion. Improving local varieties without altering their genetic background, which is linked to traditions and cultural legacies, might encourage more farmers to grow these landraces and expand their market while allowing the preservation of these genotypes.

Moreover, their capacity of easily regenerate *in vitro* might open new possibilities of commercialization that are independent from seeds production.

2.5 Supplementary material

Supplementary Table S1. Media composition for the regeneration protocol.

Component	Growing Medium*	Induction Medium*	Regeneration Medium*	Rooting Medium*
MS	1x	1x	1x	1x
Sucrose	3%	3%	3%	3%
Plant agar	0.7%	agar 0.7%	agar 0.7%	agar 0.7%
2,4 D (mg/L)	-	0.1	-	-
IAA (mg/L)	-	0.35	0.35	0.35
IBA (mg/L)	-	-	-	0.1
T-Zeatin (mg/L)	-	0.7	0.7	

***** pH 5.8

Chapter 3

A CRISPR-Cas9 approach to improve tomato fruit firmness and shelf-life

3.1 Introduction

Clustered Regularly Interspaced Palindromic Repeat (CRISPR), firstly described in *Escherichia coli* by Ishino et al. (1987), together with *cas* (CRISPR-associated) proteins, function as adaptive defense systems against viruses and plasmids in approximately 40% of bacterial and 80% of archaeal species (Burstein et al., 2016). The CRISPR-Cas locus contains two main components: i) an array of identical sequences interspersed with viral DNA, which encode a CRISPR RNA (crRNA), and ii) the *cas* operon, which encodes the protein components. Once the bacterium gets infected by a virus, a short sequence of the invader-DNA is inserted as a spacer in the CRISPR array and in case of new infections it undergoes the transcription process to generate a pre-crRNA. After maturation, the crRNA will guide the Cas proteins to the viral nucleic acid, at sites that are complementary to the crRNA spacer sequence, to direct its cleavage and enable the virulence capacity of the bacteriophage. In order for the Cas protein to recognize and bind the target region, a protospacers adjacent motif (PAM), a short sequence in the viral DNA neighboring the crRNA complementary sequence, is necessary (Doudna and Charpentier, 2014). Taking advantage of this precise mechanism, the CRISPR-Cas9 technology has been developed. The Cas9, an endonuclease unique to bacteria (Makarova et al., 2011), operates double-stranded DNA breaks directed to specific sequences, thanks to a dual system consisting of a trans-activating crRNA (tracrRNA):crRNA duplex. This RNA complex is able to match a complementary DNA target sequence, allowing a site-specific DNA cleavage (Deltcheva et al., 2011; Jinek et al., 2012). To optimize the process, the tracrRNA:crRNA duplex has been engineered in a single guide RNA (sgRNA) (Jinek et al., 2012), encompassing a 20-nucleotide sequence complementary to the target, at the 5'end, and the double strand structure (mature tracrRNA and crRNA), at the 3' end, to bind the Cas9 protein (Figure 3.1).

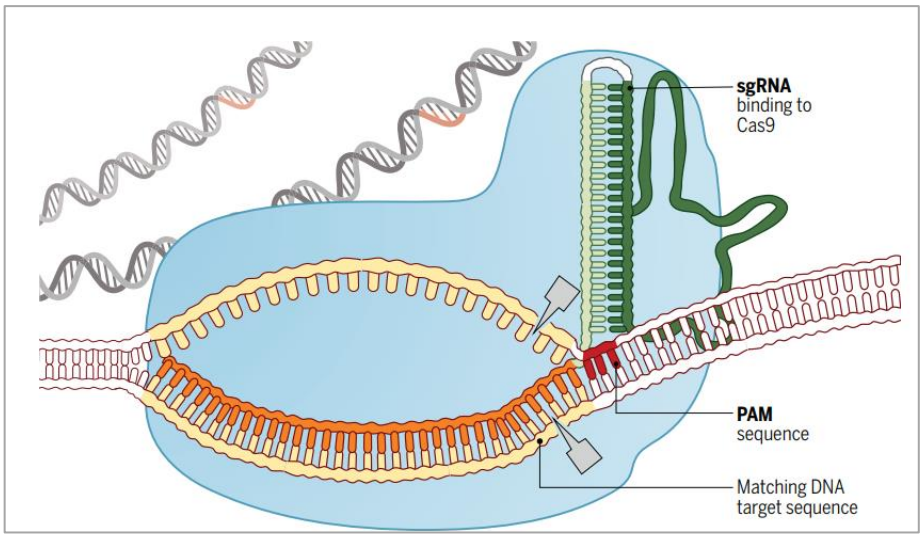

Figure 3.1. The Cas9 enzyme (blue) causes breaks in the double-stranded DNA by its two catalytic sites (blades) to cleave the DNA target site (yellow), neighboring the PAM sequence (red) and matching the 20-nucleotide sequence (orange) of the single guide RNA (sgRNA). The sgRNA includes a dual-RNA sequence comprising the CRISPR RNA (crRNA, light green) and a transcript RNA (tracrRNA, dark green) that binds and stabilizes the Cas9 protein. (Doudna and Charpentier, 2014).

After the cleavage occurred, endogenous cellular DNA repair mechanism, driven by non-homologous end joining (NHEJ) pathway, introduces small insertions/deletions that cause gene disruption and that can be used to introduce site-specific modifications in genomes of interest (Doudna and Charpentier, 2014).

Avoiding post-harvest losses, estimated to be up to 50% in the tomato market (Arah et al., 2016), and preserving post-harvest quality, is of foremost importance to reduce the negative impact on both food waste and food safety. Different strategies have been adopted over the years, with tomato breeders relying on natural mutations to generate hybrids, and researchers looking for new useful alleles. To achieve this goal, several genes encoding for cell wall-remodeling enzymes, like *SlPG2a*, *SlTBG4*, *SlXTH5* (Wang et al., 2023) and *SlPL* (Uluisik et al., 2016; Yang et al., 2017; Wang et al., 2019), and TFs, like *SlLOB1* (Shi et al., 2021) and *NOR-like1* (Peng et al., 2024) have been proposed as suitable targets for genetic transformation in order to improve the post-harvest quality of tomato fruits.

To increase our understanding of cell wall remodeling effect on fruit firmness and shelf-life, and to transfer the gained knowledge obtained by previous researches to local varieties, a gene editing approach was set up and two target genes (*SlLOB1* - *Solyc11g072470* and *SlPL* - *Solyc03g111690*) were hereby chosen to generate CRISPR/Cas9 mutants in different traditional genetic backgrounds.

Lateral organ boundaries (LOB) domain (LBD) proteins are plant-specific transcription factors that play key roles in lateral organ development, pollen and root development, plant regeneration capacity, photomorphogenesis and pathogen responses (Xu and Hochholdinger, 2016). In tomato, 47 LOB-encoding genes have been identified (PlantTFDB v5.0: https://planttfdb.gao-lab.org/family.php?sp=Sly&fam=LBD). Among them, *SlLOB1*, which is expressed in the locular gel and in the pericarp of tomato fruit, has been involved in cell wall-remodeling by up-regulating a suite of cell wall-associated genes (i.e. *EXP1* and *CEL2*, among others). By silencing the gene through RNAi in the Ailsa Craig tomato variety, inhibition of fruit softening, reduction in water loss, extension of shelf-life and no alteration of ripening initiation have been achieved; furthermore, an increase in lycopene and β-carotene content has been observed (Shi et al., 2021).

PLs are a class of cell wall-remodeling enzymes that have first been described in the pathogens *Erwinia carotovora* and *Bacillus* spp. (Starr and Moran, 1962), where they act as virulence factors and play an essential role in infection processes (Uluisik and Seymour, 2020). Once the pathogen penetrates the cutin layer, pectins act as a barrier to prevent infections, stimulating the plant immune response (Wan et al., 2021). The modification of the expression of genes encoding pectin-degrading enzyme, like the disruption of *PME3* (McMillan et al., 1993) or the overexpression of PME inhibitors *PMEI3* and *PMEI2* in *Arabidopsis* (Lionetti et al., 2007) enhanced the plant resistance to *Botrytis cinerea* and *Pectobacterium carotovorum*. Moreover, the elimination of the *PL1332* gene in a *Alternaria brassicicola* strain, reduced the pathogen virulence (Cho et al., 2015). As the pathogen threat is likely to worsen because of the ongoing climate changes (Velásquez et al., 2018), finding new ways to face crops diseases has become of great importance.

In tomato, 22 *PL* genes have been identified, however only *SlPL* is highly expressed in fruits, thus indicating its major role in softening (Yang et al., 2017).

The plant cell wall is an intricate structure made up by three predominant polymers: i) cellulose, composed of β-1,4-glucan chains; ii) hemicellulose, a combination of different polysaccharides, like xylan, xyloglucan, mannan and glucomannan; iii) pectin, formed by different polysaccharides, such as homogalacturonan (HG), rhamnogalacturonan-I (RG-I), rhamnogalacturonan-II (RG-II) and xylogalacturonan (XGA), with HG, homopolymer of α(1-4) galacturonic acid, being the most abundant one. The interaction among different enzymes is responsible for these polymers' degradation, leading to cell wall remodeling during ripening and fruit softening. The cellulose polymer is cleaved by the action of β-glucosidase (β-Glu; EC

3.2.1.21); hemicellulose, which in eudicots is prevalently composed of xyloglucan (Barnes and Anderson, 2018), is disassembled by the action of different glycosidases, including the β-galactosidase (β-Gal; EC 3.2.1.23) and β-glucosidase. As for pectin, different enzymes work together to operate the depolymerization of the homogalacturonan structure. PMEs (EC 3.1.1.11) remove the methyl-ester groups from the polygalacturonic acid chains, making them accessible to PGs (endo-polygalacturonase: EC 3.2.1.15 and exo-polygalacturonase: EC 3.2.1.67) and PLs (EC 4.2.2.2), both needing the de-esterification of pectate in order to hydrolyze the HG backbone. The contribution of β-Gal in pectin degradation, through the cleavage of galactose residues in RG-I, has also been described (Figure 3.2). Its action increases pectin solubilization, thus facilitating the access of PMEs and PGs to their substrate (Brummell and Harpster, 2001). Lastly, the α-galactosidase (α-Gal), may also have a role in fruit ripening and softening. The enzyme is prevalently allocated in the cytosol and the vacuole, but Keller and Pharr (1996) and Marraccini et al., (2005) reported it in the cell wall as well. Furthermore, the capacity of α-Gal to hydrolyze cell wall materials and solubilize pectin has been described in orange juice (Burns, 1990), and avocado (De Veau et al., 1993) and papaya (Soh et al., 2006) fruits.

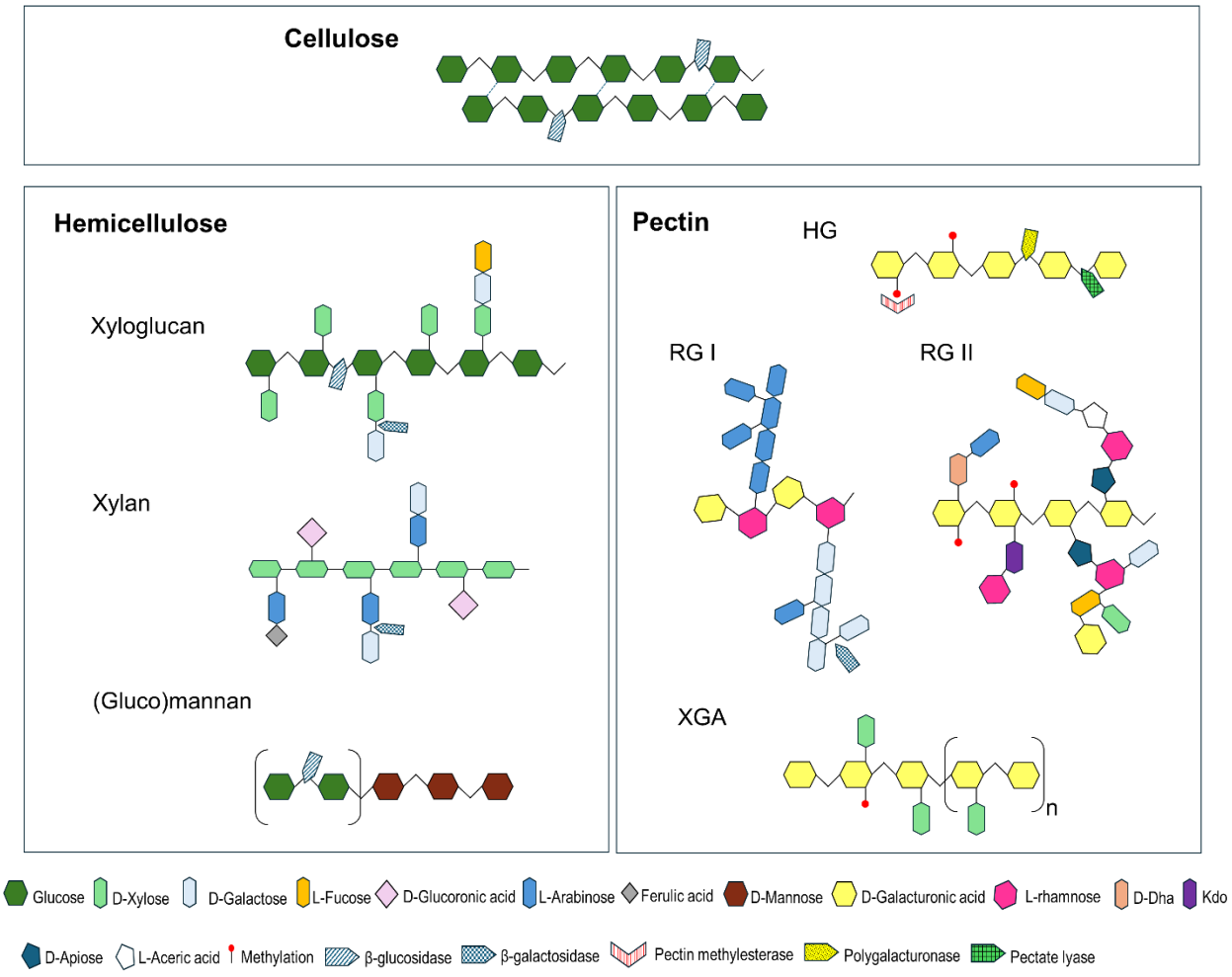

Figure 3.2. Cell wall polysaccharides and main cell wall-remodeling enzymes

No results about *SlLOB1* CRISPR/Cas9 editing in tomato landraces are publicly available to date and we wanted to increase our understanding of the effect of *SlPL* knock out on fruit firmness, shelf-life, cell wall remodeling and pathogen susceptibility. For this reason, a gene editing approach was set up in three different genetic backgrounds: Scatolone di Bolsena (SCA), Spagnoletta di Gaeta e Formia (SPA) landraces and Micro-Tom (MTO) model varieties, used as control.

3.2 Materials and methods

3.2.1 Plant material

Seeds from SCA and SPA traditional varieties and MTO as control, were *in vitro* germinated at 25°C to obtain cotyledons for transformation. Cotyledonary explants and regenerated plantlets were grown in a growth chamber under standard conditions (16 h light/8 h dark at 25°C) and fruits at the ripening stages of breaker (BR)+4 and red ripe (RR), equivalent to breaker +7, were collected for the phenotypic characterization and the cell wall enzyme-activity evaluation.

3.2.2 Construct assembly and plant transformation

3.2.2.1 sgRNA design and CRISPR/Cas9 vector construction

The constructs for the CRISPR/Cas9 transformation were assembled through the GoldenBraid (GB) cloning system (Sarrion-Perdigones et al., 2011). GB is a modular toolbox which consists of three levels of cloning, modulable by the *Bsa*I and *Bsmb*I restriction enzymes: i) level 0, represented by a universal domesticator vector (pUPD2) to clone DNA fragments (i.e. gRNAs); ii) level 1, represented by alpha vectors (pDGB α1 and α2) and iii) level 3, represented by omega vectors (pDGB ω1 and ω2). pDGBs are destination vectors in which the restriction sites for *Bsa*I and *Bsmb*I are placed in opposing orientations, allowing the assembly of the different transcriptional units (TUs).

For the *SlLOB1construct* the sgRNAs were designed to target the first exon of *SlLOB1* using the CRISPOR v5.2 tool (Concordet and Haeussler, 2018). Guides were selected by the best on-target specificity score and the lowest number of predicted off-target. To verify that the target genotypes did not contain SNPs in the region of interest, Sanger sequencing was performed on SCA, SPA and MTO DNA, using primers listed in the Supplementary Table S3.1 and PCR conditions reported in the Supplementary Table S3.2.

For the construct assembly, *E. coli* DH5α electrocompetent cells were used. First, the two sgRNAs were domesticated (together with tRNA and scaffold sequences) into two separate pUPD2 vectors, and positive colonies, grown on LB-agar medium supplemented with

chloramphenicol, were selected by the IPTG/Xgal screening method. Then, the two domesticated guides and the *Arabidopsis thaliana* U626 promoter were cloned into a single pDGBα2 vector, and selection was made on a medium supplemented with kanamycin, IPTG and Xgal. Finally, the assembled TU was cloned together with the NptII:Cas9:DsRed-marker cassette into a pDGB3-ω1 vector and selected over a medium containing spectinomycin. The final construct (Figure 3.3 A-C), containing the TUs Tnos:NptII:Pnos-35S:Cas9:Tnos-AtPU626:sgRNA1:sgRNA2:scaffold (Figure 3.3 D), was eventually transferred by electroporation into *Agrobacterium tumefaciens* electrocompetent cells and used for transformation of cotyledonary explants.

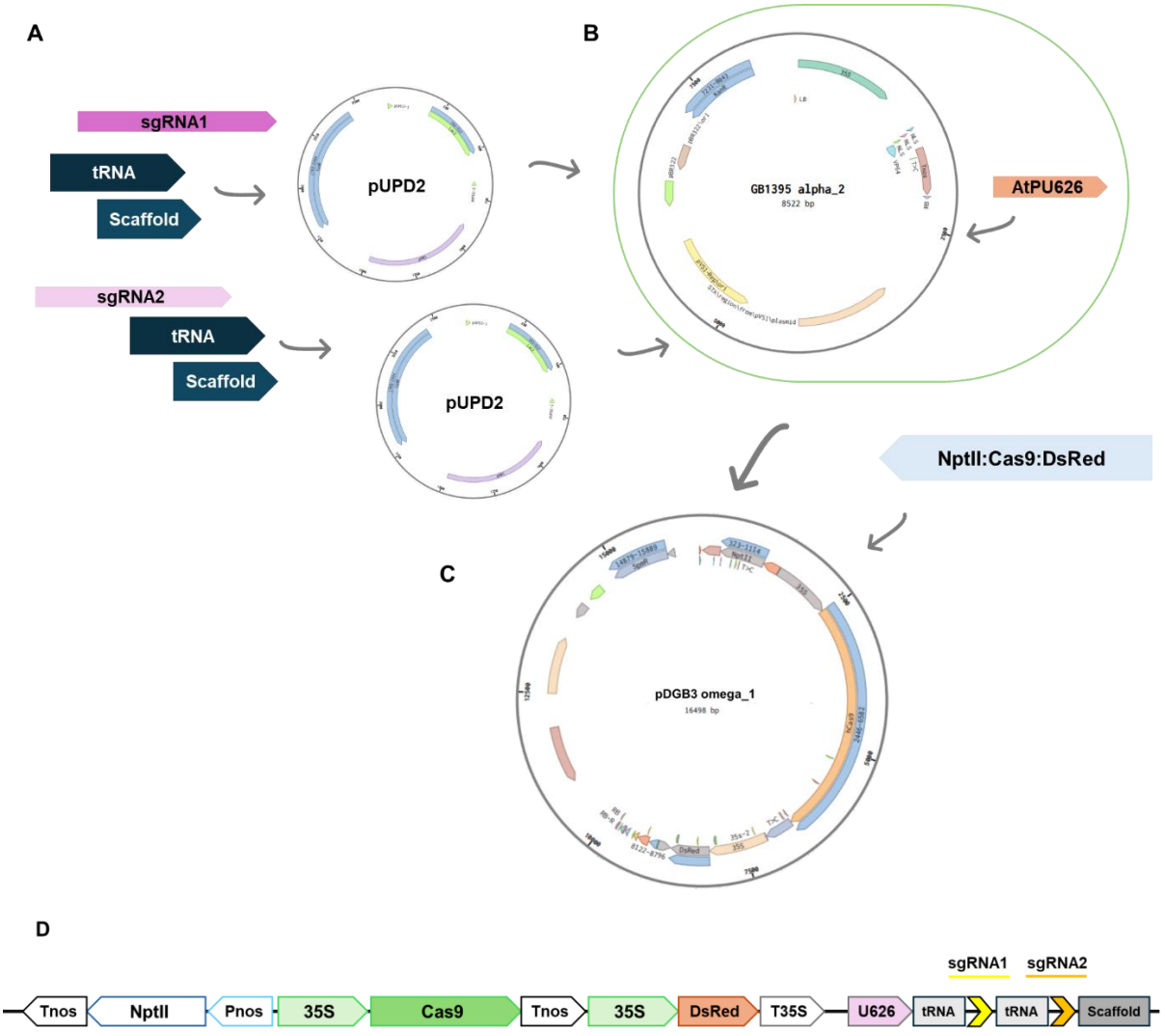

Figure 3.3. (A) Domestication of sgRNAs into pUPD2 vectors, **(B)** cloning of domesticated guides and the *Arabidopsis thaliana* U626 promoter (AtPU626) into the pDGBα2 destination vector, **(C)** assembly of the final pDGB3-ω1 construct containing **(D)** the Tnos:NptII:Pnos-35S:Cas9:Tnos-AtPU626:sgRNA1:sgRNA2 transcriptional units.

The construct for the *SlPL* transformation was assembled at "Instituto de Biología Molecular y Celular de Plantas (IBMCP), Consejo Superior de Investigaciones Científicas (CSIC) – Universitat Politécnica de Valéncia (UPV)", Valencia, Spain, following the same cloning system. A 20 nt sgRNA was designed to target the second exon of *SlPL* using the CRISPR-P v2.0 tool (Liu et al., 2017) and was selected by the best on-target and the lowest off-target score (Table 3.2).

Table 3.2. sgRNA information from CRISPR-P v2.0. PAM sequence is reported in italic bold, mismatched nucleotides in red.

sgRNA sequence	GGGCGCTAGCGTACACATAG***CGG***
On-score	0.2768
%CG	60%
No. of off-target (mismatches)	1 (4 MMs)
Off-target sequence	GGG**T**GCTAG**A**G**A**ACACATA**T*****TGG***
Off-score	0.388
Off-target region	Intron one of Solyc02g088550

The final pDGB3-ω1 construct, containing the TUs Tnos:NptII:Pnos-35S:Cas9:Tnos-PAtU626:sgRNA:scaffold (Figure 3.4 A-B) was transferred by electroporation into *A. tumefaciens* electrocompetent cells and used for transformation of cotyledonary explants.

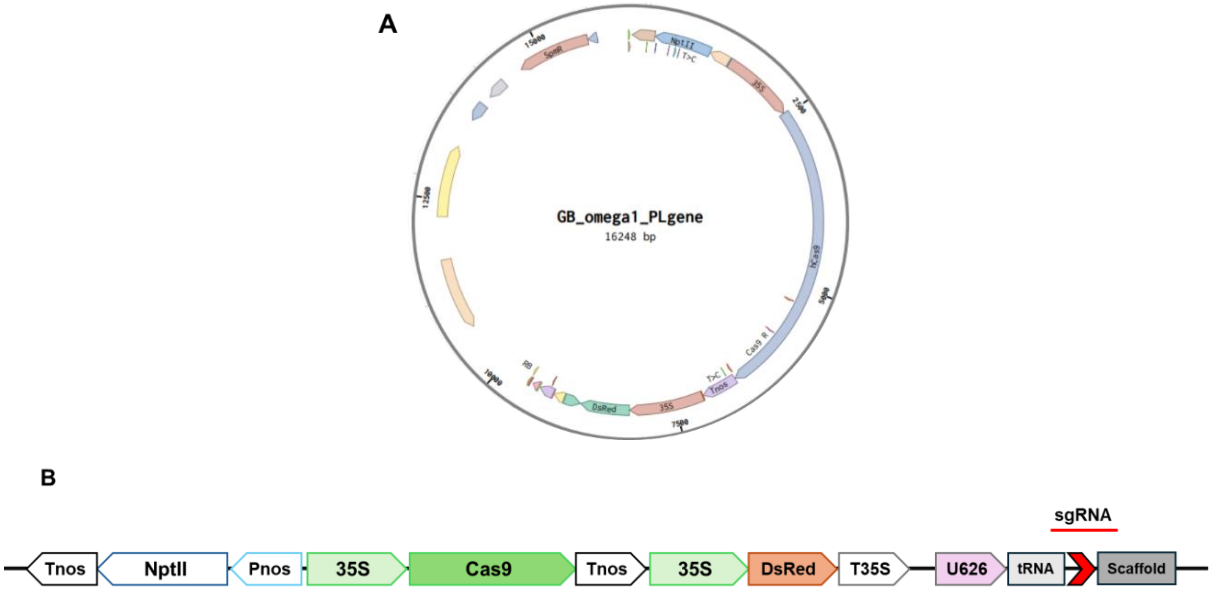

Figure 3.4. (A) Final *SlPL* pDGB3-ω1 vector and **(B)** transcriptional unit.

3.2.2.2 *Agrobacterium*-mediated transformation

Transformation was carried out according to Olimpieri et al. (2011). Sterile seeds of SCA, SPA, PAN and MTO genotypes were germinated in Petri dishes at 25°C, transferred in a growing medium containing 1 X Murashige and Skoog (MS) salts, 3% sucrose and 7 g/L plant agar (pH 5.8) and kept in a growth chamber under standard conditions (16 h light/8 h dark at 25°C). Once the cotyledons emerged, they were cut and placed in the dark onto a pre-conditioning medium supplemented with 0.1 mg/L 2,4-dichlorophenoxyacetic acid (2,4D), 0.35 mg/L indole-acetic-acid (IAA), 0.7 mg/L trans-zeatin (T-zea) and 200 µM acetosyringone. After 48 h, explants were inoculated for five min with *Agrobacterium* culture (OD_{600}: 0.4), grown in LB medium, and placed on the same pre-conditioning medium at dark for 24 h. Then, cotyledons were kept on an induction medium containing 0.35 mg/L IAA, 0.7 mg/L T-zea, 200 mg/L cefotaxime and 50 mg/L vancomycin for one week and finally transferred onto the regeneration medium, supplemented with 0.35 mg/L IAA, 0.7 mg/L T-zea, 500 mg/L carbenicillin and 100 mg/L kanamycin. Shoots of approximately 1 cm were eventually placed in the rooting medium containing 0.35 mg/L IAA, 0.1 mg/L indole-3-butyric-acid (IBA), 200 mg/L cefotaxime and 50 mg/L kanamycin (Supplementary Table S3.3) and transformation efficiency was calculated as: number of transformed shoots/number of explants * 100. Two different *Agrobacterium* strain (LBA4404 for *SlLOB1* and *SlPL* SCA/SPA; EHA105 for *SlPL* MTO) were used.

3.2.3 Molecular screening and sequencing

DNA was extracted from rooted shoots according to the CTAB method (Doyle and Doyle, 1987) and screened for the transgenic cassette by the amplification of Cas9 and NptII regions, using primer pairs listed in Supplementary Table S3.1. Transformed T_0 plants were transferred in pots and their sgRNA sites were Sanger sequenced and analyzed by the Tracking of Indel by DEcomposition (TIDE) tool (https://tide.nki.nl/).

For *SlPL*, seeds were collected from T0 plants, T_1 plants were self-pollinated until the mutations were in homozygous state and finally the 10 X whole genome resequencing of T_3 Cas-free plants (one for each obtained mutations, plus MTO as control) was performed (BGI Genomics, Shenzhen, China), and screened for on-target/off-target editing. Possible Cas9 off-target sites were identified using the Cas-OFFinder software (http://www.rgenome.net/cas-offinder/), using the *S. lycopersicum* SL2.50 genome assembly as reference and setting the maximum number of mismatches (MMs) at five.

3.2.3.1 T7EI endonuclease assay on *SlPL* mutants

For the T7EI endonuclease assay, primers were designed to amplify a 816 bp region containing the CRISPR target site, with the expected Cas9 cut site located 250-300 bp downstream of the 5' end of the fragment (Supplementary Table S3.1). The assay procedure was carried out according to the protocol supplied by New England Biolabs Inc (https://www.neb.com/en/protocols/2014/08/11/determining-genome-targeting-efficiency-using-t7-endonuclease-i).

3.2.4 Protein prediction of *SlPL* mutants

The protein sequences of mutants were predicted with the Expasy Translate tool (https://web.expasy.org/translate/) and aligned against the MTO wild type sequence on Clustal Omega Multiple Sequence Alignment (https://www.ebi.ac.uk/jdispatcher/msa/clustalo). The effect of mutations on the protein, the protein structures and the ligand-binding-site of native Micro-Tom PL and mutated proteins were inferred by I-TASSER tool (https://zhanggroup.org/I-TASSER/).

3.2.5 Fruit phenotyping of *SlPL* mutants

3.2.5.1 Fruit weight, fruit shape index, total soluble solids and pH

Weight for 25 red ripe fruits per mutated genotype plus the control was recorded. For fruit shape index (FSI) and total soluble solids (TSS) determination, ten fruits for each line were analyzed. FSI was calculated as the ratio of the polar to equatorial diameter of the fruit and TSS was obtained by two measurements of the juice per each fruit taken by a digital pocket refractometer (ATAGO™ PAL-1, ATAGAO CO., LTD, Tokyo, Japan). pH was measured in triplicate, by Fisherbrand™ Set pH meter accumet™ AE150 (Thermo Fisher Scientific, Waltham, MA, USA), on 250 mg of frozen pericarp resuspended in 15 mL pH 7 distilled water.

3.2.5.2 Firmness and weight loss

Firmness measurement was performed by Instron® Universal Testing Machine (model 4301, Instron, Canton, Mass., USA). Thirty fruits per genotype were harvested at the BR+4 and RR stages. Fruits at BR+4 were stored at room temperature and firmness was measured over a period of 10 d, for a total of four measurements; RR fruits were measured and immediately frozen for further analysis. The tomato fruit was placed over the plate of the Instron (Figure 3.5) and compressed with a flat compression anvil (55 mm diameter) at a rate of 10 mm min -1. The deformation of whole fruit to a load of 3 N was recorded and reported as “deformation to 3 N”.

Figure 3.5. Firmness measurement by Instron® Universal Testing Machine.

Weight loss assessment was performed only on RR fruits. Fifteen fruits per genotype were collected and weighed every three d up to 18 dph. Weight loss percentage was calculated as follows:

$$\frac{W_0 - W_{1,\,2,\,\ldots,\,n}}{W_0} \text{ x } 100$$

where W_0 was the weight recorded at harvest, W_1 the weight recorded at three dph, W_2 the weight at six dph, and so on, until $n = 6$ (18 dph). Before all analyses, fruits were rinsed with distilled water and cleaned with ethanol.

3.2.5.3 Determination the external color

Tomato external color was determined on 20 fruits per genotype for each ripening stage (BR+4, RR) with a Minolta colorimeter (Minolta C2500; Konica Minolta, Ramsey, NY, USA). Two values, taken on the equatorial region in two different sides of the fruit, were recorded for each CIEL*a*b* parameter, where L* indicates the lightness of the color, a* represent the red-green coordinates and b* the yellow-blue values. Hue angle ($H^* = [\tan^{-1} (b^*/a^*)*360]/(2*\pi)$) and a*/b* ratio were later calculated.

3.2.6 Enzymatic activity of *SlPL* mutants

Fruits from MTO and mutant lines were harvested at RR and pericarp tissue was grinded by IKA® A11 basic analytical mill (IKA, Staufen, Germany) and stored at -80°C to evaluate the activity of the main cell wall-remodeling enzymes. Assays were carried out on three biological and three technical replicates. Protein quantification was performed by Qubit™ Protein Broad Range (BR) Assay Kits (Invitrogen™, Thermo Fisher Scientific, Waltham, MA, USA).

3.2.6.1 Pectin methylesterases

For PME activity, 2 g of frozen pericarp were homogenized in 8 mL of 0.2 M potassium phosphate dibasic at pH 7.5, containing 1 mM EDTA, 1% (w/v) % polyvinylpolypyrrolidone (PVPP) and 8.8% (w/v) NaCl. After 2 h of incubation at 4°C on a tilting shaker, samples were

centrifuged at 11,000×*g* for 30 min. The supernatant was then filtered through a cotton gauze and the pH adjusted to 7.5. To assess the enzyme activity, the Hagerman and Austin (1986) protocol was followed. The reaction mixture was prepared by adding 100 µL of crude enzyme extract to 750 µL of distilled water, 2 mL of 0.5% citrus pectin and 150 µL of 0.01% (v/v) bromothymol blue. The linear decrease in absorbance at 620 nm occurring during the first minute of reaction was recorded and a standard curve of D-galacturonic acid was used to calculate the concentration of the reaction product. PME activity was expressed as unit (U = µmol of D-galacturonic acid produced per min) per mg of protein under the assay conditions.

3.2.6.2 Pectate lyase

PL activity was assessed by the Pectate Lyase Microplate Assay Kit (#CAK1093, Cohesion Biosciences), following the manufacturer's instruction. To determine the level of 4,5-unsaturated reaction products, the absorbance of the supernatant was measured at 235 nm and activity was expressed as U (1 U= µmol of oligogalacturonic acid produced per min) per mg of protein.

3.2.6.3 Polygalacturonases

For PG activity, the protocol described by Shakir et al. (2022), with slight modifications, was followed. One g of frozen tomato fruit was mixed with 8 mL of 40 mM cold sodium acetate buffer (NaAcB) (pH 5.5) and 2 mL of 0.2 M NaCl and kept for 15 min at 4°C on a tilting shaker. After incubation, the samples were centrifuged at 12,000×*g* for 30 min at 4°C and the supernatant was collected. 100 µL of supernatant was added to 500 µL of 0.2 M NaAcB (pH 4.5) and 400 µL of 0.5% (w/v) poligalacturonic acid and incubated for 30 min at 37°C. After incubation, 1 mL of 0.1% dinitrosalicylic acids (DNSA) was added into the mixture and heated at 100°C for 5 min. Samples were then centrifuged and cooled down before reading the absorbance at 540 nm. The same procedure but with boiled-inactivated extract was followed for the blank and NaAcB/DNSA mixture was used to calibrate the spectrophotometer. PG activity was expressed as U (1 U = µmol of D-galacturonic acid liberated per min) per mg of protein under the assay conditions and product concentration was assessed by a standard curve of D-galacturonic acid.

3.2.6.4 Glycosidases

Glycosidases extraction was performed according to Fils-Lycaon and Buret (1991), with modifications. Two g of grinded tomato pericarp were homogenized in 4 ml (1:2 w/v) of 50mM NaAcB (pH 5.5) containing 1.4 M NaCl, 0.2% (w/v) L-cysteine and 0.5% (w/v) PVPP. After 1 h of incubation at 4°C on a tilting shaker, samples were centrifuged at 11,000×*g* for 30 min at 4°C and the supernatant was filtered using a cotton gauze. α-D-galactosidase, β-D-galactosidase and β-D-glucosidase activity was assessed using 950 µL of the appropriate *p*-nitrophenyl glycoside, at a final concentration of 2.0 mM, 2.0 mM and 2.5 mM respectively, in a 50 mM NaAcB buffer at pH 5.8, 4.3 and 5.1 respectively. Twenty-five µL of enzyme extract for the α-D-galactosidase and 50 µL for β-D-galactosidase and β-D-glucosidase were added to the solution and the mixture was incubated at 37°C for 15 min. The reaction was stopped by adding 1 mL of 0.1 M Na_2CO_3 and the absorbance was measured at 405 nm. Boiled extract was used as sample blank and NaAcB/Na_2CO_3 mixture was used to calibrate the spectrophotometer. Glycosidase activity was expressed as U (1 U = µmol of *p*-nitrophenol liberated per min) per mg of protein under the assay conditions, using a molar extinction coefficient of 1.77 x 10^4 (Konozy et al., 2012).

3.2.7 Pathogenicity assay of *SlPL* mutants

The pathogenicity assays were performed in collaboration with prof. De Lorenzo group (Department of Biology and Biotechnology Charles Darwin, La Sapienza University, Rome, Italy).

For the analysis, fifty seeds from MTO and T_3 homozygous mutated lines were surface sterilized with 70% ethanol, followed by a 50% bleach treatment. After thoroughly rinsing them with distilled water, seeds were incubated on wet filter paper for 48 h in darkness at room temperature to allow germination. Afterward, germinated seeds were transferred to autoclaved soil and grown in a controlled growth chamber with a 16-h-light/8-h-dark cycle at 25°C. Leaves from five-weeks-old plants were collected in triplicate and infected with *B. cinerea*, *Phytophthora capsici*, and *Pseudomonas syringae* pathogens.

3.2.7.1 *Botrytis cinerea* infection

For the *B. cinerea* assay, the protocol of Lian et al. (2018) was followed with slight modifications. The fungal strain SF-1 was routinely maintained on malt extra agar medium at 20°C under a 12 h photoperiod prior to spore collection. Spore concentration was measured with a counting chamber under a microscope and adjusted to 5 x 10^5 spores/mL before inoculation. Leaflets from the third true leaf were detached from the plants and placed onto 0.8% agar medium, with the petiole embedded in, to ensure proper hydration during the infection period. Five µL of spore suspension was used to infect leaves and, after 48 h of incubation, disease symptoms were evaluated. Sterile distilled water was used as control treatment. Lesion development and lesion area on the infected leaflets were assessed via ImageJ software (https://imagej.net/ij/index.html).

3.2.7.2 *Phytophthora capsici* infection

For spore induction, *P. capsici* culture was grown on V8 agar plates in darkness at 25°C for 7 d. Portions of fungal culture were transferred to fresh plates containing sterile water and incubated under continuous light for 3 d to induce sporangia formation. Sporangia were observed under the microscope and harvested by centrifuging at 5,000×*g* for 10 min. The resulting pellet was resuspended in 2 mL of sterile water to prepare the spore suspension. The inoculation procedure was the same as for *B. cinerea*. Disease progression was observed after three d of incubation, and lesion area was measured using ImageJ software.

3.2.7.3 *Pseudomonas syringae* infection

P. syringae pv. *tomato* (Pst) DC3000 was grown on LB liquid medium, supplemented with 50 µg/mL rifampicin, at 28°C for 36 to 48 h. After growth, bacterial cells were suspended in sterile distilled water to create the inoculum with an optical density (OD) of 1.0 at 600 nm. Leaves of each genotype were syringe-infiltrated with Pst DC3000 suspension or sterile water as control. Two leaf discs with a total area of 0,392 cm^2 were collected three d post inoculation, surface sterilized with 70% ethanol, rinsed with sterile distilled water and subsequently homogenized in 1 mL of sterile water. Serial dilutions of the homogenate were prepared, and 5 µL of each

dilution were plated onto LB agar plates containing 50 µg/mL rifampicin. After 48 h of incubation at 28°C, bacterial colonies were counted.

3.2.8 Data analysis

Data were analyzed by one-way analysis of variance ANOVA, and statistical differences were determined by Dunnett's Multiple Comparison *post hoc* test, implemented on DescTools R package (Signorell, 2024) and performed in RStudio v4.3.3 (Posit team, 2022). The same statistical analysis was performed on phenotypic data, enzymatic activity and pathogenicity assays. Results were expressed as mean ± standard error and differences were considered significant at $p \leq 0.05$.

3.3 Results

3.3.1 sgRNAs design and CRISPR/Cas9 vector construction

Two 20 nt sgRNAs targeting the first exon of *SlLOB1* were selected, based on the best specificity and lowest off-target number (Table 3.1).

Table 3.1. sgRNAs information from CRISPOR v5.2. PAM sequence is reported in italic bold, mismatched nucleotides in red.

sgRNA sequences	**1) ACCCCCGTCAATGACAGTGG*TGG*** **2) GCGCCGCCTGTAAAATATTA*CGG***
Specificity score	1) 100 2) 100
No. of off-target (mismatches)	1) 2 (4 MMs) 2) 2 (4 MMs)
Off-target sequence	1) GTCTTCGTCAATGACAGTGG***TGA*** ACCGCCGTCAGTGGCGGTGG***TGG*** 2) GTGCCACCTGTTAAGTATTA***TGG*** ACGAAGCCTCTAAAATATTA***AGA***
Off-target region	1) Intergenic 3’ UTR of Solyc01g098030/exon one of Solyc01g098040 2) Intergenic Intergenic

In MTO, SCA and SPA no sequence differences were detected at the target region (Figure 3.6), thus the final pDGB3-ω1 construct was used to transform SCA, SPA and MTO cotyledons by *Agrobacterium*-mediated transformation.

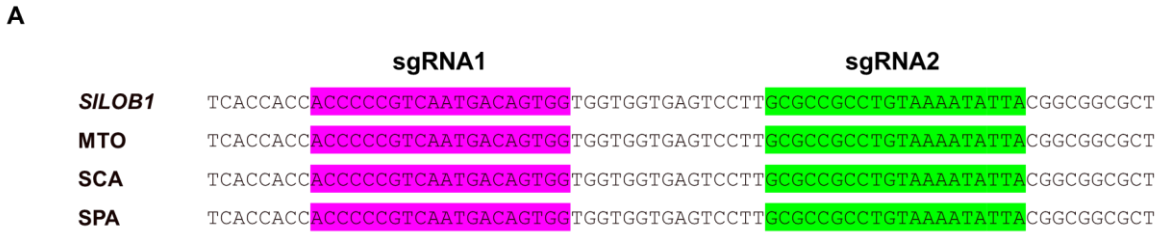

Figure 3.6. Target region of *SlLOB1* in Micro-Tom (MTO), Scatolone di Bolsena (SCA) and Spagnoletta di Gaeta e Formia (SPA).

3.3.2 *Agrobacterium*-mediated transformation

For *SlLOB1* transformation, out of the three genotypes, only SCA produced transformed shoots (Figure 3.7). From seven calli, 21 shoots were transferred in the rooting medium, with a regeneration rate of 8%. Ten shoots could produce roots and nine of them resulted positive to the Cas9/NptII PCR screening, with a final transformation efficiency of 3.6% (Supplementary Table S3.4).

SPA could not regenerate, while MTO had a callus production of 1.2% and regenerated six shoots, none of which rooted in kanamycin-supplemented medium (Supplementary Table S3.4).

Figure 3.7. Scatolone di Bolsena shoots in rooting medium

The transformed shoots obtained from SCA were transferred into pots but none of them survived the *ex-vitro* environment

For the *SlPL* construct, the transformation trial on the SCA and SPA landraces, as for the *SlLOB1* one, was not successful. Out of three formed calli, four shoots were regenerated in SCA, with an efficiency of 1.7%, and no one was transformed. For SPA, a higher number of calli (12) formed. 13 shoots were produced, with a regeneration efficiency of 5.5%, but as for SCA, no rooting in presence of kanamycin occurred, thus indicating a transformation efficiency equal to zero (Supplementary Table S3.5).

For the MTO (hereafter referred as wild type - WT) transformation with the *SlPL* construct, from 43 calli produced by the explants, 81 regenerated shoots were obtained. Among these, only seven were able to root in kanamycin-supplemented medium and just five of them (PL1, PL7, PL8, PL9, PL17) resulted positive to Cas9/NptII PCR screening, with a final transformation efficiency of 2.5%. Sanger sequencing was performed on the target locus of T_0 transformed plants. No events were detected in PL7 and PL8, thus indicating that no editing happened in the two T_0 lines. Further, one heterozygous and two chimeric events occurred. The latter occurred in PL1, which retained the WT allele and exhibited a 1 bp insertion and a 3 bp deletion, and in PL17, which retained the WT allele as well and exhibited a 1 bp insertion and 2 bp deletion. Finally, PL9 was heterozygous for the WT and a 1 bp insertion allele. The percentage of each predicted allele with $p < 0.05$ were reported (Supplementary Table S3.6). Seed was collected from each T_0 line and T_1 progeny plants were grown and further analyzed as above. Alleles predicted in T_0 were not yet fixed, with all lines showing the same allelic distribution as T_0, except for PL1, which lost the 1 bp insertion allele, and PL7, in which a new allele appeared (Supplementary Table S3.6). As PL1 and PL7 did not produce seeds and PL8 did not carry any mutation, only PL9 and PL17 were grown to the T_2 generation. T_2 DNA was screened for mutations by T7EI endonuclease assay.

In the assay, after a PCR cycle, if insertions or deletions are present in the target region, heteroduplex, with one or more mismatches, form. Afterwords, the PCR product is re-annealed and digested with T7EI endonuclease, a structure-specific enzyme which is able to recognize and cleave in correspondence of such mismatches (Vouillot et al, 2015). If *indel* are present, three bands are expected, one from the undigested homoduplex DNA (from either allele), and two resulting from heteroduplexes digestion.

Since none of the PL9 plants displayed the mutation digestion-pattern, only PL17 Cas-free plants were sequenced in the target region to assess the type of mutation. By TIDE

decomposition, all the screened plants exhibited an heteroallelic configuration (Supplementary Table S3.6) and finally, only in T_3, homozygous lines (Supplementary Table S3.6) could be evaluated for their phenotypic traits. In Figure 3.8, the two fixed mutations are shown. The 1 bp insertion mutant will be hereafter referred to as PL^{INS} and the 2 bp deletion mutant as PL^{DEL}.

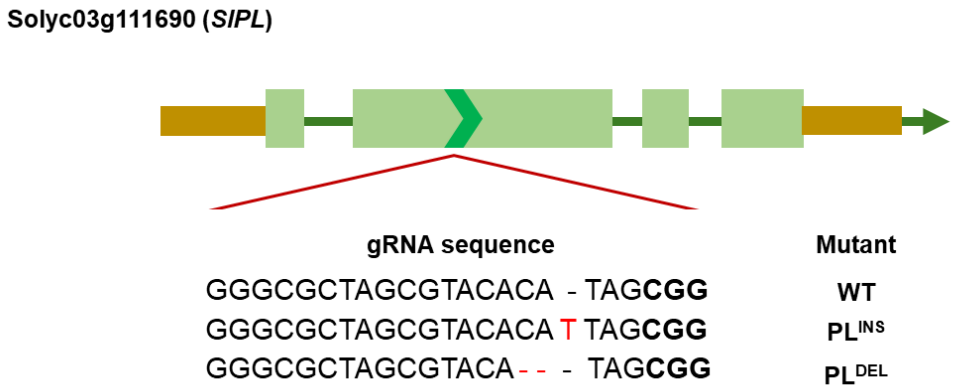

Figure 3.8. Target sequence of the *Solyc03g111690* (*SlPL*) gene and genetic lesions obtained. The PAM sequence is reported in bold. Mutations for PL^{INS} and PL^{DEL} are reported in red.

Cas-OFFinder identified a total of 20 potential off-target sites: one with 4 MMs and 19 with 5 MMs (data not shown). Out of these 20, only the one with 4 MMs falls within a genic region (first intron of Solyc02g088550) and no mutations were detected at any predicted site in the two CRISPR edited lines (Supplementary Figure S3.1).

3.3.3 Protein prediction of *SlPL* mutants

SlPL encodes a 403 amino acids (aa) protein. The two mutations caused a predicted frameshift that introduces a premature stop codon, with the 1 bp insertion resulting in a 176 aa truncated protein and the 2 bp deletion resulting in a 175 aa truncated protein. As shown by the alignment of the native and mutated PL proteins, PL^{INS} and PL^{DEL} are identical, except for an isoleucine (I) residue that is retained in PL^{INS}, as in the WT sequence (Supplementary Figure S3.2). Additionally, the Interpro domain IPR002022 Pectate lyase/Amb_all (from aa 128 to 325) resulted to be partially truncated in both the mutated proteins, lacking the aa responsible for the substrate binding-activity (D224, K248, L251, R285) and the active site residues (D202, M280) (Figure 3.9), as predicted by the I-TASSER tool (Supplementary Figure S3.2).

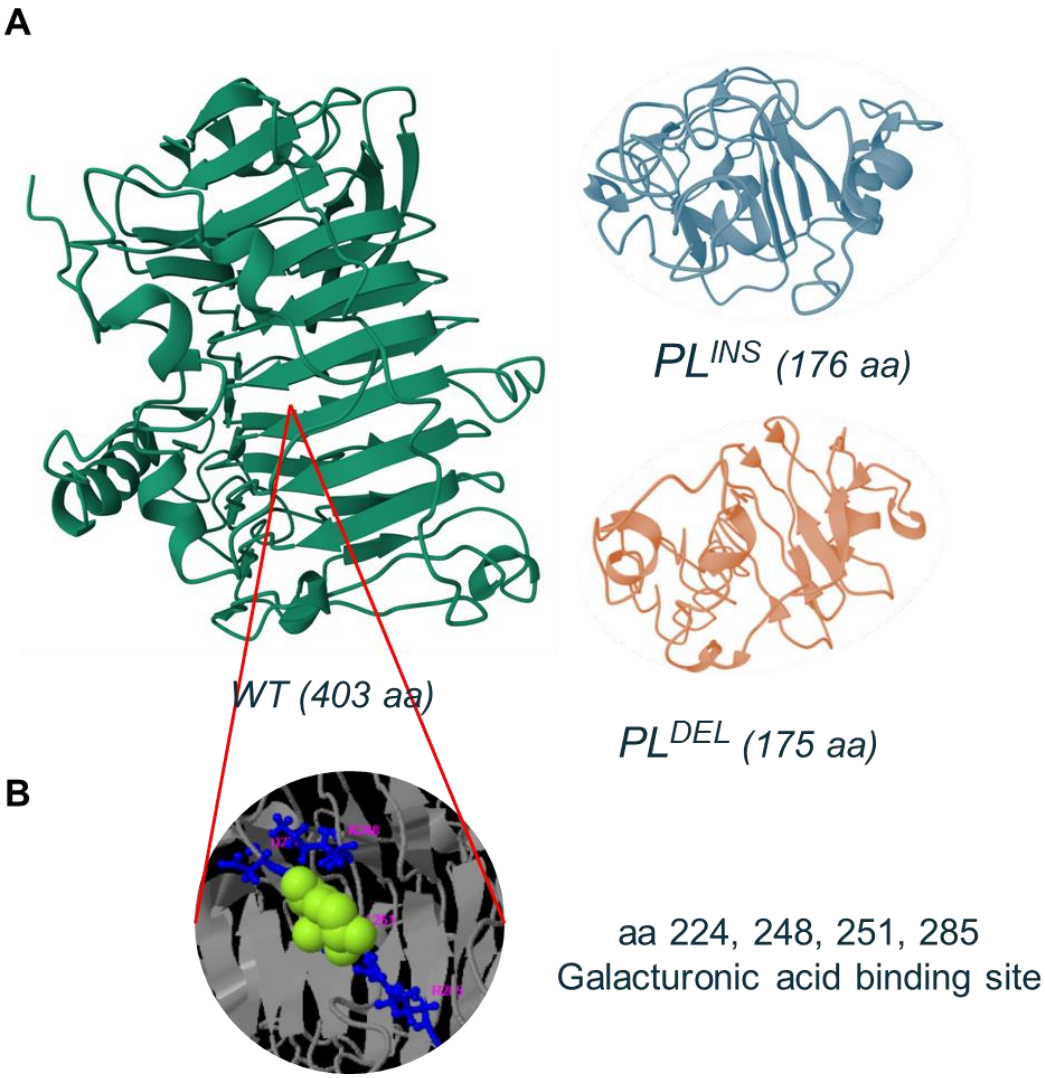

Figure 3.9. (A) Structure of native (WT) and mutated (PL^{INS}, PL^{DEL}) PL protein, inferred by I-TASSER, and **(B)** amino acids (aa, in blue) responsible for the substrate (galacturonic acid, in green) binding activity.

3.3.4 Fruit phenotyping of *SlPL* edited plants

3.3.4.1 Fruit weight, fruit shape index, total soluble solids and pH

Fruit wight, FSI, TSS and pH were measured at the RR stage in WT, PL^{INS} and PL^{DEL} fruits. No significant difference was detected in any of the traits analyzed between the WT and the mutated lines (Figure 3.10).

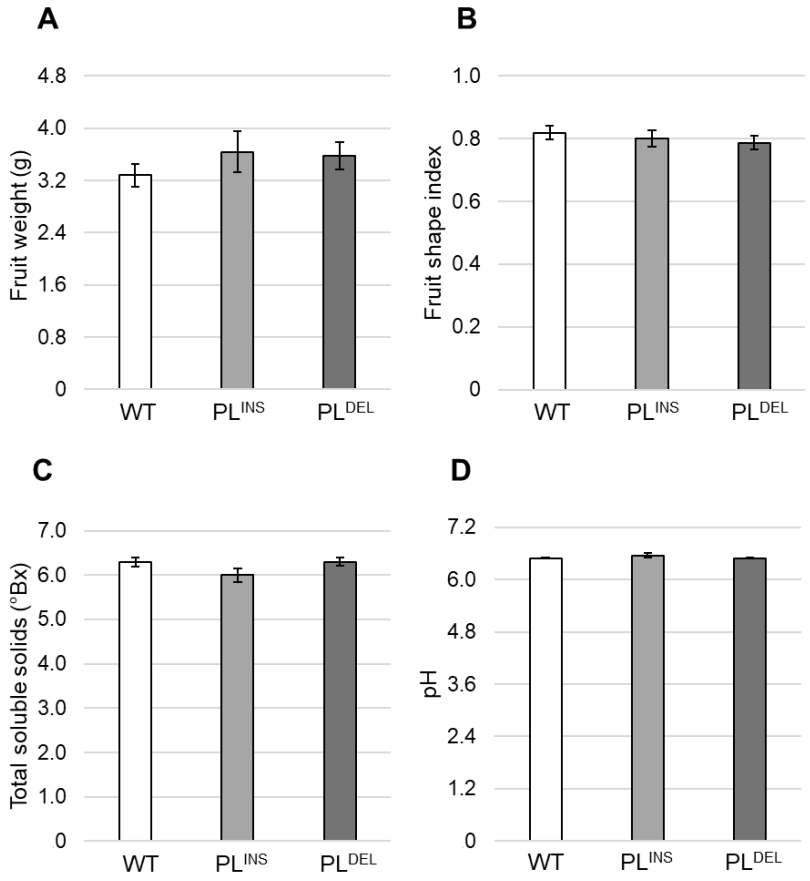

Figure 3.10. Fruit quality parameters in the wild type (WT) and in the mutated lines by insertion (PL^{INS}) and deletion (PL^{DEL}). **(A)** fruit weight; **(B)** fruit shape index, **(C)** total soluble solids, **(D)** pH under the assay conditions. Data are expressed as mean ± standard error of 25 (A), ten (B-C) and three (D) replicates.

3.3.4.2 Firmness and weight loss

Fruit firmness was assessed at the BR+4 and RR ripening stages. Furthermore, fruits at BR+4 were stored at room temperature to evaluate the firmness decay up to 10 dph. Both PL^{INS} and PL^{DEL} fruits exhibited a highly significant difference ($p<0.001$) in fruit firmness in comparison to WT. Fruit deformation was 19% and 17% lower than WT for PL^{INS} and PL^{DEL} at BR+4 and 21% and 22% lower than WT at RR (Supplementary Figure S3.3). For firmness decay, PL^{DEL} fruits always exhibited a significantly reduced softening compared to WT, while PL^{INS}, even showing a general increase in firmness, resulted to be significantly firmer only at the first, third and fourth measurement (Figure 3.11 A).

To assess the weight loss beyond the commercial life of fruits, all the samples were weighed every three d over a period of 18 d. Similar to fruit firmness, PL^{DEL} fruits always exhibited a significantly lower percentage of weight loss loss than the WT fruits did, while PL^{INS} showed a significant difference compared to WT starting from 9 dph (Figure 3.11 B). Fruits of all genotypes appeared wrinkled after 18 dph, but for PL^{INS} and PL^{DEL} wrinkling was visibly reduced (Figure 3.11 C).

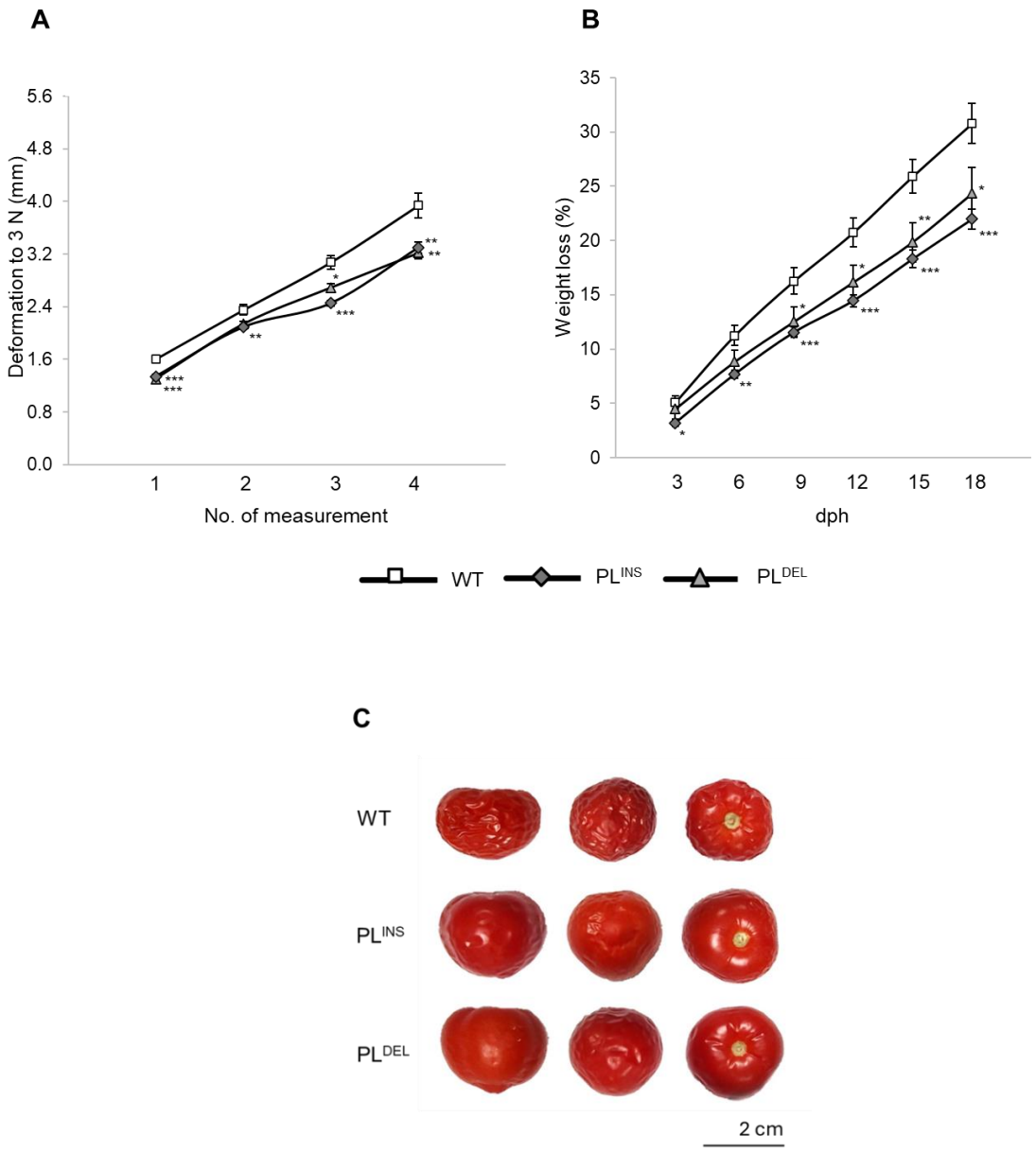

Figure 3.11. Dynamics of **(A)** fruit firmness and **(B)** weight loss in fruits of the wild type (WT) and mutated lines (PL^{INS}, PL^{DEL}) after storage, and **(C)** lateral, stylar, and stem side views of representative fruits stored at room temperature for 18 days post-harvest (dph). Data are expressed as mean ± standard error of 30 (A) and 15 (B) replicates. Asterisks indicate significant differences, determined by Dunnett's test, between each mutated line and the WT (* $p \leq 0.05$, ** $p \leq 0.01$, *** $p \leq 0.001$).

3.3.4.3 Determination of the external color

PL^{INS} always showed a significantly different value for any parameter, except for the a* value at both BR+4 and RR stages. In contrast, no significant difference between WT and PL^{DEL} was found at both ripening stages, except for a* and b* at the RR stage, which resulted significantly lower in the mutant (Table 3.3).

Table 3.3. External fruit color parameters. Values for L*, a*, b*, a*/b* ratio and hue angle (H*) are reported for two ripening stages, breaker plus 4 d (BR+4) and breaker plus 7 d (RR). Data are expressed as mean values ± standard error of 20 replicates. Significant differences against WT were determined by ANOVA followed by Dunnett's test (* $p \leq 0.05$, ** $p \leq 0.01$, *** $p \leq 0.001$)

Stage	Genotype	L*	a*	b*	a*/b*	H*
BR+4	WT	40.51±0.45	22.04±0.70	34.69±1.26	0.65±0.03	57.24±1.18
	PL^{INS}	42.43±0.54**	22.22±0.53	41.78±1.38***	0.56±0.03*	61.41±1.37*
	PL^{DEL}	39.24±0.45	21.75±0.58	34.15±0.90	0.64±0.02	57.37±0.81
RR	WT	35.31±0.59	29.24±0.60	28.85±0.74	1.02±0.02	44.54±0.47
	PL^{INS}	37.32±0.49*	28.76±0.43	32.22±0.78**	0.90±0.02**	48.16±0.65**
	PL^{DEL}	35.12±0.35	27.00±0.55**	26.90±0.58*	1.01±0.01	44.89±0.40

3.3.4.4 Activity of cell wall-remodeling enzymes

The activity of the main cell wall-remodeling enzymes was evaluated at the RR harvesting time in WT and mutated lines to elucidate the fruit softening process and the regulatory mechanisms behind texture increase in *SlPL* knock-out lines. Both PL^{INS} and PL^{DEL} exhibited a significant reduction in the activity of all the tested enzymes (Figure 3.12).

PL activity was reduced by 37.4% and 16.6% in the PL^{INS} and PL^{DEL} lines, respectively. PME activity decreased by 43.6% and 37% for PL^{INS} and PL^{DEL}, respectively, in comparison to WT. For PGs, the activity decreased by 47.5% for PL^{INS} and by 50.6% for PL^{DEL}. Finally, all the analyzed glycosidases showed lower activity in the mutated lines in comparison to the WT: α-Gal activity was reduced by 46% in PL^{INS} and 45.5% in PL^{DEL}; β-Gal activity decreased by

60.7% and 56% in PL^{INS} and PL^{DEL}, respectively; and the decrease in β-Glu activity was 62% in PL^{INS} and 57.2% in PL^{DEL}.

PME was the enzyme that presented the highest overall activity in all the genotypes, followed by α-Gal, PG, PL, β-Gal and lastly β-Glu.

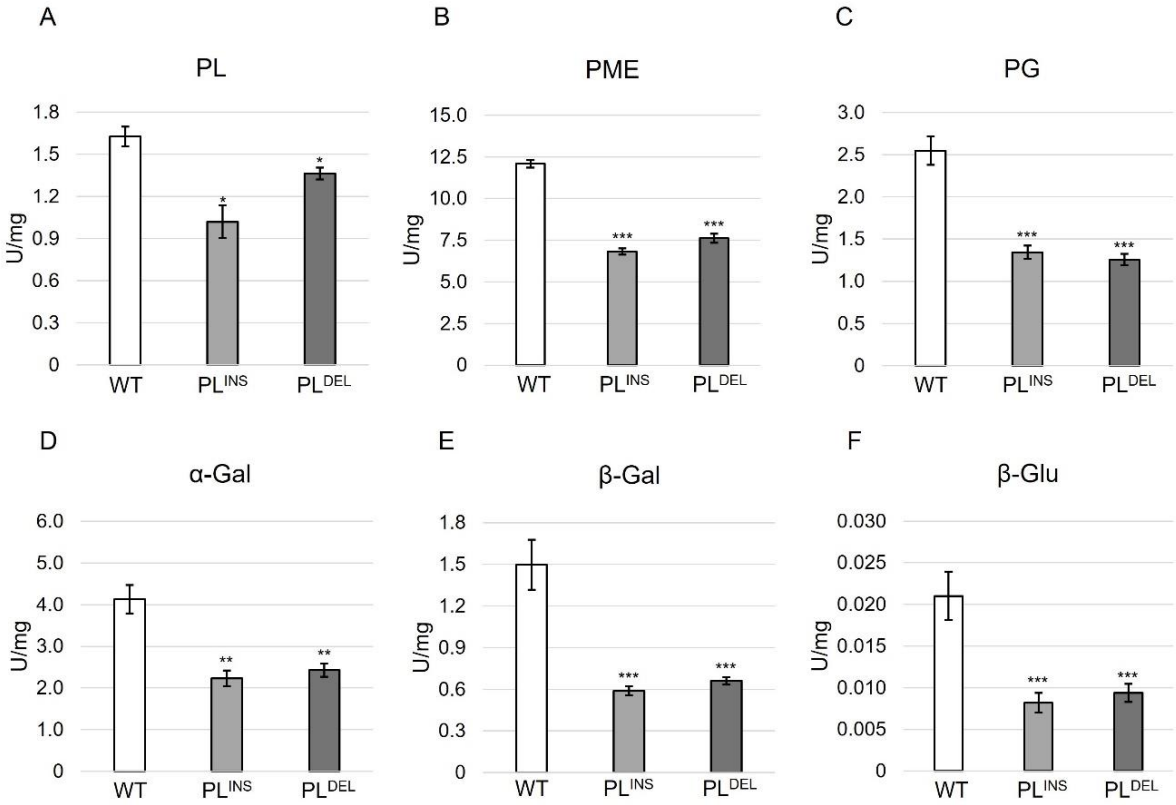

Figure 3.12. Activity of cell wall-remodeling enzymes. **(A)** Pectate lyase (PL), **(B)** pectin methylesterase (PME), **(C)** polygalacturonase (PG), **(D)** α-galactosidase (α-Gal), **(E)** β-galactosidase (β-Gal) and **(D)** β-glucosidase (β-Glu). Data are expressed as mean ± standard error of three replicates. Asterisks indicate significant differences, determined by Dunnett's test, between each mutated line (PL^{IN}, PL^{DEL}) and wild type (WT) (* $p \leq 0.05$, ** $p \leq 0.01$, *** $p \leq 0.001$).

3.3.5 Pathogenicity assay

Compared to the WT plants, both the PL^{INS} and PL^{DEL} genotypes presented increased resistance to *B. cinerea* and *P. capsici* infection, since both lesion size and disease severity were significantly reduced in the mutants (Figure 3.13 A-B). For *B. cinerea*, PL^{INS} showed a reduction of 22.7% and PL^{DEL} of 18.2%. For *P. capsici*, the infection severity was reduced by 20% in PL^{INS} and by 30% in PL^{DEL}.

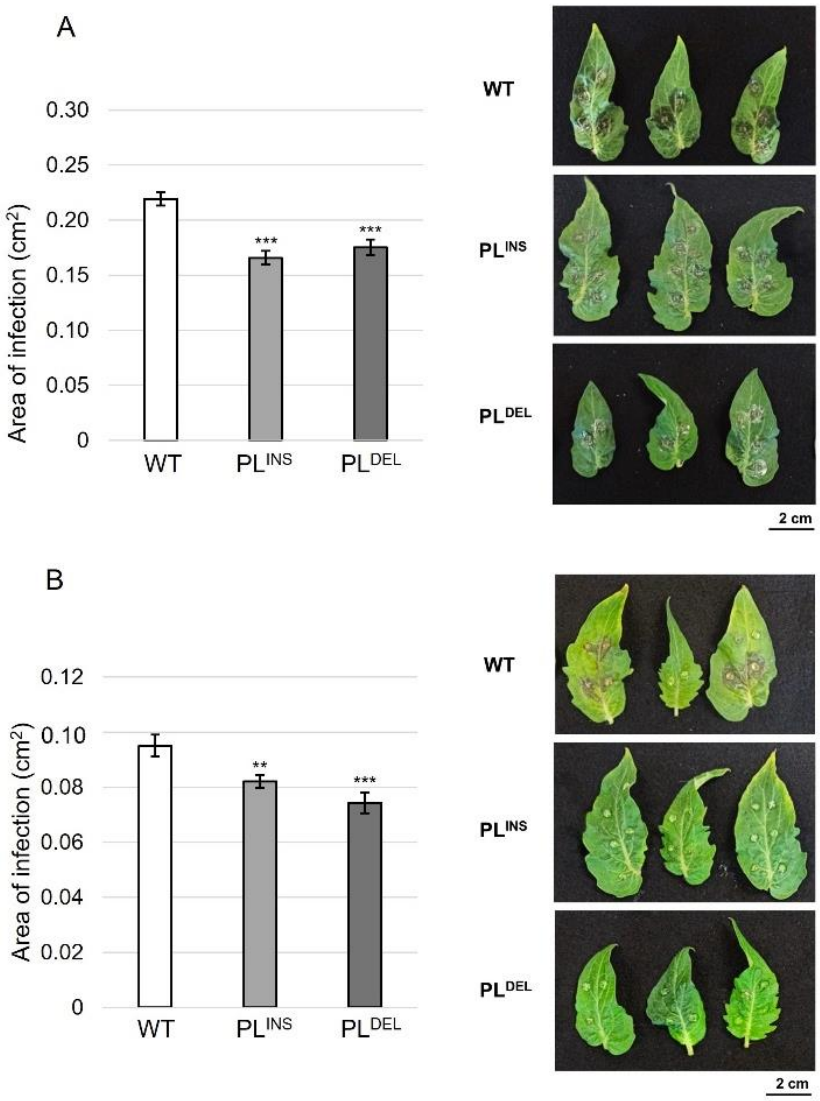

Figure 3.13. Response of wild type (WT), and mutated lines (PL^{INS}, PL^{DEL}) to **(A)** *B. cinerea* and **(B)** *P. capsici* infection. Data are expressed as mean ± standard error of three replicates. Asterisks indicate significant differences, determined by Dunnett's test, between each mutated line and WT (** $p \leq 0.01$, *** $p \leq 0.001$).

In the bacterial infection assay involving *P. syringae* pv *tomato*, both *SlPL* mutants exhibited higher levels of resistance, outdoing the WT genotype (Figure 3.14), with PL^{INS} and PL^{DEL} showing 22% and 27.4% fewer bacterial cells, respectively.

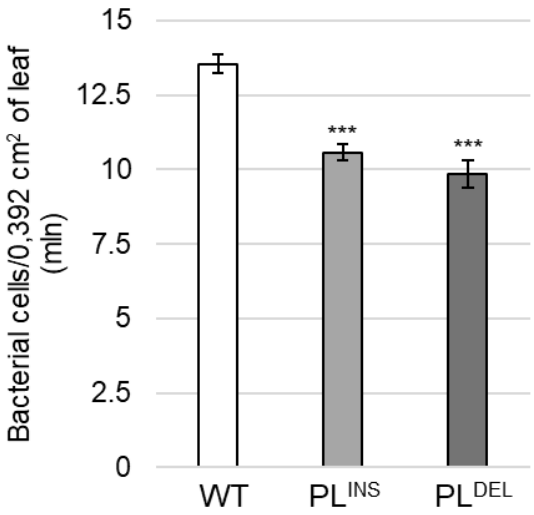

Figure 3.14. Estimated number of *P. syringae* pv. *tomato* cells in wild type (WT) and mutated lines (PL^{INS}, PL^{DEL}) leaves after three days (d) of infection. Data are expressed as mean ± standard error of three replicates. Asterisks indicate significant differences, determined by Dunnett'stest, between each mutated line and WT (*** $p \leq 0.001$).

3.4 Discussion

3.4.1 Transformation with *SlLOB1* construct

The poor response of the traditional genotypes to the *Agrobacterium*-mediated transformation may indicate a sensitivity of this material to the utilized protocol. However, considering that few transformants could be obtained from SCA, the *SlLOB1* construct may also have had a deleterious effect on the shoots/plants development. Furthermore, the presence of lethal mutations could be excluded as the plants mortality' cause, since the normal phenotype of the RNAi-silenced-plants obtained by Shi et al. (2021) indicates that *SlLOB1* is not essential for tomato plant grow (unlike, for example, the *DET1* gene, where the null mutation is lethal in *Arabidopsis* (Kang et al., 2015), as well as its silencing (Davuluri et al., 2004) and CRISPR knock-out (unpublished data) in tomato.

3.4.2 Transformation of landraces with *SlPL* construct

Unlike the *SlLOB1* transformation, where few transformed shoots were obtained in SCA, no transformation events occurred for the *SlPL* construct. Moreover, regeneration efficiency continued to remain low as for the *SlLOB1* transformation trial. This confirmed the sensitivity of the tested genotypes to the utilized protocol. While having an exceptional response to regeneration, the introduction of antibiotics to the media seems to highly affect the viability of the explants. Antibiotics toxicity depends on different factors, i.e. organism, species, genotype and concentration, (Ahmed et al., 2023), therefore, genotype-specific protocols should be developed in order to achieve genetic transformation of Scatolone di Bolsena and Spagnoletta di Gaeta e Formia traditional varieties.

3.4.3 Transformation and editing efficiency of Micro-Tom genotype with *SlPL* construct

In our experiment, the estimated regeneration capacity of the explants was 190.7%, with 81 shoots regenerated from 43 calli. Of these, just five appeared to be transformed. In Micro-Tom, transformation efficiency has been reported to reach 40% (Sun et al., 2006), and our outcome did not match such findings, suggesting very low efficiency of the protocol. Different tomato transformation protocols showed variable transformation efficiencies. ranging from 3.5 to 28 % (Kombat, R., 2023), depending on different factors, such as genotype, type and age of explants, *Agrobacterium* strain and density, and co-cultivation time (Cheng et al., 1997; Opabode, 2006; Van Eck, 2019).

Based on chromatogram decomposition analysis carried out on the TIDE software, no homozygous events were detected and just three out of five Cas-positive T_0 plantlets resulted to be edited in the target *SlPL* site. For PL7, a new allele (1 bp insertion) appeared in the T_1 generation. This is probably due to residual Cas9 activity, since the only PL7 T_1 seed that could germinate did not segregate the transgenic cassette, retaining the Cas9 sequence. Mutations not detectable in T_0 but appearing for the first time in the T_1 generation were previously reported in wheat by Zhang et al. (2021). Among the screened samples of the T_2 progeny, only PL17 showed the T7EI assay expected pattern, indicating that none of the screened PL9 plants carried the newly appeared mutant allele (Supplementary Figure S3.4). Consequently, only PL17 plants were sequenced in the target region, and analyzed by TIDE. Through decomposition analysis, the heteroallelic configuration for 1 bp ins/2 bp del was still present in all the screened samples (Supplementary Figure S3.5), making it necessary to grow a further generation to obtain homozygosity. Therefore, T_3 plants were eventually genotyped to confirm the mutations sequences and to select homozygous mutants (Supplementary Figure S3.6). Sequencing of all grown plants was required, because few individuals were still heteroallelic, indicating that it was not possible to completely get rid of the chimeric asset even after three generations.

In plants, the most common CRISPR/Cas9-induced mutations are single nucleotide insertions, mainly A/T, as reported for different crop species (Ma et al., 2015; Gianoglio, 2018; Dono, 2020), and up-to-10 nucleotides deletions (Jansing et al., 2016), with breakpoints mainly at 3 bp upstream of the PAM sequence. PL^{INS} and PL^{DEL} have a 1 bp insertion (+T) and a 2 bp deletion (-AC), respectively, occurring 3 bp upstream of PAM. The +T insertion has already been reported in tomato variety Ailsa Craig by Uluisik et al. (2016). A +G insertion, two bp

downstream of T insertion site, has also been described by Wang et al. (2019), while no deletions have been reported yet at our target region of the *SlPL*.

3.4.3.1 *SlPL* mutants show increased fruit firmness and lower weight loss while maintaining fruit quality features unchanged

As the world is facing growing challenges, like climate changes, overpopulation and food scarcity (United Nations, Global issues, last consultation in December 2024), improving quality, agronomic, and post-harvest traits in crop species turned into a very important goal in plant breeding. In tomato, preserving fruit firmness during handling and transporting, and improving storage-life for large-retailers distribution, are among the key factors to allow market suitability of the product. While natural ripening mutants, like *rin* and *nor*, have been largely used to develop commercial varieties with higher firmness and extended shelf-life (Wang and Seymour, 2022), targeting cell wall-remodeling enzymes has appeared to be a more effective way to improve post-harvest quality without causing detrimental effects on fruit color and flavor (Uluisik et al., 2016). To get a general indication of taste and overall tomato fruit quality, TSS measurement can be helpful (de Brito et al., 2021) because it indicates the proportion of the major taste determinants in tomato (Balibrea et al., 2006; Kader, 2008). No differences were detected in TSS between the two mutants and Micro-Tom WT fruits, indicating that no alteration in this organoleptic-quality-indicator has occurred, with no pleiotropic effect of the *SlPL* knock-out, nor unwanted events from *in vitro* transformation. Moreover, *SlPL* editing affected neither fruit weight, FSI or pH, proving that CRISPR/Cas9 system can be a precise and valuable method to induce specific mutations without altering non-target sites. Previous authors demonstrated that silencing *SlPL*, in Ailsa Craig through CRISPR/Cas9, and in Micro-Tom by RNAi, can have positive impact on delaying fruit softening (Uluisik et al., 2016; Yang et al., 2017; Wang et al., 2019). Here, we described two *SlPL* mutations induced by CRISPR/Cas9 system in a Micro-Tom background, which affect fruit texture at different ripening stages, maintaining a higher firmness in mutated genotypes even after 10 dph storage. This was paralleled by a reduced level of weight loss in comparison to the WT over a period of 18 d. Similar to pectin, changes in cuticle composition have also an impact on the fruit softening process, reducing water loss and delaying softening (Lara et al., 2019). The cuticle interacts with the cell wall of the outer epidermal layer (Domínguez et al., 2011), and changes in the cell

wall structure might affect its permeability, decreasing transpiration and consequently reducing weight loss.

With respect to external fruit color, the decrease in L* and b* values together with the a* value increase obtained from BR+4 to RR in all genotypes, reflected the darkening of the fruits due to carotenoid biosynthesis, mainly lycopene, and chlorophyll degradation (Ayuso-Yuste et al., 2022). Since the a* index provides redness-greenness values and the b* index indicates the yellowness-blueness component, H* values between 0 and 90 approximates the appearance of red and highest values of a*/b* ratio indicate a more intense red color (Ayuso-Yuste et al., 2022; Durmus and Davis, 2019). Taken together, this information show that PL^{INS} fruits tend to have a more orangish outer pericarp, which may indicate a color change delay in comparison with WT and PL^{DEL}.

3.4.3.2 Knocking out *SlPL* reduce the overall activity of cell wall-remodeling enzymes

The processes of plant cell wall remodeling and reorganization involve many players, ranging from phytohormones (especially ABA and ethylene) to enzymes and ripening-related expansins (Forlani et al., 2019). During plant growth, cell walls continuously change, and the disassembly mechanism peaks during fruit softening. In fleshy fruits, pectin depolymerization occurs (Forlani et al., 2019) and the integrity of the middle lamella is affected, leading to a decrease in cell-to-cell adhesion and thus a reduction in fruit texture (Brummell and Harpster, 2001). Pectins undergo the most relevant changes, being remodeled, disassembled and solubilized by the action of a variety of enzymes, like PGs, PLs, PMEs, β-Gal and EXP (Wang et al., 2018). In the *SlPL* CRISPR mutants, PL alteration caused a decrease in the overall activity of cell wall remodeling enzyme, resulting in firmer fruits and lower weight loss during storage.

PMEs act upstream of PLs and PGs and are necessary for their activity to take place (Barnes and Anderson, 2018). They remove the methyl-ester groups from the HG polygalacturonic acid chains, making them accessible to pectate lyase and polygalacturonase. While the reduction in PGs and β-Gal activity observed in the mutated lines may be explained by the indirect interaction between these two enzymes and PL, which acts on de-methylated pectin chains, fostering a more extensive degradation of HG and RGI (Ortega-Salazar et al., 2024), the decrease in PME activity, which acts before PL, and α-Gal and β-Glu, which prevalently degrade other substrates, might be due to changes in the regulatory process of cell wall

remodeling. Previously published work on silencing of different tomato *PL*s (*Solyc03g111690* and *Solyc06g083580*) by RNAi showed a down-regulation of various cell wall-remodeling genes, including *SlXTH5* (*Solyc07g009380*), *SlTBG4* (*Solyc12g008840*), *SlEXP1* (*Solyc06g051800*) (Ren et al., 2023), and *SlPG* (*Solyc06g060170*) (Yang et al., 2017). Moreover, Yang et al. (2017) reported the up-regulation of *SlPGIP* (*Solyc07g065090*), a polygalacturonase inhibitor encoding gene. The reduction in activity of PL, PME, PG, α-Gal, β-Gal, and β-Glu in PL^{INS} and PL^{DEL} is consistent with the previously reported alteration of cell wall metabolism in *SlPL*-silenced lines. By interpreting these results, we might hypothesize that the PL protein is involved in a feedback mechanism that regulates the expression of a pool of genes, or enzymes, responsible for cell wall-remodeling. PL expression might be necessary to maintain enzyme-encoding genes transcriptionally active and to repress inhibitor protein, like *SlPGIP*. Furthermore, since no alteration in the expression of polygalacturonase-encoding genes *SlPG2a* and *SlPGA3* was detected in the CRISPR-PL lines described by Ortega-Salazar et al. (2024), we infer that *SlPL* mutations obtained through genome editing may be *gain-of-function* mutations and that the muted PL proteins, in case they are produced, may trigger a negative feedback mechanism, causing a reduction in the activity of other enzymes, acting at post-translational level (Goulao et al., 2007). Finally, none of the analyzed enzymes showed a complete inhibition. The residual activity may be due to the expression of paralogous genes, to the activity of different enzymatic isoforms, or to the inability of the mutated PL to totally restrain the catabolic capacity of other enzymes, which is also necessary for the natural development of cells (Barnes and Anderson, 2018).

3.4.3.3 Altering pectin metabolism reduces Micro-Tom susceptibility to different pathogens

The tomato is vulnerable to numerous pathogens that can severely impact crop production. Among these, *B. cinerea* and *P. syringae* are particularly harmful, leading to widespread infections at different stages of the plant growth (El-Fatah et al., 2023, Rhouma et al., 2023). Effective management of these diseases requires a deep understanding of the pathogen life cycles and their interactions with host plants. *P. capsici* is an oomycete pathogen responsible for a range of destructive diseases in vegetable crops such as peppers, cucumbers, squash and tomatoes (Lamour et al., 2012). Although it is not a true fungus, it exhibits many fungal-like traits in terms of infection patterns and lifecycle. The response of tomato plants to pathogen attack is largely determined by their genetic composition, which influences both susceptibility

and resistance (Campos et al., 2021). Pathogenicity assays revealed that the *SlPL* knockout mutants exhibited enhanced resistance to three taxonomically different pathogens at the foliar level.

Reduced susceptibility to grey mold in *SlPL*-silenced lines was previously reported in fruits by Yang et al. (2017) and Ortega-Salazar et al., (2024), but no evidence for effects after foliar infection have been described yet. The enhanced resistance to all the tested pathogens suggests that the loss of PL activity impairs the pathogen's ability to cause infection, potentially by altering cell wall integrity, which reduces the ability of the pathogen to degrade the plant cell wall through pectin degradation, a key process in *B. cinerea* pathogenicity (Silva et al., 2023).

Additionally, the improved resistance of the mutants to *P. capsici* suggests that the knockout of the *SlPL* gene can also confer resistance to oomycete pathogens. The mechanism underlying this resistance could involve altered pectin structure, which may limit the pathogen’s ability to establish infection or to efficiently penetrate plant tissues.

Finally, the higher level of resistance to *P. syringae* pv *tomato*, displayed by both PL^{INS} and PL^{DEL} mutants, may indicate that the disruption of *SlPL* activity possibly leads to a stronger defense response or reduced susceptibility to bacterial colonization.

The results suggest that PL plays a significant role in the susceptibility of Micro-Tom plants to fungal, bacterial, and oomycete pathogens. PL is known to break down pectin in plant cell walls, facilitating the invasion and spread of pathogens (Uluisik and Seymour, 2020). The loss-of-function of *SlPL* likely disrupts this process, resulting in a stronger cell wall that is less prone to pathogen degradation. Likewise, it is possible that knocking out *PL* triggers compensatory defense mechanisms in the plant, including the activation of innate immune responses that contribute to the observed resistance. Additionally, since an overall reduction in the activity of several cell wall-remodeling enzymes in the fruits of PL^{INS} and PL^{DEL} mutants was detected, further investigation of the same enzymes in leaves could provide a more extensive understanding of the mechanisms underlying the plant–pathogen interaction.

3.5 Conclusions

Tomato is a widespread crop that is consumed worldwide. Among the main challenges of the Century, reducing food waste, increasing food security and facing agricultural threats like pathogens, is of utmost importance, with particular relevance for fleshy fruits like tomato.

In-vitro regeneration of Scatolone di Bolsena, Spagnoletta di Gaeta e Formia and Pantano di Ardea traditional varieties can be easily accomplished, whilst for *Agrobacterium*-mediated transformation further studies are needed in order to implement new specific protocols. Besides, new attempts, by either changing protocol or trying different constructs, should be made to edit the promising *SlLOB1* TF.

By knocking out the pectin-degrading-enzyme-encoding gene *SlPL* in Micro-Tom genetic background, a triple effect on fruit texture, pathogen resistance and modulation of cell wall-remodeling enzymes activity, has been achieved. Future directions will include a deeper characterization of the mutant lines by the analysis of *SlPL* transcripts, and possibly the modified SlPL protein, in both leaves and fruits to study the interaction with other enzymes and to clarify its mode of action.

The insights gained from this study will help elucidate the complexity of cell wall-remodeling pathway and guide future breeding efforts to develop tomato varieties that are not only improved in fruit quality but also resistant to biotic stresses, contributing to more sustainable agricultural systems. These results can also serve as a basis for future efforts to improve resistance and fruit quality of other commercially important tomato varieties, including landraces, using similar CRISPR-based approaches.

Meanwhile, the new alleles obtained at the *SlPL* locus can be transferred into landraces of interest by conventional breeding to exploit new variants that act downstream of TFs like NAC-NOR and MADS-RIN, having lower negative impact on fruit quality, and verify if these mutations have a tangible impact on firmness of traditional varieties' flat-ribbed fruits.

3.6 Supplementary material

Supplementary Table S3.1. List of primers used for T_0 screening, sequencing of *SlPL* target region and T7EI enzymatic assay

Amplified region	Primers	Ta
Cas9	F: 5'-TTGAGACACGCCAGATCACC-3' R: 5'-AGAAGCCTCCGGTCTGTACT-3'	63°C
NptII	F: 5'-ACAAGATGGATTGCACGCAGG-3' R: 5'-AACTCGTCAAGAAGGCGATAG-3'	56°C
SlPL target region	5'-GGCACGCAGTGATTCAGACT-3' 5'-ACCCGTAATGCGATGGACTG-3'	55°C
T7EI_PL	5'-TTGGGAGAAAAACCGTCAGC-3' 5'-TCAGCACTTCCACCAATAGCA-3'	62°C

Supplementary Table S3.2. PCR conditions for amplification of target region of *SlPL*

Step	Temperature	Time	Cycles
Initial denaturation	94°C	4 minutes	1
Denaturation	94°C	30 seconds	30
Annealing	55°C	30 seconds	
Extension	72°C	25 seconds	
Final extension	72°C	7 minutes	1

Supplementary Table S3.3. Media composition for the transformation protocol.

Component	Growing Medium*	Co-cultivation Medium*	Induction Medium*	Regeneration Medium*	Rooting Medium*
MS	1x	1x	1x	1x	1x
Sucrose	3%	3%	3%	3%	3%
Plant agar	0.7%	agar 0.7%	agar 0.7%	agar 0.7%	agar 0.7%
2,4 D (mg/L)	-	0.1	0.1	-	-
IAA (mg/L)	-	0.35	0.35	0.35	0.35
IBA (mg/L)	-	-	-	-	0.1
T-Zeatin (mg/L)	-	0.7	0.7	0.7	-
Acetosyringone (200uM)	-	2ml (100mM)	-	-	-
Cefotaxime (mg/L)	-	-	200	-	200
Vancomycin (mg/L)	-	-	50	-	-
Carbenicillin(mg/L)	-	-	-	500	-
Kanamycin (mg/L)	-	-	-	100	50

***** pH 5.8

Supplementary Table S3.4. *SlLOB1* transformation efficiency in Scatolone di Bolsena (SCA), Spagnoletta di Gaeta e Formia and Micro-Tom (MTO) vairieties.

Variety	No. of explants	Calli	Calli %	No. of shoots	Shoots % (shoots/explants)	Rooted shoots	No. of transformed shoots	Transformed shoots % (transf/explants)
SCA	247	7	2.8	21	8	10	9	3.6
SPA	281	-	-	-	-	-	-	-
MTO	166	2	1.2	6	3.6	-	-	-

Supplementary Table S3.5. *SlPL* transformation efficiency in Scatolone di Bolsena (SCA), Spagnoletta di Gaeta e Formia and Micro-Tom (MTO) vairieties.

Variety	No. of explants	Calli	Calli %	No. of shoots	Shoots % (shoots/explants)	Rooted shoots	No. of transformed shoots	Transformed shoots % (transf/explants)
SCA	240	3	1.25	4	1.7	1-	-	-
SPA	237	12	5	13	5.5	-	-	-
MTO	203	43	21	82	40	7	5	2.5

Supplementary Table S3.6. Genotyping of T_0-T_3 transformants by PCR amplification of the target locus, direct sequencing and TIDE chromatogram decomposition. The R^2 value indicates the percentage of variance explained by the model. Overall efficiency is calculated as the difference between R^2 and the amount of wild type allele. Values in the remaining columns indicate the percentage of each predicted allele with $p < 0.05$. Data from representative samples are shown.

Generation	Sample	Overall efficiency	R^2	Alleles			
				WT	Insertion	Deletion	
					+1 bp	-2 bp	-3 bp
T_0	PL1	28.8 %	0.97	75.7 %	7.2 %		11.2 %
	PL7	0.4 %	0.97	96.8 %			
	PL8	1 %	0.97	95.8 %			
	PL9	36.9 %	0.98	61.5 %	36.9 %		
	PL17	48.8 %	0.98	49.3 %	0.8 %	48 %	
T_1	PL1	7.5 %	0.96	88.3 %			7.3 %
	PL7	1.2 %	1	98.4 %	0.9%		
	PL8	1 %	1	98.7 %			
	PL9	8 %	0.95	88.6 %	4 %		
	PL17	22 %	0.94	72.3 %	9.2 %	12.5 %	
T_2	PL17	86.4 %	0.86		42.8 %	42.5 %	
T_3	PL17a	96.4 %	0.97		95.9 %		
	PL17b	97.9 %	0.98			97.2 %	

Supplementary Figure S3.1. Bam file of whole genome re-sequencing of PL^{INS} and PL^{DEL} visualized in IGV_2.18.4. The intragenic off-target region (first intron of Solyc02g088550) with 4 MMs is underlined in red. No modification at the sequence locus have occurred. Data from 5 MMs off-target are not shown.

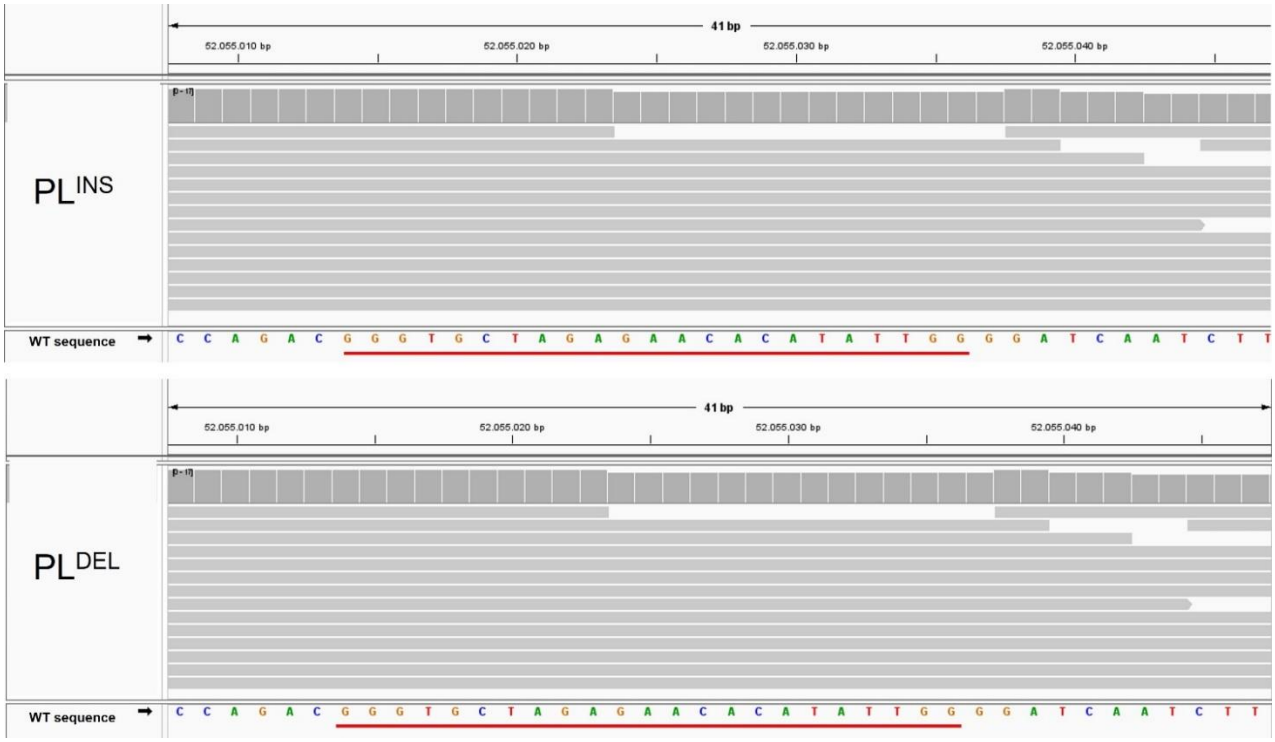

Supplementary Figure S3.2. Alignment of the native and mutated PL proteins. In yellow: isoleucine residue retained by PL^{INS} and lost by PL^{DEL}. Underlined: sequence change caused by the frameshift. In blu: active residues. In green: amino acids responsible for the binding activity. In bold: Interpro domain IPR002022 Pectate lyase/Amb_all.

```
WT          MGTSSVSLLFLLSFLLLLPSLLASSNPQQVVDEVHRSINGSRRNLGYLSCGTGNPIDDCW 60
PL_INS      MGTSSVSLLFLLSFLLLLPSLLASSNPQQVVDEVHRSINGSRRNLGYLSCGTGNPIDDCW 60
PL_DEL      MGTSSVSLLFLLSFLLLLPSLLASSNPQQVVDEVHRSINGSRRNLGYLSCGTGNPIDDCW 60
            ************************************************************

WT          RCDPNWEKNRQRLADCAIGFGKNAIGGRDGKIYVVTDSGDDNAVTPKPGTLRHAVIQTEP 120
PL_INS      RCDPNWEKNRQRLADCAIGFGKNAIGGRDGKIYVVTDSGDDNAVTPKPGTLRHAVIQTEP 120
PL_DEL      RCDPNWEKNRQRLADCAIGFGKNAIGGRDGKIYVVTDSGDDNAVTPKPGTLRHAVIQTEP 120
            ************************************************************

WT          LWIIFARDMVIQLKEELIMNSFKTIDGRGASVHIAGGPCITIQYVTNIIIHGIHIHDCKQ 180
PL_INS      LWIIFARDMVIQLKEELIMNSFKTIDGRGASVHISGWSVYNNTVRNEYYYTRNSYT---- 176
PL_DEL      LWIIFARDMVIQLKEELIMNSFKTIDGRGASVH-SGWSVYNNTVRNEYYYTRNSYT---- 175
            ******************************** :*    .    .:

WT          GGNAMVRSSPSHYGWRTVSDGDGVSIFGGSHVWVDHCSLSNCKDGLIDAIMGSTAITISN 240
PL_INS      ------------------------------------------------------------ 176
PL_DEL      ------------------------------------------------------------ 175

WT          NYMTHHDKVMLLGHSDSYTQDKNMQVTIAFNHFGEGLVQRMPRCRHGYFHVVNNDYTHWE 300
PL_INS      ------------------------------------------------------------ 176
PL_DEL      ------------------------------------------------------------ 175

WT          MYAIGGSADPTINSQGNRFLAPDIRFSKEVTKHEDAPESEWKNWNWRTDGDLMLNGAFFT 360
PL_INS      ------------------------------------------------------------ 176
PL_DEL      ------------------------------------------------------------ 175

WT          RSGVRTGSSSYAKASSLSARPSSLVANLVSSSGALNCKKGSRC   403
PL_INS      ---------------------------------------------   176
PL_DEL      ---------------------------------------------   175
```

Supplementary Figure S3.3. Fruit firmness at BR+4 and BR+7 stages. Significant differences against WT were assessed by Dunnet test (*** $p \leq 0.001$).

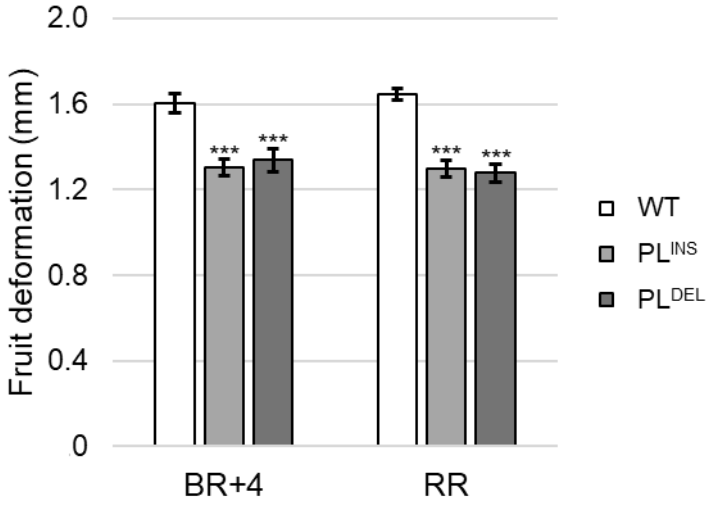

Supplementary Figure S3.4. T7EI endonuclease assay on PL17 and PL9 T_2 plants. Mutated samples display three bands; WT allele results in an undigested band. C-: negative control (non-edited plant); C+: positive control (edited plant).

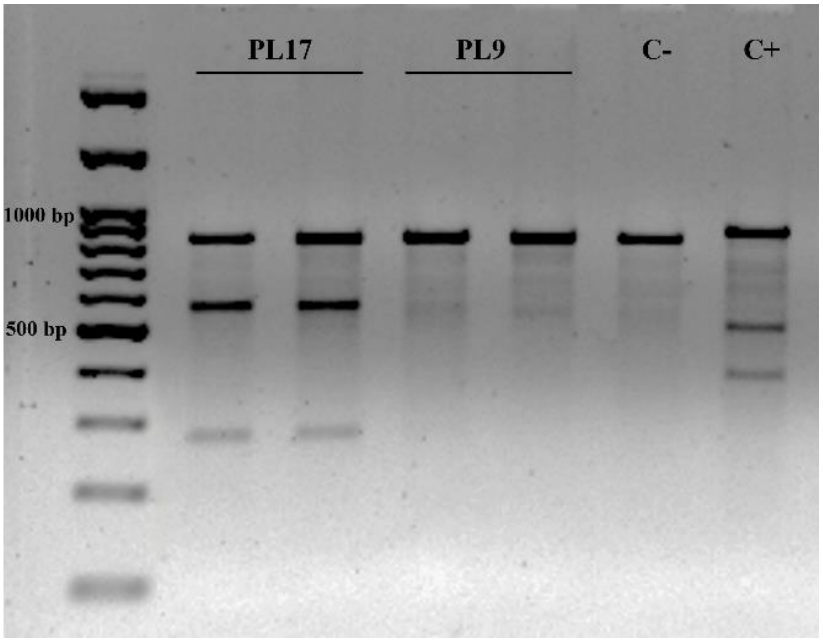

Supplementary Figure S3.5. TIDE *indel* prediction of a representative T_2 plant showing heteroallelic configuration.

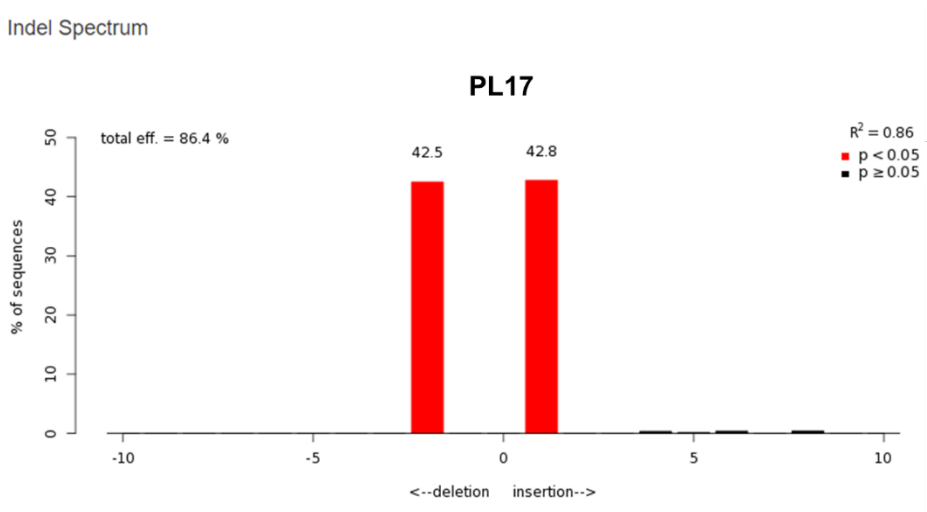

Supplementary Figure S3.6. TIDE *indel* prediction of representative T_3 plants showing homozygous configuration for 1 bp insertion (PL17a) and 2 bp deletion (PL17b).

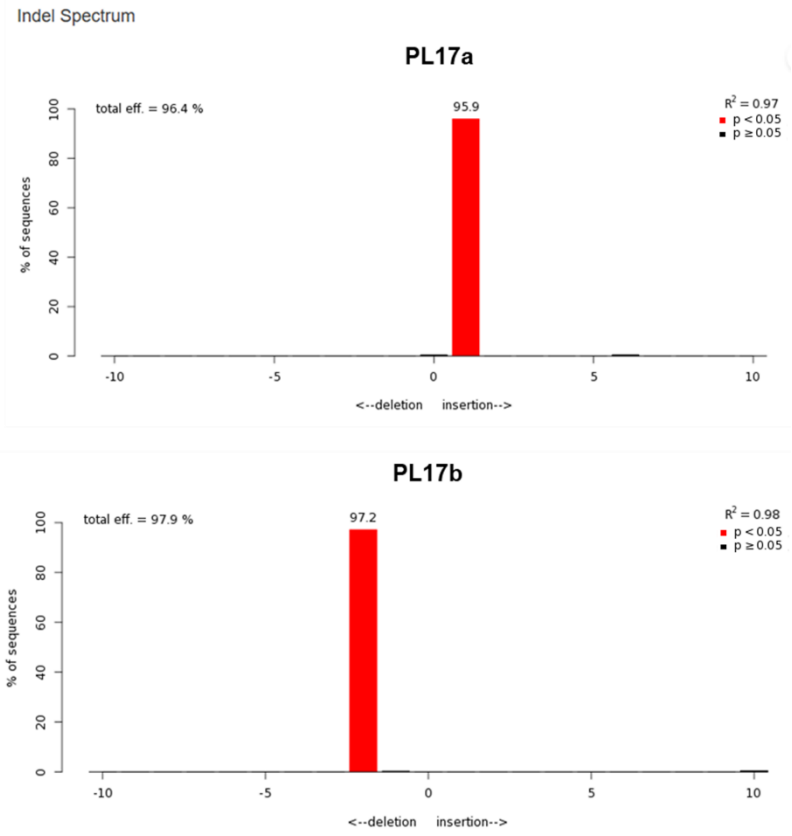

Chapter 4

Genome Wide Association Studies (GWAS) for the identification of QTLs involved in fruit softening

4.1 Introduction

Since its first application in crops genetics back in the 2010s, starting with cereals such as rice (Huang et al., 2010) and maize (Lu et al., 2010), GWAS became more and more popular in the agricultural-genetic field and many studies on a wide range of crops, including soybean (Hwang et al., 2014; Leamy et al., 2017), lettuce (Zhang et al., 2017), cucumber (Zhang et al., 2015), peach (Cao et al., 2016) and cotton (Ma et al., 2018) were published during the last decade.

In tomato, several studies helped decipher the genetics behind agronomic and qualitative traits. Many GWA studies were carried out on different populations and allowed the identification of QTLs and candidate genes for numerous traits like flowering time, plant vigor, plant growth, fruit weight (Bauchet et al., 2017a), growth habit, inflorescence type, fruit locule number, pericarp thickness (Sacco et al., 2015), fruit firmness, TSS content, fruit metabolites and volatile compounds (Ruggieri et al., 2014; Sauvage et al., 2014; Bauchet et al., 2017b; Tieman et al., 2017; Kim et al., 2021).

In this chapter, a GWAS analysis was performed on the HARNESSTOM repository to dissect QTLs that may control the fruit softening process and can thus affect the fruit firmness.

The European Horizon 2020 HARNESSTOM (HARNESSing the value of TOMato genetic resources for now and the future, http://harnesstom.eu/en/index.html) project (Figure 4.1) aims to improve the accessibility and to consolidate the use and the knowledge of tomato genetic resources. It brings together different stakeholders, from academy to private industry and from farmers to consumers, to face the emerging agricultural challenges, to try to overcome

the consequences of climate change and to create an efficient interaction among partners to easily transfer materials, knowledge and skills.

Figure 4.1. HARNESSTOM project logo

To achieve these objectives, HARNESSTOM collected and centralized germplasm and phenotypic/genotypic data of a large number of accessions coming from past EU-funded projects and developed four pre-breeding programs addressing the major challenges of the field: i) introducing resistances against major emerging diseases, ii) improving tomato tolerance to climate change, iii) improving fruit quality and iv) increasing resilience in traditional European tomato by participatory breeding.

Among the activities carried out within the project, the "Tomato Plant and Fruit Phenotyping Training Course", held at the Maritsa Vegetable Crops Research Institute (Plovdiv, Bulgaria), gathered all the academic partners to participate in the phenotyping of the HARNESSTOM repository, in which several qualitative and quantitative traits related to production and fruit quality were collected (i.e. number of fruits, yield, fruit set, inflorescence type, fruit shape, fruit color, fruit firmness, fruit chemical composition etc.). Data collected within the training course will be analyzed in collaboration with other partners, and this chapter will specifically focus on fruit firmness and association analysis on this trait.

4.2 Materials and methods

4.2.1 Plant material and growing conditions

For the HARNESSTOM project, a repository collection (RH) of promising materials coming from previous EU-funded projects was set up. It comprised 234 accessions from different European countries, spanning from traditional varieties to breeding lines, selected for their excellent agronomic performance, the presence of resistance-to-pathogen genes and good fruit quality. The collection includes the control variety Moneymaker. The plants were grown in greenhouse at the Maritsa Vegetable Crops Research Institute (Plovdiv, Bulgaria), in a randomized block design with three blocks and five plants/genotype per block.

4.2.2 Genotyping and phenotyping

The Commercial Tomato PlexSeq™ SNP Panel by AgriPlex Genomics (Cleveland, OH, USA), which contains 1039 SNPs that span across all 12 tomato chromosomes (Chr), was used for the amplicon-based genotyping of the plant material. For the fruit firmness, measurements were taken at three different ripening stages (mature green: MG, turning: TUR and red ripe: RR) on three plants per genotype and two fruits per plant, on two different sides on the equatorial region of the fruit using a portable digital durometer (T.R. Turoni srl, Forlì, Italy). Fruit weight was retrieved from the yield of the third and fourth trusses of three plants per block and fruit shape was assigned according to the following categories: flat, rectangular, ellipsoid, obovoid, round, oxheart, long, heart.

4.2.3 Data analysis

Data were analyzed using the PROC GLM, PROC CORRESP and Duncan's Multiple Range *post-hoc* test ($\alpha = 0.05$) implemented in the SAS software package (v9.4M6, SAS® University Edition, SAS Institute Inc., Cary, NC, USA). A multivariate correspondence analysis was performed between fruit shape and fruit firmness and the results were plotted according to the first two dimensions. The Pearson correlation coefficient between fruit weight and fruit

firmness was calculated in RStudio v4.3.3 (Posit team, 2022) by "*corrplot*" v0.92 R package (Wei and Simko, 2024).

4.2.4 SNP filtering

The filtering of the SNP panel was performed on TASSEL v5 (Bradbury et al., 2007). Missing genotypes were imputed using LD k-nearest neighbor imputation (LD-kNNi) and markers were filtered with a call rate value lower than 95% and for a minor allele frequency (MAF) lower than 5%.

4.2.5 Population structure analysis

The population structure was inferred as described by Tripodi et al. (2021). The analysis was performed on STRUCTURE v.2.3.4 (Pritchard et al., 2000) and to determine the best number of clusters (K) five independent runs for each K (ranging 1-14) were done using 20,000 burn-in cycles followed by 10,000 Monte Carlo-Markov Chain (MCMC) iterations. The most probable numbers of sub-populations were determined according to the Evanno's method (Evanno et al., 2005) using StructureHarvester.py (Earl and VonHoldt, 2012) and once the optimal K was defined, a second run at the best K value with a 150,000 burn-in period and 100,000 MCMC iterations was performed to maximize the accuracy in determining the membership of each accession. According to the best number of sub-populations, a structure matrix (Q matrix) was then generated.

4.2.6 Association analysis

For the association analysis, different models were utilized, and the results were eventually compared. The general linear model (GLM) and the mixed linear model (MLM) were performed in TASSEL v5, whereas the BLINK (Huang M. et al., 2019), farmCPU (Liu X. et al, 2016) and SUPER (Wang Q. et al., 2014) models were implemented in the GAPIT v3.4.0 R package (Wang and Zhang, 2021), performed in RStudio v4.3.3. To minimize effects such as the stratification of the population, the Q matrix, the PCA and the kinship matrix (K matrix),

the latter being estimated using the centered identity by state (IBS) for accounting relationships among individuals, were incorporated in the models. To determine the threshold for significant marker-trait association, the p value required for significance was calculated by Bonferroni correction method, setting alpha = 0.05, according to the following formula:

$$p \text{ value } = \frac{0.05}{No.\ of\ markers}$$

4.2.7 Linkage disequilibrium and confidence intervals

The R^2 statistic was estimated on all the inter-chromosomal SNPs pairwise using Plink v1.09 (Chang et al., 2015) to investigate the linkage disequilibrium (LD) decay in the population. LD threshold was estimated on the 95th percentile of R^2 values, mean R^2 values were computed into 1 Kbp interval and LD decay curves were obtained using the LOWESS non-parametric regression, fitting the distance (Mb) values on the x-axis and R^2 values on the y-axis. Confidence interval regions were defined based on a window size length of intra-chromosomal LD decay and centered around the lead SNP.

4.2.8 Identification of candidate genes

For candidate genes (CGs) identification two strategies have been adopted. First, for the associated markers that fell within an intergenic region the SNPs effect on the protein was predicted by the EnsemblPlants VEP tool (https://plants.ensembl.org/tools.html) and genes with missense variants (no nonsense variants were predicted) were selected. Second, genes falling within the calculated confidence intervals were analyzed on the TomExpress database (http://tomexpress.toulouse.inra.fr/) and genes mainly expressed in fruit were chosen. Genes were retrieved from the SL4.0 tomato genome (https://solgenomics.net/) and ITAG4.1 annotation version.

4.3 Results and discussion

4.3.1 Phenotyping

Among the phenotypic traits recorded on the HARNESSTOM collection, fruit firmness, fruit weight and fruit shape will be hereafter discussed.

For fruit firmness, measurements were performed at three ripening stages (Figure 4.2, Supplementary Figure S4.1). At the MG stage, firmness values ranged from 84.4 to 101.4, with Moneymaker having a durometer index of 96.7. At TUR, the lower value was 44.8 and the highest 87.1, with the control having a value of 74.3. For the RR stage, the softest genotype exhibited a value of 4.1, the firmest of 41.5 and the control of 21.3.

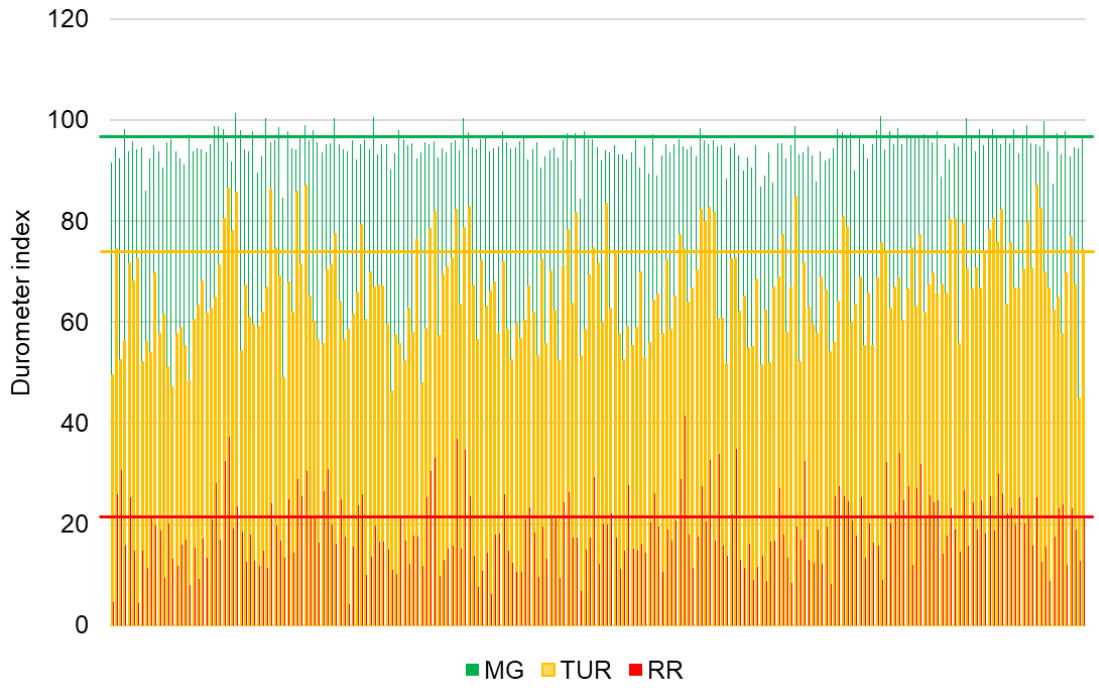

Figure 4.2. Firmness distribution in the HARNESSTOM population at three ripening stages: mature green (MG), turning (TUR) and red ripe (RR). Lines represent firmness values of the control genotype at the three ripening stages.

For fruit weight, most genotypes produced fruits weighing less than 50 g (41%). 36% of the accessions produced fruits from 51 to 100 g and almost 23% of the material had fruits weighing more than 100 g (Figure 4.3).

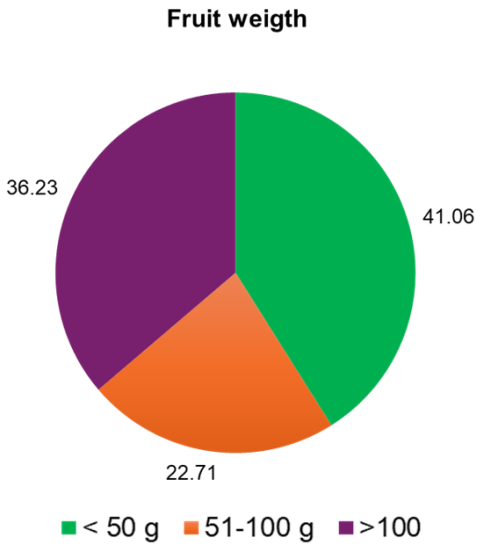

Figure 4.3. Fruit weight distribution in the HARNESSTOM population.

In our population, the Pearson correlation revealed a significant but weak negative correlation between fruit firmness and fruit weight at all three ripening stages (Figure 4.4). At the MG stage, the Pearson coefficient (R) was -0.26, with p = 0.00024; at TUR R was equal to -0.37, with p = 4.476e-08, and at RR, R = -0.34 and p = 6.142e-07. In literature, contrasting information about the correlation between fruit firmness and fruit weight are reported. Chaïb et al. (2007) did not find any correlation between the two traits; Khapte and Jansirani (2014) described a positive correlation, while Solieman et al. (2013) find a negative but not significant correlation between weight and firmness.

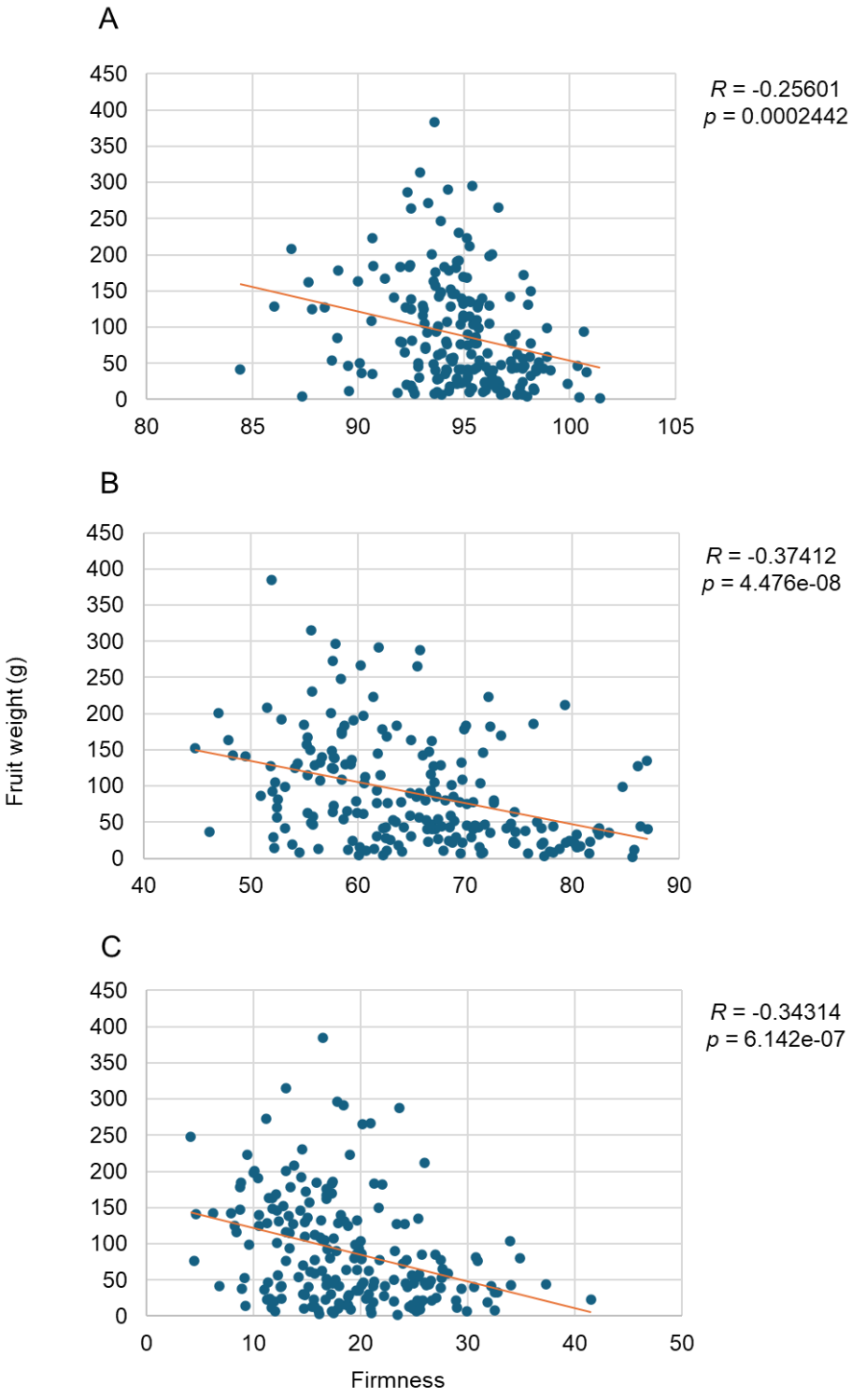

Figure 4.4. Correlation analysis of fruit firmness and fruit weight at mature green (A), turning (B) and red ripe (C) stages. *R*: Pearson correlation coefficient; *p*: statistical significance.

For the fruit shape all eight categories were represented in the population, with the "round" and the "flat" shapes accounting for almost 60% of the genotypes. The "obovoid" shape was present in 8.14% of the accessions; the "ellipsoid", the "oxheart", the "heart" and the "rectangular" types were equally distributed, being present in the 7.69% each for "ellipsoid", "oxheart" and "heart, and in the 6.33%" for rectangular shape. The remaining "long" type accounted for 4.52% of the population (Figure 4.5).

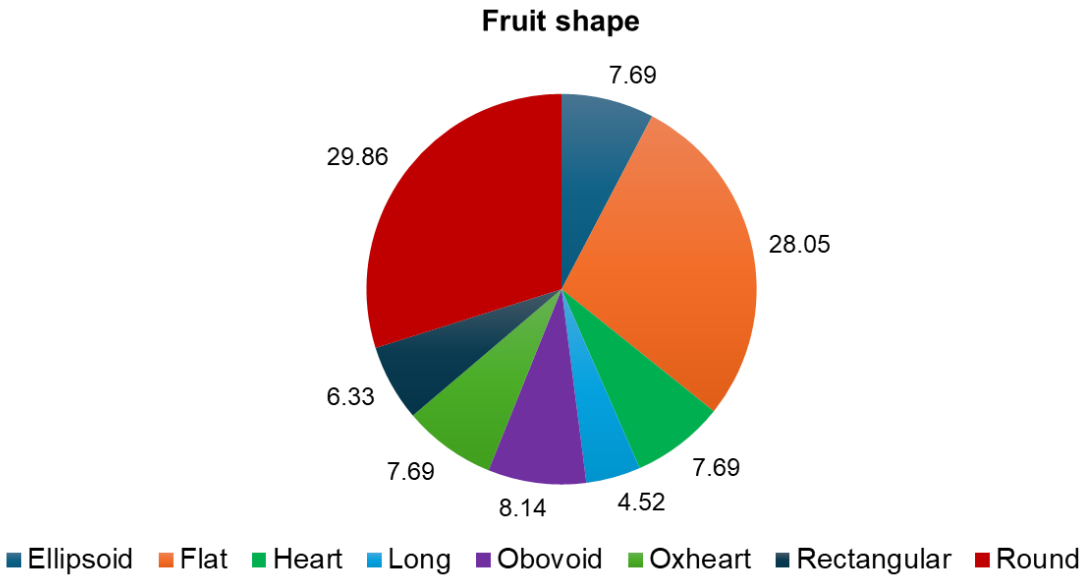

Figure 4.5. Fruit shape distribution in the HARNESSTOM population.

In relation to shape, the firmness trend was consistent among the different ripening stages (Figure 4.6). Ellipsoid, heart-shaped and rectangular fruits were the firmest at MG, TUR and RR. At MG, fruits belonging to "oxheart" and "long" categories were the one with lowest firmness values; similarly, at TUR stage, the same categories plus the "flat" types showed the lowest indexes. At the RR stage "flat", "oxheart", "obovoid", "long" and "round" shapes grouped all together, being significantly less firm then the other three categories.

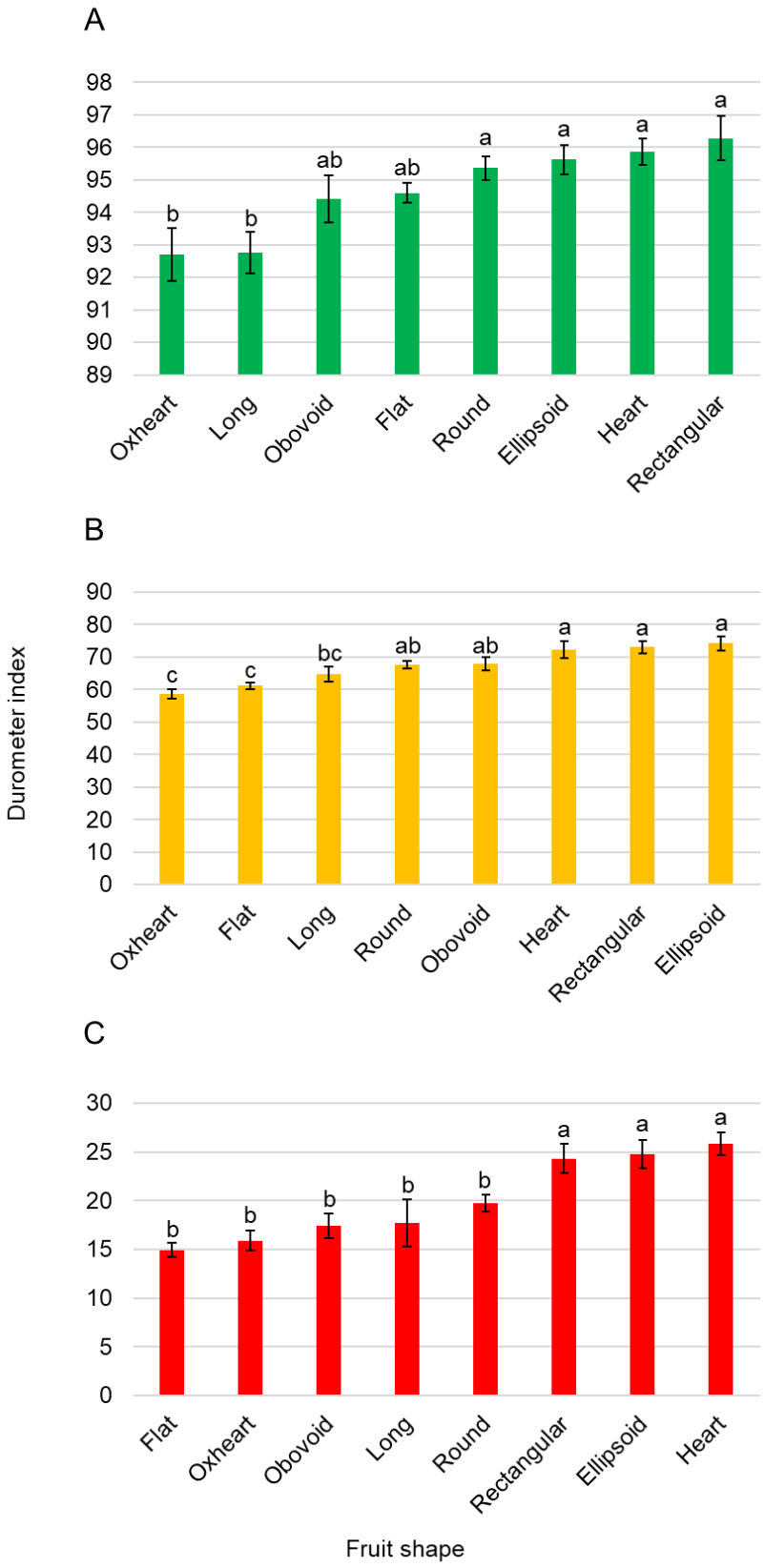

Figure 4.6. Fruit firmness in relation to fruit shape, at mature green (A), turning (B) and red ripe (C) stages. Letters indicate significant difference among the samples calculated by Duncan *post hoc* test (α = 0.05). Data are expressed as mean ± standard error.

To confirm the relationship between fruit firmness and fruit shape at the RR stage, a correspondence analysis was performed (Figure 4.7). To include the numerical variables in the correspondence analysis procedures, firmness was categorized into four classes, based on the quartile distribution (Q1, Q2, Q3 and Q4), with Q1 comprising the lowest values and Q4 the highest. As shown in the Figure 4.7, the firmer shapes are the "ellipsoid", the "heart" and the "rectangular", which clustered together within the Q4 class. The long and round-shaped fruits clustered along within the Q3 class, the "obovoid" type with Q2 and the oxheart and flat categories within the lowest firmness class Q1.

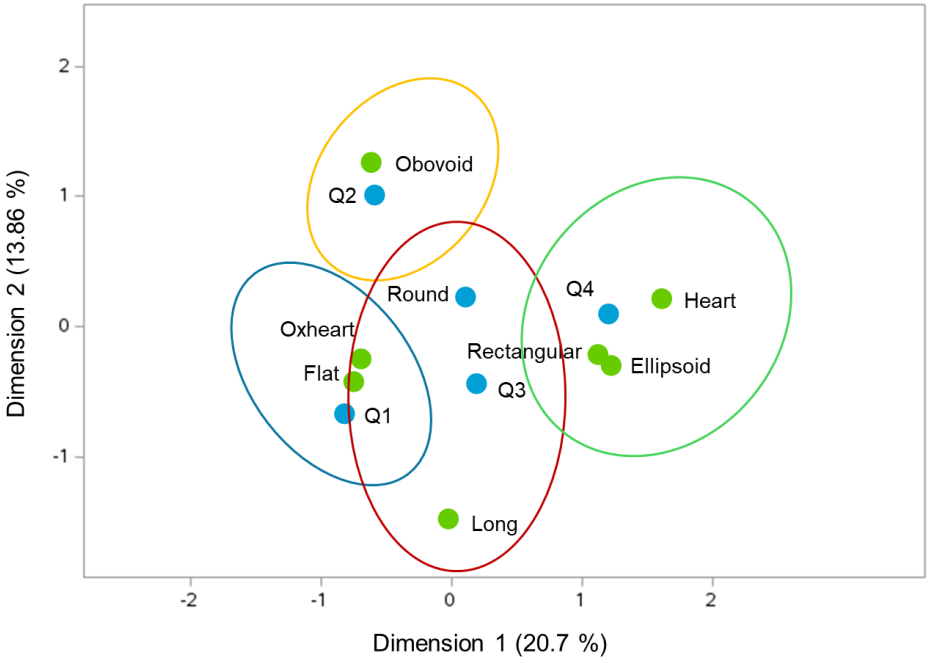

Figure 4.7. Correspondence analysis of fruit firmness (Q1-Q4) and fruit shape variables.

4.3.2 Population structure

After the dataset of 1039 SNPs was filtered, a total of 550 homozygous markers were used in the subsequent STRUCTURE analysis. Based on the Evanno ΔK method, the analysis showed K=3 as the most likely number of sub-populations (Supplementary Table S4.1) and accessions were considered to belong to a specific group if its membership coefficient (qi) was ≥ 0.90. Genotypes with qi lower than 0.90 at each K were considered as admixed. Most of the genotypes (144) belonged to the latter category, while 54 genotypes grouped in K=1, just two in K=2 and 35 in K=3 (Figure 4.8). Most of the accessions (69%) clustering in K= 1 had

firmness values at RR higher than 20, whereas the majority of the K=3 accessions (91%) had firmness values lower than 20. With respect to fruit shape, most of the K=1 genotypes had "round" shape (29%), "flat" shape (16%) and "heart" and "ellipsoid" shapes (12%), followed by minor percentage of the remaining shape categories. In K=3, the flat-shaped fruits were predominant (53%), followed by "oxheart" (21%) and "obovoid" (18%). Only two genotypes had "round" and "ellipsoid" shapes, and no "rectangular", "heart" and "long" types were present in the cluster. Based on the fruit weight, 72% of the K=1 genotypes had fruits ≤ 50 g, 12% up to 100 g and 16% ≥100 g. In the K=3 group, there were no genotypes with fruits weighing less than 50 g, and the 12.5% and 87.5% exhibited 51-100 g and ≥100 g fruits, respectively.

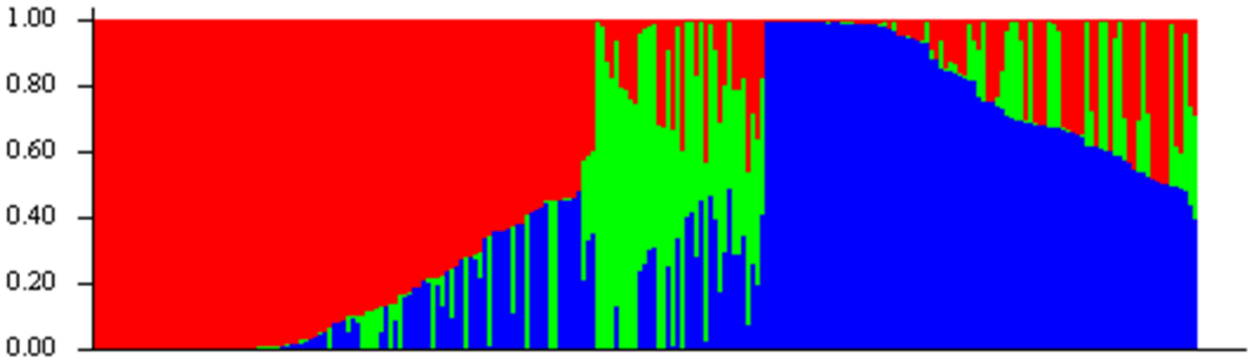

Figure 4.8. Genetic structure of the HARNESSTOM collection. Accessions were inferred to cluster in three ancestral populations (red, green and blue). Each bar represents a genotype, which is partitioned into color segments based on the estimated membership to each K cluster.

Large and mixed populations are the most suitable genetic material to conduct GWAS in tomato (Hall et al., 2010; Chen, 2013), therefore an association analysis was performed on the HARNESSTOM collection.

4.3.3 Linkage disequilibrium and association analysis

The extent of LD was examined within each Chr. The R^2 values were plotted against the genetic distance, and curves of LD decay were fitted using locally weighted scatterplot smoothing (LOWESS) (Cleveland, W. S., 1979). A R^2 baseline value of 0.20 was estimated using the 95th percentile method, being in line with what Sim et al. (2012) reported. The distance of LD decay ranged from 0.17 Mb on Chr07 to 0.79 Mb on Chr8, with an average value of 0.42 Mb (Supplementary Table S4.2).

The association analysis was performed using different models. The GLM and the MLM were performed in TASSEL; the BLINK, the farmCPU and the SUPER models were performed in RStudio, as implemented in the GAPIT v3.4.0 package. For all models, structure covariates (Q matrix and PCA) as fixed effects, and genetic relatedness (kinship matrix) as random effect, were considered in different combinations (in Supplementary Table S4.3 are reported the combinations that gave significant associations). The analyses considering the GLM+Q and GLM+Q+PCA approach detected a total of 56 and 12 associations, respectively, for all MG, TUR and RR firmness traits. From the MLM+Q+K and MLM+Q+PCA+K, only two significant associations (one for each, at TUR and RR stages, respectively) were detected. BLINK+Q, farmCPU+Q and SUPER+Q, returned six, nine and eight associations, respectively, for TUR and RR stages.

To choose the associated markers to focus on, a first screening choosing markers represented in at least two models (Table 4.1), also considering their fitness by checking the QQ plots to avoid false-positive and false-negative associations, was performed. Secondly, to determine significant marker-trait association, the significant *p* value threshold was calculated by Bonferroni correction method and markers with *p* value < 9.97E-05 in at least one model, were selected. After applying these screening methods a total of 13 associated SNPs were maintained (Supplementary Table S4.4): one for the MG stage, eight for TUR and four for RR stages. Manhattan and QQ plots for each model/matrix combination are reported in Supplementary Figure S4.2 A-D.

Table 4.1. Associated markers in at least two models. X represents the model that gave association for that specific marker.

Chromosome and position (SL4.0)		Marker	Ripening stage	Model						
				GLM +Q	GLM +Q, PCA	MLM +Q, K	MLM +Q, PCA, K	BLINK +Q	farmCPU +Q	SUPER +Q
Chr01	315590	solcap_snp_sl_15051	TUR	**X**					**X**	
Chr01	3070555	solcap_snp_sl_15000	RR	**X**				**X**		
Chr01	88561886	solcap_snp_sl_13404	RR	**X**	**X**				**X**	**X**
Chr03	56363131	solcap_snp_sl_7939	TUR	**X**					**X**	
Chr04	59706268	UFTLP1_1898	TUR	**X**					**X**	**X**
Chr05	59470745	solcap_snp_sl_22572	TUR	**X**				**X**	**X**	
Chr06	40466450	UFTLP1_2001	MG	**X**	**X**					
Chr07	63252547	UFTLP2_240	TUR	**X**					**X**	
Chr08	49736	solcap_snp_sl_7232	RR		**X**				**X**	
Chr10	4054660	solcap_snp_sl_9598	TUR	**X**				**X**	**X**	**X**
Chr10	48519186	SL4.0ch10.48519186	TUR	**X**	**X**	**X**		**X**		**X**
Chr10	54728653	solcap_snp_sl_5191	TUR	**X**						**X**
Chr12	611723	solcap_snp_sl_3159	RR	**X**	**X**		**X**	**X**		

To identify CGs associated with the firmness trait (Table 4.2), two strategies were followed. The first aimed to look for the associated makers that fell within an intragenic region and check if the SNP influenced the respective protein. Out of 13 associated markers, five fell in intergenic regions or UTRs (solcap_snp_sl_15000, solcap_snp_sl_7939, UFTLP1_1898, solcap_snp_sl_22572, SL4.0ch10.48519186), two fell within intronic regions (UFTLP1_2001, UFTLP2_240) and six in coding sequence (CDS) regions (solcap_snp_sl_15051, solcap_snp_sl_13404, solcap_snp_sl_7232, solcap_snp_sl_9598, solcap_snp_sl_5191, solcap_snp_sl_3159). Among these latter, that were analyzed on VEP tool, four of the corresponding SNP produced a synonymous variant, while for solcap_snp_sl_9598 and solcap_snp_sl_3159, the SNPs were responsible for missense variants that causes a shift from serine (S) to asparagine (N) and from aspartate (D) to asparagine (N), respectively. The S to N change occurs in the open reading frame of *Solyc10g011960*, a heavy metal-associated isoprenylated plant protein, and the D to N change occurs in the 7th exon of *Solyc12g005980*, a WLM domain-containing protein/PUB domain-containing protein, both expressed in fruit (Supplementary Figure S4.3).

The second approach was based on confidence intervals. The confidence region for each significant SNP was defined as a window size defined by the SNPs with an R^2 higher than the inter-chromosomal linkage disequilibrium (LD) at the 95th percentile (R^2 baseline value > 0.2002) and the confidence interval regions were defined based on the window size length (bp) of intra-chromosomal LD decay and centered around the lead SNP. Genes mapping within the boundaries defined by the intra-chromosomal LD were analyzed in TomExpress and the ones that were mainly expressed in fruit were considered (Figure 4.9), for a total of 23 identified potential CGs.

Even if 13 significant associations were detected by the GWAS, after screening the dataset for CGs, only in the LD blocks of 11 markers (one for MG, seven for TUR and three for RR) were found potential candidates.

Table 4.2. List of candidate genes (CGs) proposed for each associated marker. References refer to gene involvement in the ripening/softening processes.

Chr	Position (SL4.0)	Marker	Ripening stage	Associated QTLs	Associated CGs	Distance from marker (bp)	Annotation	References
Chr01	3070555	solcap_snp_sl_15000	RR		*Solyc01g008710*	368,226	Mannan endo-1,4-beta-mannosidase	*Schröder et al. (2009)*
Chr01	88561886	solcap_snp_sl_13404	TUR		*Solyc01g109110*	68,106	Extra-large guanine nucleotide-binding protein 2	*Agarwal et al. (2009)* *Lawson et al. (2020)*
					Solyc01g108470	453,254	Carboxypeptidase	*Mattoo, K. (1996)* *Mehta and Mattoo (1996)*
					Solyc01g108770	274,208	Methylesterase 3 isoform .1	
					Solyc01g108780	245,044	Methylketone synthase 1a	*Khuat et al. (2019)* *Urrutia et al. (2021)*
					Solyc01g108880	189,823	2-oxoglutarate (2OG) and Fe(II)-dependent oxygenase superfamily protein	*Szymanski et al., (2017)* *Wei et al. (2021)*
Chr03	56363131	solcap_snp_sl_7939	TUR	*firm3.1* *(Diouf et al., 2018)*	*Solyc03g111010*	247,033	Glyceraldehyde-3-phosphate dehydrogenase	*Luo et al. (2020)* *Zhao et al. (2024)*
					Solyc03g111550	199,033	GDSL esterase/lipase	*Segerson, N. A. (2018)*
					Solyc03g111690	389,732	Pectate Lyase	*Uluisik and Seymour (2020).*
					Solyc03g111720	426,595	Peptide methionine sulfoxide reductase	*Gao et al. (2018)* *Zhou et al. (2024)*
Chr04	59706268	UFTLP1_1898	TUR		*Solyc04g076850*	43,920	Transcriptional repressor of auxin signaling	*Zia et al. (2018)* *Saito et al. (2011)*
Chr05	59470745	solcap_snp_sl_22572	TUR		*Solyc05g050230*	191,477	Ubiquitin-conjugating enzyme	*Wang et al. (2014)* *Miricescu et al. (2018)* *Li et al. (2022c)*
Chr06	40466450	UFTLP1_2001	MG		*Solyc06g069120*	68,616	BnaA05g33450D protein	
Chr07	63252547	UFTLP2_240	TUR		*Solyc07g055020*	169,928	F-box protein	*Deng et al., Guo et al. (2018)* *Su et al. (2022)*
Chr08	49736	solcap_snp_sl_7232	RR		*Solyc08g005630*	457,797	Long-chain-alcohol oxidase	*Yeats et al. (2010)* *Sützl et al. (2019)* *Hattery, T. (2022)*
					Solyc08g005770	567,335	Alcohol acyl transferase	*Cao et al. (2021)* *Fang et al. (2023)*
					Solyc08g005800	589,012	Pectin acetylesterase	*Wu et al. (2021)*

Table 4.2. (continued)

Chr	Position (SL4.0)	Marker	Ripening stage	Associated QTLs	Associated CGs	Distance from marker (bp)	Annotation	References
Chr10	4054660	solcap_snp_sl_9598	TUR		*Solyc10g011960*	0	Heavy metal-associated isoprenylated plant protein	-
Chr10	54728653	solcap_snp_sl_5191	TUR		*Solyc10g054560*	71,025	V-type proton ATPase proteolipid subunit	-
					Solyc10g054670	30,403	Unknown protein	-
Chr12	611723	solcap_snp_sl_3159	RR		*Solyc12g005860*	103,577	Aconitate hydratase	*Liu et al. (2022)*
					Solyc12g005980	0	WLM domain-containing protein/PUB domain-containing protein	-
					Solyc12g006470	351,352	Gamma aminobutyrate transaminase isoform 2	*Gramazio et al. (2020)* *Pan et al. (2023)* *Yan et al. (2024)*
					Solyc12g006540	445,403	Signal peptidase I	*Margossian et al. (1988)*
					Solyc12g006560	459,654	Early nodulin-93	*Franssen et al. (1992)* *Küster et al. (1995)*

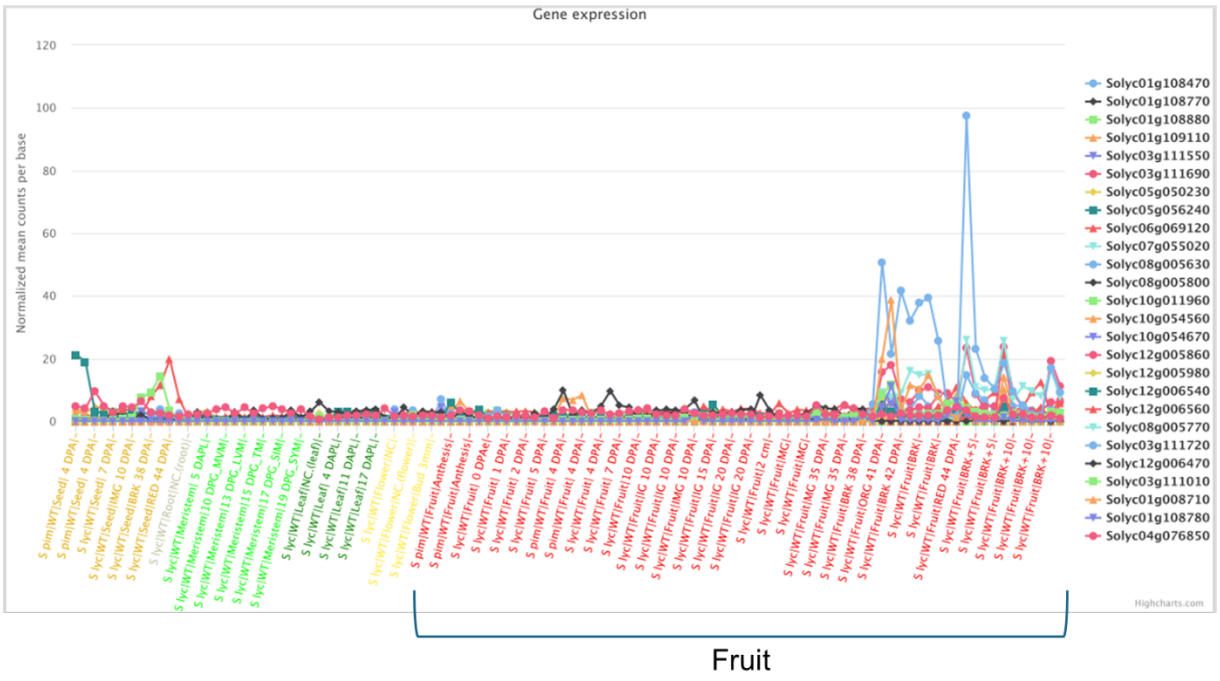

Figure 4.9. Expression of candidate genes mainly expressed in fruit.

On Chr01, *Solyc01g008710*, encoding for a mannan endo-1,4-beta-mannosidase was associated with firmness at the RR stage (solcap_snp_sl_15000). Endo-β-mannanases are hydrolytic enzymes that cleave the mannan backbone of hemicellulose, thus being involved in cell wall-remodeling (Schröder et al., 2009). For TUR stage, five CGs associated to solcap_snp_sl_13404: *Solyc01g109110*, *Solyc01g108470*, *Solyc01g108770*, *Solyc01g108780* and *Solyc01g108880*, encoding for an extra-large guanine nucleotide-binding protein 2, a carboxypeptidase, a methylesterase 3 isoform.1, a methylketone synthase 1a and a 2-oxoglutarate (2OG) and Fe(II)-dependent oxygenase (2ODDs) superfamily protein, respectively, were identified.

Rabs proteins, which contain guanine nucleotide binding domains, play a vital role in several plant physiological processes including fruit ripening, regulating hormone signaling (Agarwal et al., 2009; Lawson et al., 2020); carboxypeptidases expressed during ripening have been describe in tomato (Mattoo, K., 1996; Mehta and Mattoo, 1996); 2ODDs, that have a role in the biosynthesis of different hormones, such as gibberellins and ethylene, showed high expression levels during fruit development after the breaker stage in tomato (Szymanski et al., 2017; Wei et al., 2021).

Arabidopsis methylesterases have shown to have a methyl jasmonate esterase activity (Yang et al., 2008). As *Solyc01g108770* is annotated as methyl jasmonate esterase in the ITAG3.2

version and the respective protein shared high percentage of identity with methyl jasmonate esterases from different *Solanaceae* species on blastp (https://blast.ncbi.nlm.nih.gov/), the role of this enzymes in fruit ripening has been investigate in the literature. Two papers describe how methyl jasmonate application delays cell wall degradation in raspberries (Shah et al., 2025) and accelerates the fruits ripening process in strawberry (Han et al., 2019).

Methylketone synthases are involved in the biosynthesis of methylketones, volatile compounds involved in plant defense but also responsible for fruit fragrance and flavor that have been found to be up-regulated during ripening in strawberry (Khuat et al., 2019; Urrutia et al., 2021). As a correlation between volatile compounds and fruit firmness has been reported in cantaloupe (Beaulieu and Lancaster, 2007) and banana (Zhu et al., 2010), the methylketone synthase 1a is here proposed as a candidate gene (CG).

On Chr03, four genes (Solyc03g111010, Solyc03g111550, Solyc03g111690, and Solyc03g111720) associated with the solcap_snp_sl_7939 at the TUR stage have been chosen as CGs. While a QTL for fruit firmness has already been reported in this region by Diouf et al. (2018), none of the cited genes were described by the authors.

Solyc03g111010 encodes for a glyceraldehyde-3-phosphate dehydrogenase (GAPDH). Even if the clear role of GAPDH in fruit ripening has not been elucidated yet, an alteration of the expression of *Solyc03g111010* has been reported in tomato mutant for the ripening-related *SlMYC2* gene (Zhao et al., 2024) and in Luo et al. (2020) work, two GAPDHs acted as negative regulators of strawberry ripening.

Solyc03g111550 encodes for a GDSL esterase/lipase, which is involved in cutin polymerization and deposition in the cuticular layer (Girard et al., 2012; Segerson N. A., 2018). Since plant cuticle functions as a barrier to water loss (Goodwin and Jenks, 2005), the gene has been considered a potential candidate. *Solyc03g111690* (*SlPL*), has been discussed in Chapter 3 and is not surprisingly correlated with fruit firmness. It encodes for a pectate lyase and has been considered a confirmation of the goodness of the GWAS analysis.

The *Solyc03g111720* peptide methionine sulfoxide reductase-encoding gene was the one with highest expression level according to TomExpress. It showed a differential expression between *nor-like1* mutant and wild type fruits at the breaker +3 stage (Gao et al., 2018) and was listed among “maturation regulator” genes by Zhou et al. (2024).

On Chr04, Chr05, Chr06 and Chr07, one CG for each associated marker (UFTLP1_1898-TUR, solcap_snp_sl_22572-TUR, UFTLP1_200-MG and UFTLP2_240-TUR) was kept. *Solyc04g076850* is a transcriptional repressor of auxin signaling (Aux/IAA9) residing at the *entire* locus. While Mazzucato et al. (2015) did not find any differences for firmness in *iaa* mutant plants, Saito et al. (2011) described different pericarp thickness, indicating that the disruption of the *IAA9* gene influenced the pericarp development, and Zia et al. (2018) described a significantly reduced ethylene production during fruit ripening in *SlAUX/IAA9* knockout mutants.

A ubiquitin-conjugating enzyme is encoded by *Solyc05g050230.* Ubiquitination controls many essential aspects of plant development, both vegetative and reproductive, including the fruit-ripening process (Miricescu et al., 2018) and ubiquitin-conjugating enzyme roles in ripening have been described in both tomato (Wang et al., 2014) and strawberry (Li et al., 2022c). *Solyc06g069120* encodes for a BnaA05g33450D protein, but its function is still unknown and *Solyc07g055020* encodes for a F-box protein, which belong to a class of proteins that participate in plants response to phytohormones and ethylene signaling (Deng et al., 2018; Guo et al., 2018; Su et al., 2022).

On Chr08, the function of three genes associated with solcap_snp_sl_7232 at RR stage (*Solyc08g005630*, *Solyc08g005770*, *Solyc08g005800*) has been investigated in the literature. The first encodes for a long-chain-alcohol oxidase, which belongs to the GMC oxidoreductase family (Sützl et al., 2019). This class of enzymes has been associated with variation in cuticular wax accumulation in maize (Hattery T., 2022) and furthermore, a tomato GMC oxidoreductase -encoding gene has been found to have high similarity to the *Arabidopsis* protein HOTHEAD (HTH), which is involved in cuticle biosynthesis (Yeats et al., 2010).
The second gene is an alcohol acyl-transferase, that plays a major role in volatile ester synthesis in tomato fruits and whose expression was reduced in the *nor* mutant (Cao et al., 2021; Fang et al., 2023). The last one is a pectin acetylesterase encoding gene and in apple, the pectin acetylesterase gene *MdPAE10* was found to contribute to prolonged fruit shelf-life (Wu et al., 2021).

On Chr10, *Solyc10g054560* and *Solyc10g054670* are associated to solcap_snp_sl_5191 at TUR stage. They encode for a V-type proton ATPase proteolipid subunit and an unknown protein, respectively. On Chr12, four genes (*Solyc12g005860*, *Solyc12g006470*, *Solyc12g006540*, *Solyc12g006560*) associated with solcap_snp_sl_3159 at RR have been selected. The first one

is an aconitate hydratase, the second encodes for a gamma aminobutyrate transaminase isoform 2, the third is a signal peptidase I and the last one produces an early nodulin-93.

An aconitate hydratase was reported to be differentially expressed during *Lycium barbarum* L. fruit softening (Liu et al., 2022). The gamma aminobutyrate transaminase isoform 2 is involved in the γ-aminobutyric acid (GABA) pathway. GABA plays important roles in different developmental processes, including fruit ripening (Gramazio et al., 2020). Treatment with this acid has shown to delay fruit softening of kiwifruits (Yan et al., 2024), and a lower expression of *Solyc12g006470* at pink and RR stages has been observed in cherry tomatoes (Pan et al., 2023). Lastly, a peptidase signal cleavage site was predicted in an ethylene-responsive inhibitor (ERI) (Margossian et al., 1988) and early nodulins have been postulated to have roles in cell structure, due to their potential localization in the cell wall (Franssen et al., 1992; Küster et al., 1995).

Several QTLs for firmness have been reported by various authors (Diouf et al., 2018; Kim et al., 2021; Pons et al., 2022, 2023). Among the QTLs described by Fulton et al. (1997, 2000) *fir1.1*, *fir1.2*, *fir4.1*, *fir6.1* and *fir10.1* might overlap with the QTLs described in this chapter. Based on the associated-markers position, *firm1.1* and *fir1.2* are 6 Mbp and 10.2 Mbp away from solcap_snp_sl_13404; *fir4.1* is 5.9 Mbp from UFTLP1_1898, *fir6.1* is 6.3 Mbp from UFTLP1_2001 and *fir10.1* is 4.2 Mbp away from solcap_snp_sl_5191.

However, we could identify associations on new chromosomic regions and propose new candidate genes that might affect different stages of tomato fruit ripening.

4.4 Conclusions

Looking for genetic variability and finding new genic/allelic variants is of pivotal importance to develop improved and resilient varieties. Studies on large populations, performed by association analysis, and more specifically by GWAS approaches, can be suitable systems to identify new genes and QTLs that can be useful to breeders.

The analyses described in this chapter allowed to identify significant associations in previously reported genomic regions as well as new candidates for ripening and softening-related processes, which can be potentially useful for fruit firmness and shelf-life improvement. Indeed, 11 QTLs comprising 25 potential CGs for fruit softening and ripening have been described on Chr01, Chr03, Chr04, Chr05, Chr06, Chr07, Chr08, Chr10 and Chr12.

Further analysis will be required to validate the actual roles of the proposed genes in the tomato ripening process. Once more solid information becomes available, it may be of interest to screen the HARNESSTOM population for variants in these genes to develop a germplasm collection of firmness-related genetic resources for use in tomato breeding.

4.5 Supplementary materials

Supplementary table S4.1. Estimation of the best number of clusters (K) by the Evanno ΔK method.

# K	Reps	Mean LnP(K)	Stdev LnP(K)	Ln'(K)	|Ln''(K)|	Delta K
1	5	-64278.8	0.9633	NA	NA	NA
2	5	-58045.1	6.6013	6233.68	1285.7	194.765
3	5	-53097.1	12.943	4947.98	5358.26	413.9906
4	5	-53507.4	4810.253	-410.28	4007.58	0.833133
5	5	-49910.1	329.4378	3597.3	1964.58	5.963433
6	5	-48277.4	322.6397	1632.72	470.48	1.458221
7	5	-47115.1	135.1964	1162.24	196.88	1.456251
8	5	-46149.8	294.9076	965.36	518.54	1.758313
9	5	-45702.9	344.5274	446.82	1789.9	5.195232
10	5	-47046	5902.171	-1343.08	4804.02	0.813941
11	5	-53193.1	20615.59	-6147.1	16213.66	0.786476
12	5	-43126.6	284.6618	10066.56	9216.06	32.37548
13	5	-42276.1	170.1554	850.5	323.26	1.899793
14	5	-41748.8	106.2901	527.24	NA	NA

Supplementary Table S4.2. Distance of LD decay.

Chromosome	bp
Chr01	458,490
Chr03	665,044
Chr04	550,312
Chr05	204,778
Chr06	302,776
Chr07	175,073
Chr08	794,932
Chr10	228,309
Chr12	480,401
Mean	482,902

Supplementary table 4.3. Different combinations of models and covariates variables (Q matrix, PCA)/kinship matrix (K) utilized for the association analysis.

Model	Covariates/Kinship matrixes
GLM	Q
GLM	Q + PCA
MLM	Q + K
MLM	Q + K + PCA
BLINK	Q
farmCPU	Q
SUPER	Q

Supplementary Table S4.4. Final set of markers associated to fruit firmness. The lowest *p* value given for any marker is reported.

Chr	Position (SL4.0)	Marker	*p* value	Reference/alternative allele
Chr01	315590	solcap_snp_sl_15051	4.03E-07	G/A
Chr01	3070555	solcap_snp_sl_15000	2.70E-07	C/A
Chr01	88561886	solcap_snp_sl_13404	1.72E-05	G/T
Chr03	56363131	solcap_snp_sl_7939	4.03E-07	T/C
Chr04	59706268	UFTLP1_1898	4.03E-07	T/C
Chr05	59470745	solcap_snp_sl_22572	4.03E-07	T/C
Chr06	40466450	UFTLP1_2001	8.13E-05	G/T
Chr07	63252547	UFTLP2_240	4.03E-07	G/A
Chr08	49736	solcap_snp_sl_7232	4.40E-05	T/C
Chr10	4054660	solcap_snp_sl_9598	4.03E-05	T/C
Chr10	48519186	SL4.0ch10.48519186	4.58E-07	G/T
Chr10	54728653	solcap_snp_sl_5191	8.69E-06	C/G
Chr12	611723	solcap_snp_sl_3159	2.70E-05	C/T

Supplementary Figure S4.1. Frequency distribution of firmness at mature green (MG), turning (TUR) and red ripe (RR) stages.

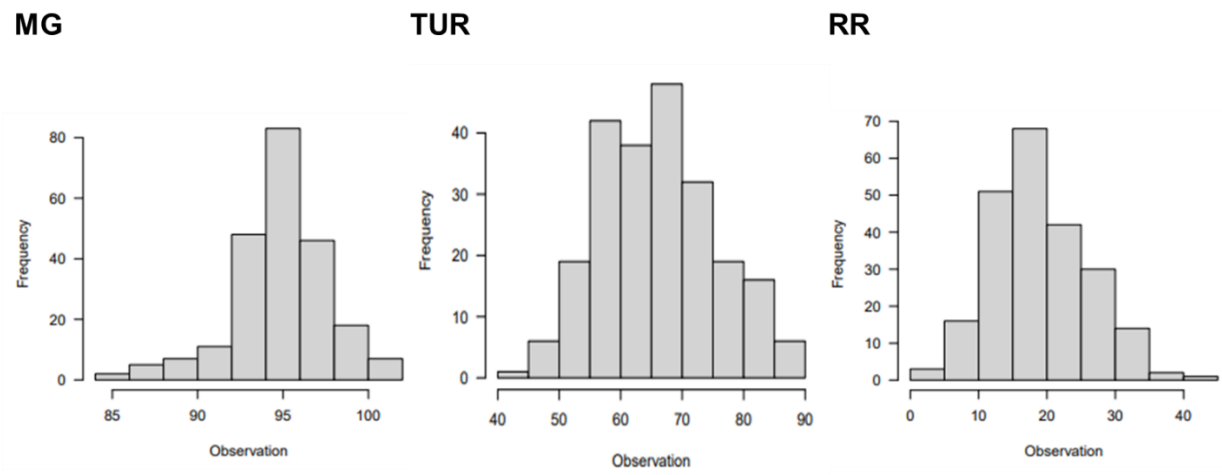

Supplementary Figure S4.2. Manhattan plot and QQ plot for the different model/matrix combinations: GLM+Q (A), GLM+Q+PCA (B), MLM+Q+K/+PCA (C) and BLINK, farmCPU, SUPER +Q (D), . Only the ripening stages for which a significant association was detected are reported.

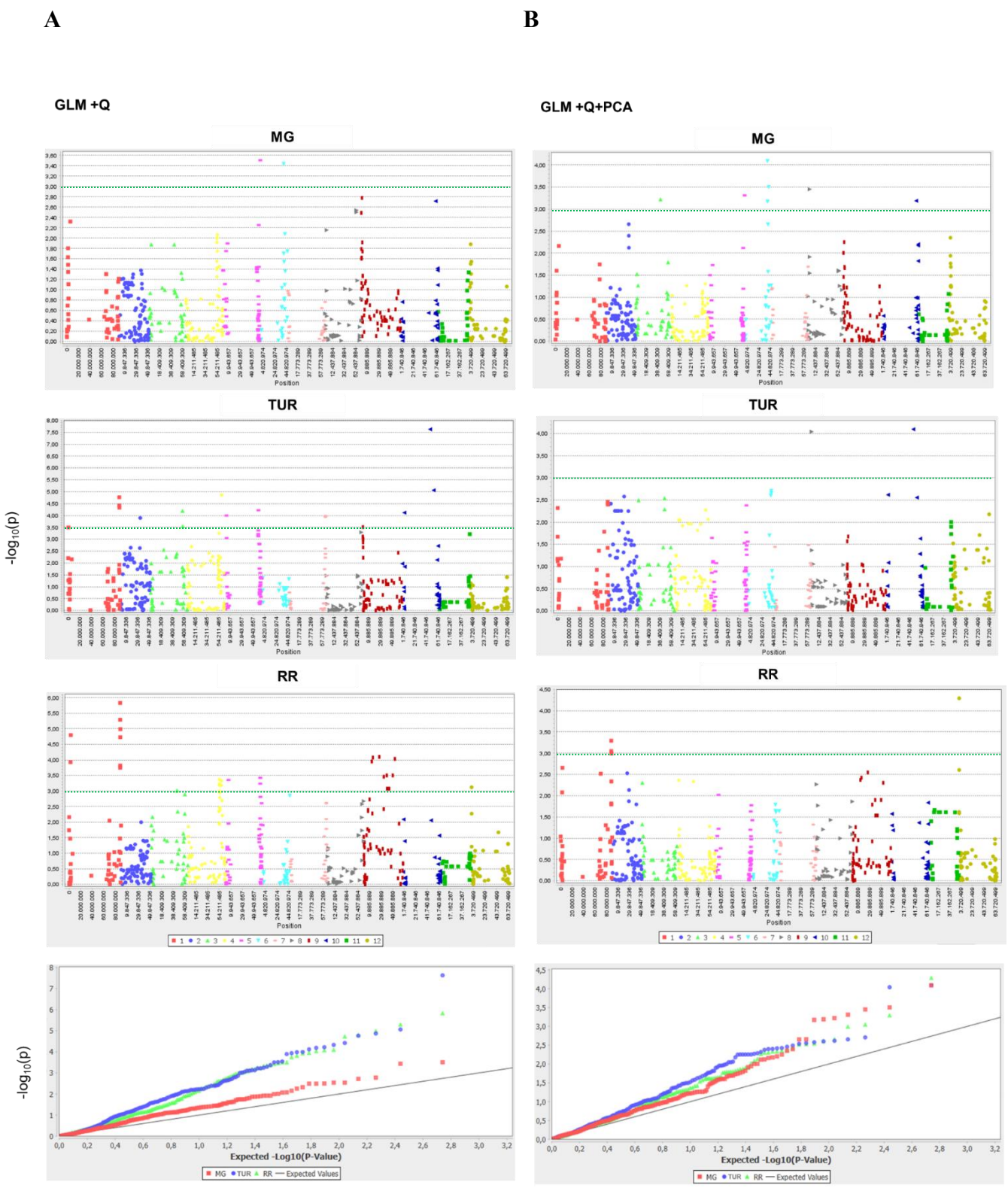

C

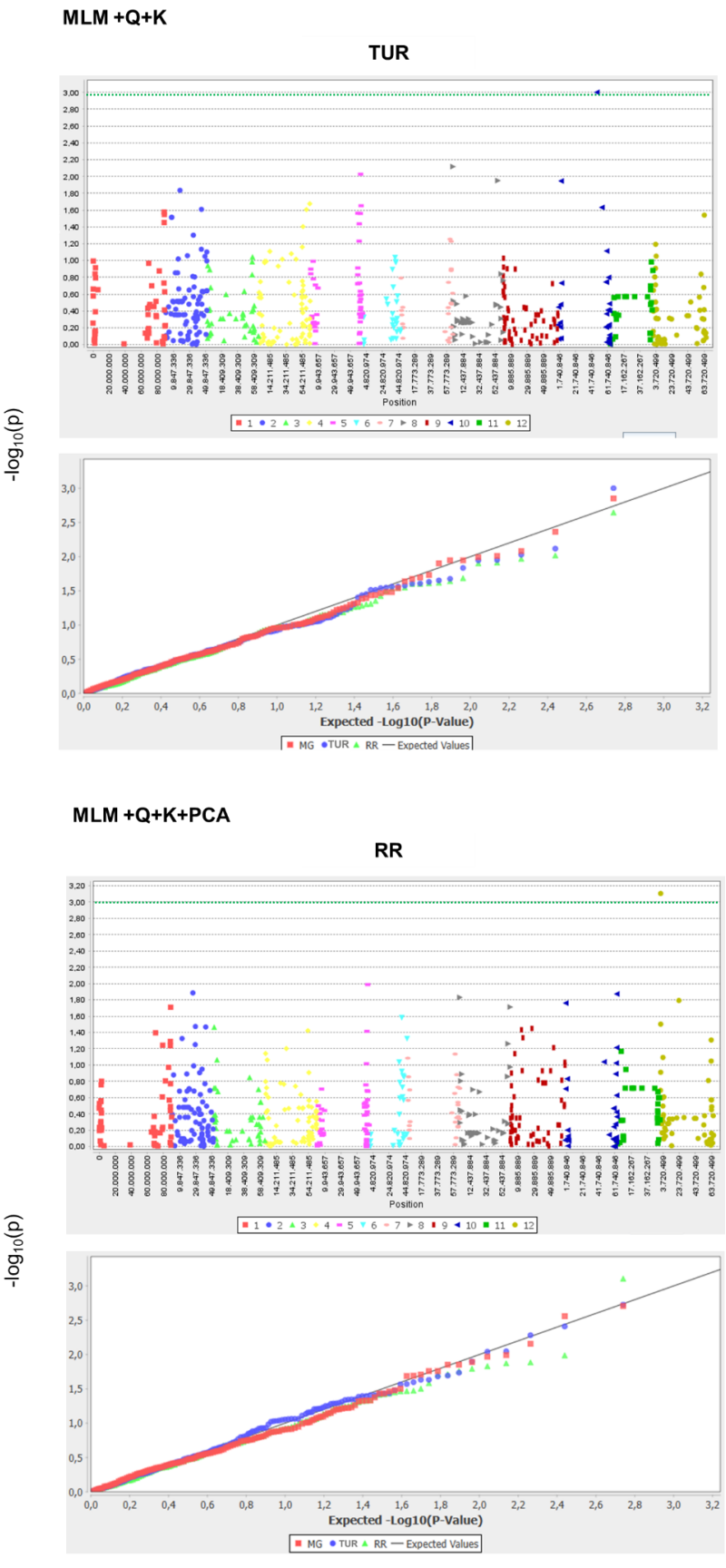
MLM +Q+K
TUR
-log10(p)
Position
Expected -Log10(P-Value)
MG TUR RR Expected Values
MLM +Q+K+PCA
RR
-log10(p)
Position
Expected -Log10(P-Value)
MG TUR RR Expected Values

D

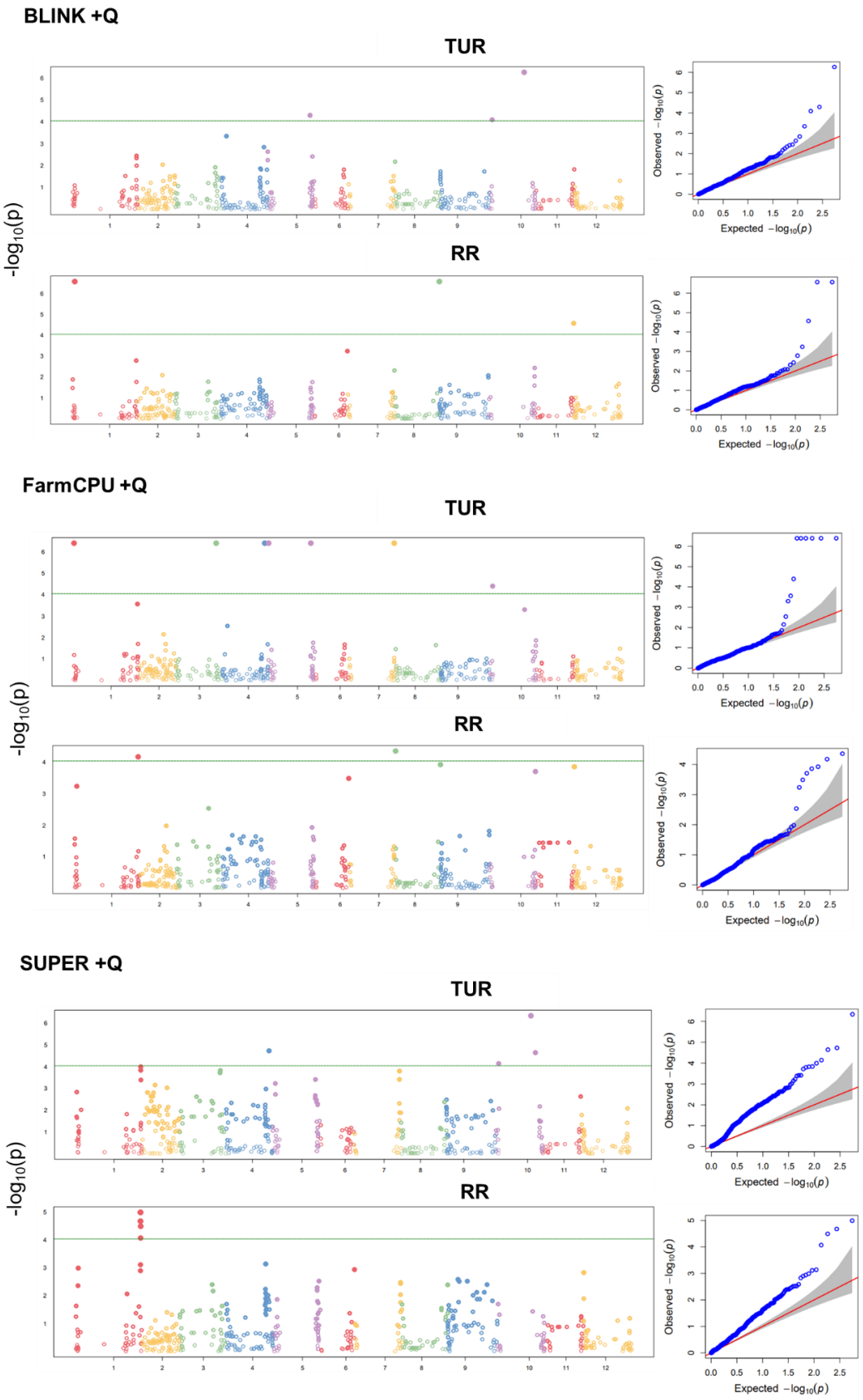
BLINK +Q
TUR
RR
FarmCPU +Q
TUR
RR
SUPER +Q
TUR
RR
-log10(p)
Observed −log10(p)
Expected −log10(p)

Supplementary Figure S4.3. Expression pattern of *Solyc10g011960* and *Solyc12g005980* candidate genes.

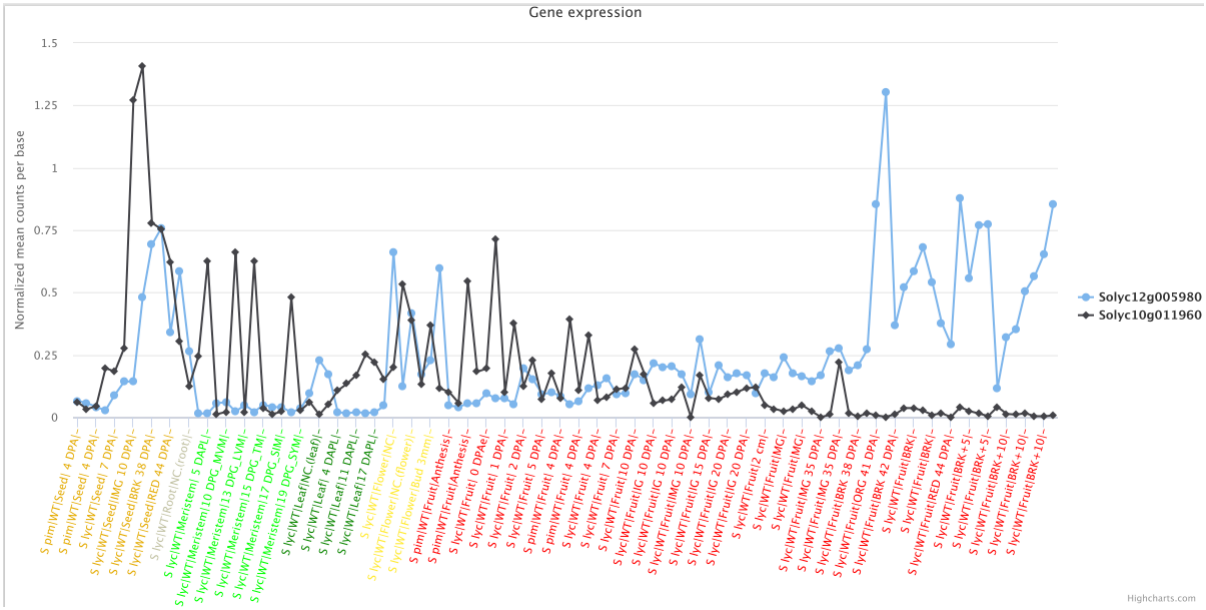

Chapter 5

Participatory selection within the HARNESSTOM project

5.1 Introduction

Among the four pre-breeding programs developed in the HARNESSTOM project, one had the objective of increasing resilience in traditional European tomato by participatory breeding. Recently, an increasing interest in Citizen Science and participatory breeding has bloomed globally. In Europe, 399 projects, involving 333 organizations, arose during the past years (https://eu-citizen.science/). Citizen Science refers to activities intended to engage the general public in scientific research (Vohland et al., 2021). It involves scientific institutions, authorities, politicians and people in all the research steps, from designing the experiment to the collection and the analysis of data.

As the EU's attention in Citizen Science is growing, several activities were included in the HARNESSTOM project and were developed in a dedicated work package: a Citizen Science *stricto sensu* experiment, the agronomic/commercial evaluation of plant material by farmers, the implementation of a survey about consumer preferences (Casals et al., 2024), the sensory evaluation of selected genotypes, and a participatory breeding initiative (Figure 5.1).

Figure 5.1. HARNESSTOM Citizen Science and participatory activities.

As defined by FAO, participatory plant breeding (PPB) is "crop breeding with farmers working firsthand to improve crops and develop resilient plant varieties in collaboration with researchers, scientists and other stakeholders" (FAO "International Treaty on Plant Genetic Resources for Food and Agriculture"). PPB is based on the principle that farmers know better what they need, so "they set breeding goals based on their local environments, conditions, tastes and cultures and then they can judge a variety's success in their own fields", enhancing crop diversity for local needs.

Generally, in a full PPB program, three breeding stages are included: the "creation" of genetic variability; the selection of desirable gene combinations; and the final testing of these combinations (Ashby, 2009). However, involving people in all stages might not be feasible, and that's why a more rapid and cost-effective form of PPB has emerged: the participatory varietal selection (PVS) (Witcombe et al., 1996). In PVS, farmers only collaborate in the final stages of the program (Ceccarelli and Grando, 2022), evaluating the material that was previously obtained by breeders and researchers.

Within the HARNESSTOM project, a "participatory selection" strategy was realized in Italy and Spain. Starting from an F_2 population and ending with F_5 material, 14 fields were implemented, and 138 evaluations were collected over a period of four years, in both countries, leading to the selection of 20 yellow and orange-fruited breeding lines.

Here after, the Italian experiment will be discussed.

5.2 Materials and methods

5.2.1 Plant material

To develop two composite populations with yellow and orange fruits, genotypes differing for alleles responsible for flesh and skin color (Supplementary Table S5.1) were crossed in different combinations (Figure 5.2 A-B) and the F_2 progenies for each color were mixed to obtain the starting material. As control, the yellow "Tomate beef" (TRVA0940), a Spanish landrace from the Core collection of the Traditom project (Pons et al., 2023), the "Santy Yellow" F_1 hybrid by Enza Zaden, the orange "DZ56" breeding line from the Traditom project, and the "Santy Naranja" F_1 hybrid (Enza Zaden) were used (Figure 5.2 C-F).

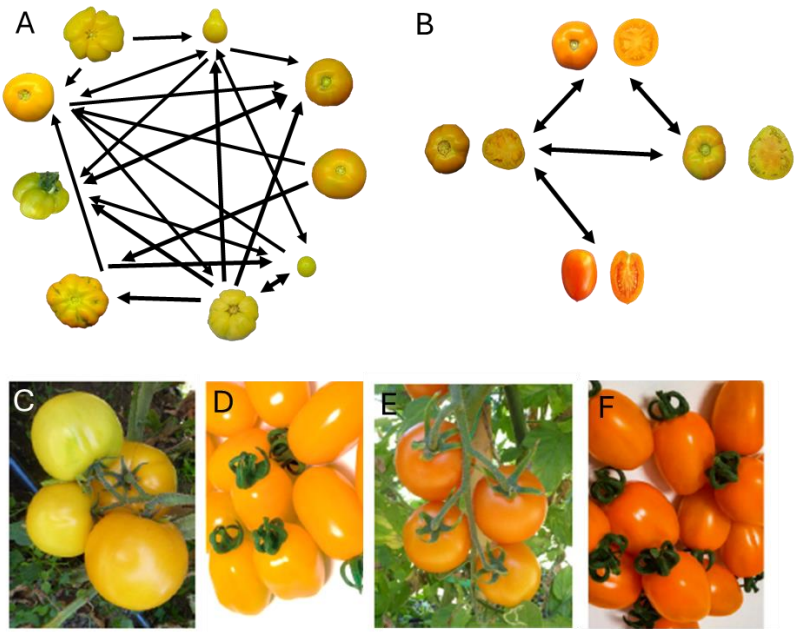

Figure 5.2. Representation of crosses carried out to develop the **(A)** yellow and the **(B)** orange population, and control genotypes: **(C)** TRVA0940, **(D)** Santy yellow, **(E)** DZ56 and **(F)** Santy naranja.

5.2.2 Growing conditions and experimental design

Plants were grown under organic farming methods. During the experimental years 2021-2023, two separate fields, one for each population, were implemented. For the last year of the

experiment (2024), a single field, comprising the best F_5 selected lines of both populations and from both Italy and Spain, was set up. Plants were cultivated following a plant-row arrangement according to a pedigree selection scheme. In 2021, 271 and 289 F_2 plants were grown in the yellow and orange fields, respectively. In 2022 and 2023, 12 plants for each progeny of the best ten plants selected were planted in rows, interspersed with single control plants (Supplementary Figure S5.1 A). In 2024, the experimental design followed a randomized block format with two replicates and six plants per plot, for a total of 12 plants for each selected line and the controls (Supplementary Figure S5.1 B). All the experiments were performed on farms from the Viterbo Province.

5.2.3 Breeding scheme

The utilized breeding scheme followed the pedigree selection method. From 2021 to 2023 (F_2 to F_4 generation), a single-plant selection was performed. Based on the participant evaluation, seed was collected from the best 20 plants for each field. For the last year (F_5 generation in 2024), the top five lines from each population and country were compared and evaluated following a “parcel-evaluation” system, with regard to the high intra-family homogeneity. In Figure 5.3, the breeding scheme is summarized.

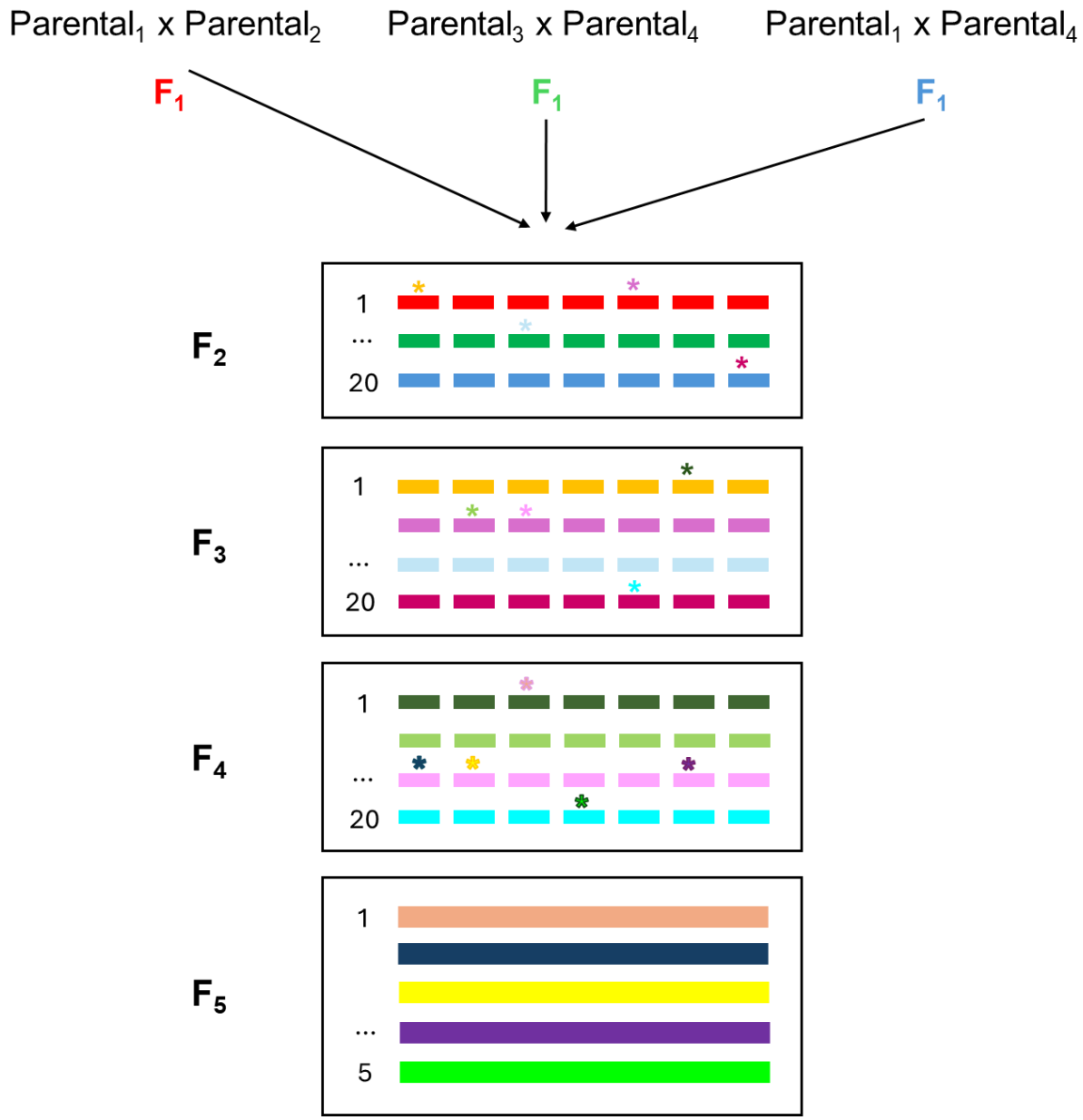

Figure 5.3. Pedigree selection method carried out in the yellow and orange populations. Seeds were collected from the best 20 plants (*) of the F_2, $F_3$and F_4 fields, and their progeny was grown and evaluated at single-plant level. The progeny (F_5) of the best five plants of the F_4 field (❋) was evaluated at parcel-level.

5.2.4 Participatory evaluation and selection

Different stakeholders (mainly farmers, but also consumers, technicians and researchers) were invited to participate in the experiment. To facilitate the evaluation process, each plant was labelled with increasing numbers from 1 to *n*, and evaluators were asked to give a single score, based on the plant general appearance, from 1 to 4 (1, scarce; 2, sufficient; 3, good; 4, excellent). The participatory selection was carried out in the fields at the ripening of the second truss and all the participants signed informed consent and data privacy documentations (ethical approval for the involvement of human subjects in this study was granted by the Research Ethics Committee of the Polytechnic University of Valencia - Reference number P10_16_11_20). To select the best material to be grown the following year, a ranking based on mean values and standard deviation of the assigned score for each plant was created, excluding the controls from the final list.

5.2.5 Data collection for the phenotypic characterization of the two populations

In addition to the score assigned by the evaluators, for every generation and on a single-plant basis, the qualitative and quantitative traits reported in Table 5.1 were recorded. For ordinal variables, data were grouped in different classes according to the values recorded for each trait.

Table 5.1. Qualitative and quantitative traits recorded on a single-plant basis for each generation.

	Trait	Categories
Qualitative traits	Plant growth habit	*Determinate* *Semideterminate* *Indeterminate*
	Inflorescence type	*Uniparous* *Fishbone* *Forked* *Irregular* *Compound*
	Green shoulder	*Uniform* *Light green* *Medium green* *Dark green*
	Fruit shape	*Flat* *Rectangular* *Ellipsoid* *Obovoid* *Round* *Oxheart* *Long* *Heart* *Long rectangular*
	Fruit color	*Yellow* *Orange* *Pink* *Red* *Purple* *Brown* *Green* *Sherry* *Non ripening*
	Flowering date	
Quantitative traits	Fruit weight	Of three representative fruits
	Fruit set	At the first three trusses
	Yield	Estimated on the first three trusses

Furthermore, on fruits of the selected plants, additional traits were eventually recorded, such as total soluble solids content (TSS) and firmness. Firmness was measured on three ripe fruits per selected plant on two different sides on the equatorial region of the fruit using a portable digital durometer (T.R. Turoni srl, Forlì, Italy). For the firmness data analysis, fruits were classified according to their size, in small (0-50 g), medium (51-100 g) and big (>100 g).

5.2.6 Data analysis

All data, except for firmness, were expressed as the frequency of values for each class. Because of the unbalanced number of samples, for the comparison of firmness values among generations, the Kruskal-Wallis test followed by the Dunn's *post hoc* test, implemented on the FSA R package (Ogle et al., 2024) in RStudio v4.3.3 (Posit team, 2022) was performed. Results were expressed as mean ± standard error and differences were considered significant at $p \leq 0.05$.

5.3 Results and discussion

5.3.1 Participatory selection on the "yellow" population

The starting F_2 population for the yellow field was obtained mixing the same quantity of F_2 seeds coming from ten different crosses (Table 5.2).

Table 5.2. Crosses that originated the F_2 yellow population.

F_1 Code	**Parent 1**		**Parent 2**		**Fixed or Segregating loci**
	Code	**Name**	**Code**	**Name**	
251F	V710108	Taxi	V710123	Golden Jubilee	rr
252F	V710108	Taxi	V711097	White Beauty	rr Y/y
254F	V711257	Bell pepper	V710123	Golden Jubilee	R/r
257F	V711104	Sherry color	V711257	Bell pepper	Sh/sh (yellow)
260F	V710049	Campanella	V710108	Taxi	rr
261F	V710108	Taxi	V710049	Campanella	rr
264F	V711259	Invernale	V710108	Taxi	R/r
265F	V711097	White Beauty	V710049	Campanella	rr Y/y
268F	V711097	White Beauty	V710123	Golden Jubilee	rr Y/y
273F	V710124	Golden Boston	V711259	Invernale	R/r

The progenies differed for two mutations causing the yellow flesh. One was a loss-of-function mutation in the phytoene synthase 1 (*PSY*-1) encoding gene at the *R* locus (Ray et al., 1992). The enzyme acts upstream of the carotenoid biosynthetic pathway and catalyzes the condensation of two molecules of geranylgeranyl diphosphate in phytoene (Dono et al., 2020). Its mutation causes the inhibition of carotenoid biosynthesis, resulting in very low levels of lycopene in the flesh (Kachanovsky et al., 2012). The other is the *sherry* (*sh*) mutation, which is not allelic to *r* and produces fruits that are tinged with red (Zscheile and Lesley, 1967). The progenies were also differing for the *y* allele, which is responsible for colorless fruit skin

(Lindstrom, 1925). The *y* mutation occurs in *SlMYB12*, causing the deficiency of the naringenin chalcone, the flavonoid behind the yellow color of the tomato peel (Adato et al., 2009).

The characterization of the different traits was carried out on single-plant level. For qualitative traits, inflorescence type (uniparous, fishbone, forked, irregular, compound), green shoulder (uniform, light green, medium green, dark green), growth habit (determinate, semideterminate, indeterminate) and fruit shape (flat, rectangular, ellipsoid, obovoid, round, oxheart, long, heart, long rectangular) were assessed. For quantitative traits, earliness of flowering, expressed in days (d), was calculated by the difference between the transplanting day and the opening of the first flower. Fruit weight and number of fruits on the first three trusses were recorded and the yield was subsequently calculated.

5.3.1.1 Qualitative traits

For the categorical variable "inflorescence type" (Figure 5.4), low variability was present since the starting of the experiment. In the starting population 79% of the plants exhibited a uniparous inflorescence, followed by a 16% having a forked inflorescence and a 4% and 1% showing the fishbone and compound types, respectively. During the four years of experimentation the fishbone and the uniparous types-selection were favored, but the fishbone eventually disappeared from the final F_5 population. None of the plants at any year of selection possessed an irregular inflorescence type.

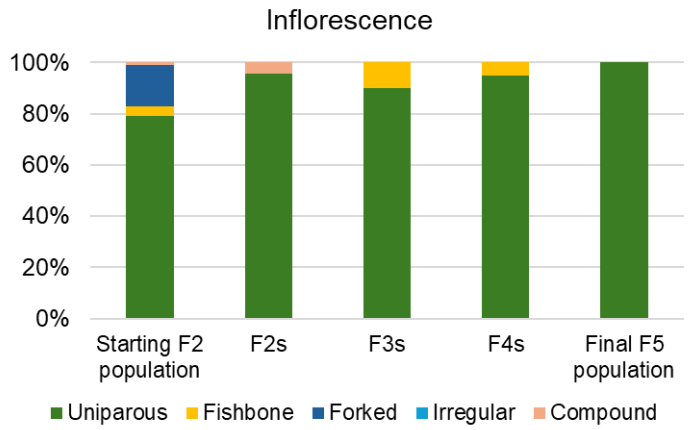

Figure 5.4. Dynamic of the inflorescence type trait under participatory selection from the original F_2 yellow population to the final F_5 population. F_2s, F_3s, F_4s: selected plants for each generation.

The composition of the yellow population for the green shoulder trait (Figure 5.5) was quite stable starting from the F_2 population (F_2p) to the selected plants of the F_2, F_3 and F_4 generations (F_2s, F_3s, F_4s), in which all the categories are represented, with the medium green being the prevalent one in the F_2 starting population, the F_2s and the F_3s. From the F_4s, the dark green shoulder became the most abundant one, being present in the 80% of the F_5 families, whereas the remaining 20% did not exhibited the green shoulder (uniform).

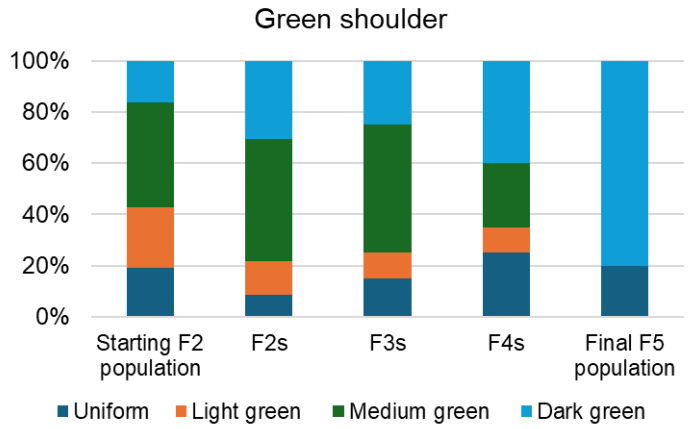

Figure 5.5. Dynamic of the green shoulder trait under participatory selection from the original F_2 yellow population to the final F_5 population. F_2s, F_3s, F_4s: selected plants for each generation.

As for the inflorescence type, the growth habit (Figure 5.6) variability was low. The indeterminate habitus was the main type in the F_2p, the F_2s and the F_3s and the only one to be selected at the end of the experiment. The 18% of the F_2p plants had a determinate growth habit and a 4% showed a semideterminate habitus. In the F_2s the determinate type was reduced to 4% and the semideterminate disappeared, appearing again in the 37% of the F_3s plants.

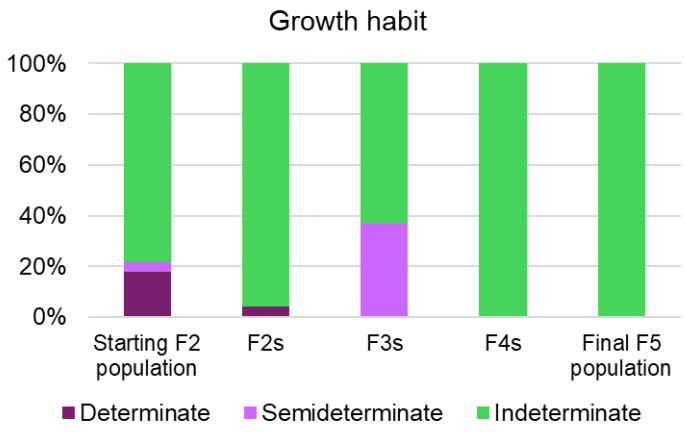

Figure 5.6. Dynamic of the growth habit trait under participatory selection from the original F_2 yellow population to the final F_5 population. F_2s, F_3s, F_4s: selected plants for each generation.

The fruit shape trait (Figure 5.7 A) was the one with the highest variability, because of the higher number of categories utilized to describe the trait (International Plant Genetic Resources Institute, 1996, *Descriptors for Tomato (Lycopersicon* Spp.). In the F_2p, F_2s and F_4s the round category was the prevalent one (54.2%, 43% and 60%, respectively), while in the F_3s plants the obovoid shape was predominant (50%). In the final F_5 population (F_5p) the fruit shape was restricted to ellipsoid (40%), obovoid (40%) and round (20%) shapes (Figure 5.7 B). Long rectangular fruits were not present in any of the plants.

A

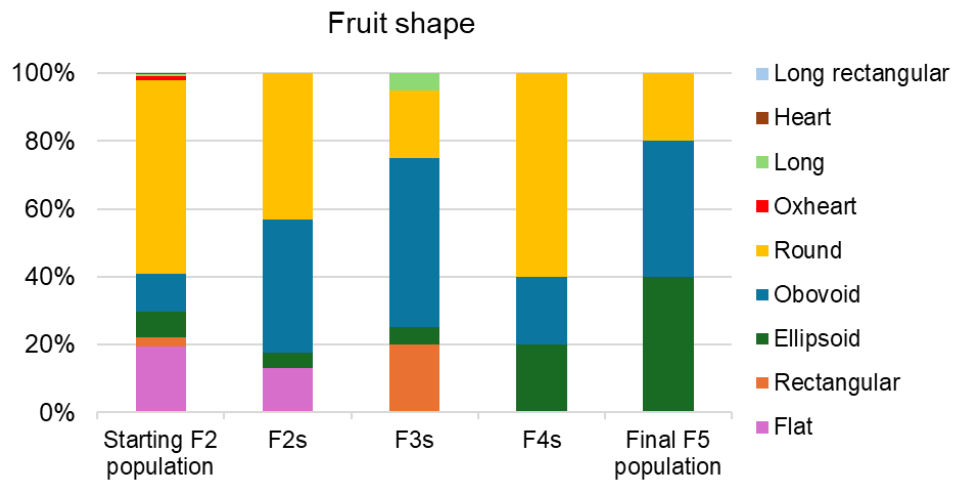

B

Figure 5.7. (A) Dynamic of the fruit shape trait under participatory selection from the original F_2 yellow population to the final F_5 population. F_2s, F_3s, F_4s: selected plants for each generation. **(B)** Representative ellipsoid, obovoid and round fruits from the selected plants.

5.3.1.2 Quantitative traits

For the earliness of flowering, most of the plants in all generations had values that ranged from zero to 40, with a balanced composition of the two classes “0-20” and “21-40” d in F_5p, and only 1% of plants in the F_2p were more tardive than the others (Figure 5.8).

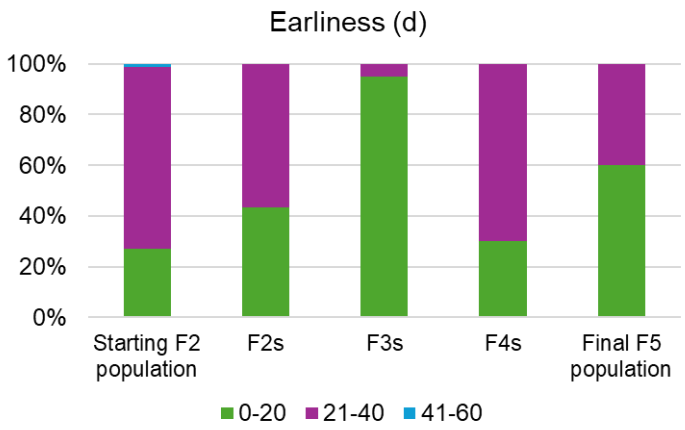

Figure 5.8. Dynamic of earliness of flowering, expressed in days (d), under participatory selection from the original F_2 yellow population to the final F_5 population. F_2s, F_3s, F4s: selected plants for each generation.

A similar trend was observed for the fruit weight (Figure 5.9), where the two categories "0-50" and "51-100" g were prevalent, especially the first one, indicating the preference of the participant to fruits of small size.

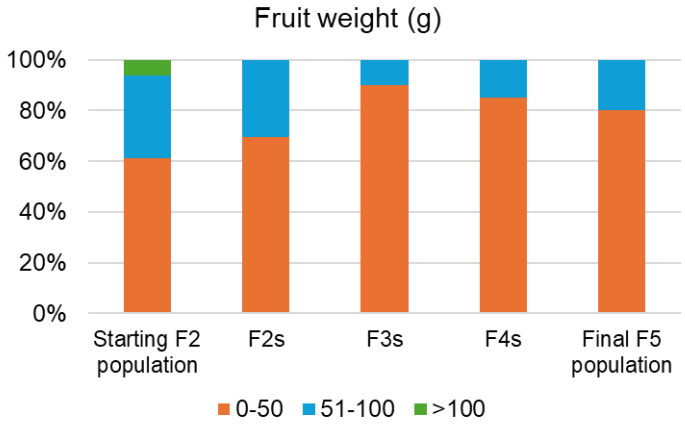

Figure 5.9. Dynamic of the fruit weight, expressed in grams (g), under participatory selection from the original F_2 population to the final F_5 yellow population. F_2s, F_3s, F_4s: selected plants for each generation.

By reading the last two plots for the number of fruits (Figure 5.10 A) and yield on the first three trusses (Figure 5.10 B), a positive selection towards an increasing production occurred, with the lower categories, both in terms of fruit number and yield, disappearing as the selection progressed. For the fruit number, 80% of the F_5 families produced 22 to 30 fruits, and the 80% had a yield ranging from 501 to 1000 g, with the remaining 20% that produced more than 1 kg.

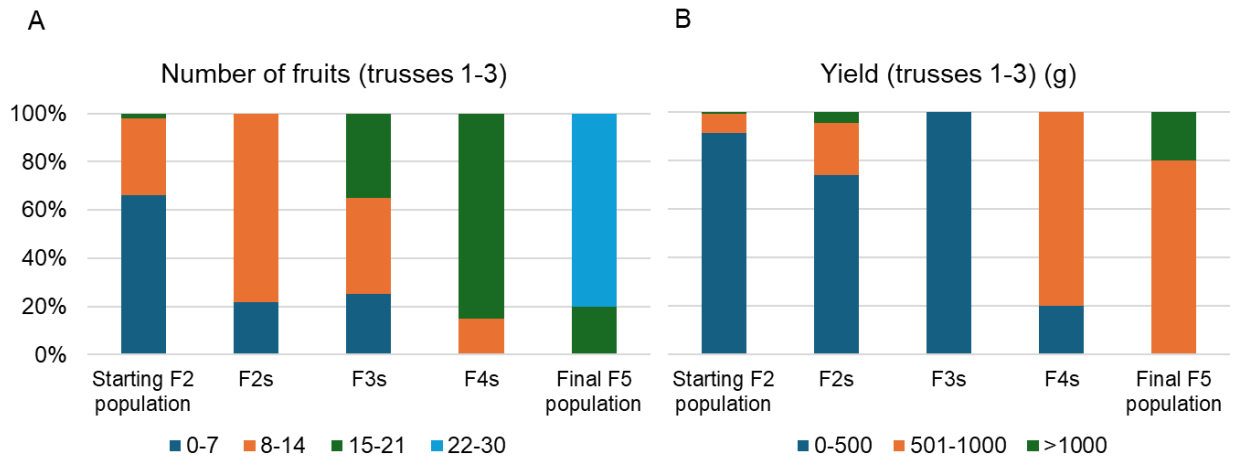

Figure 5.10. Dynamic of **(A)** number of fruits and **(B)** yields, expressed in grams (g), under participatory selection from the original F_2 yellow population to the final F_5 population. F_2s, F_3s, F_4s: selected plants for each generation.

As the selection process was based just on the plant's general appearance, fruits were not tasted, however, a positive selection was made for the TSS.

The TSS content is a refractometric index that indicates the percentage of solids, mainly sugars, organic acids and other minor components such as amino acids, phenols and minerals, dissolved in a solution. It is inversely proportional to fruit size, as it is dependent on the dry matter content, so that large sized tomato has TSS content ranging from 3 to 5%, medium sized tomato from 5 to 7% and cherry tomato may exceed the 9% (Beckles, 2012). During the first two years of selection, plants with °Brix (°Bx) ranging from 3 to 5 (Figure 5.11) represented 80% of the selected material. Starting from F4s generation, fruits with °Bx from 5.1 to 7 became prevalent, overcoming the other two categories in the final F_5p, reflecting the selection of small and medium sized fruits.

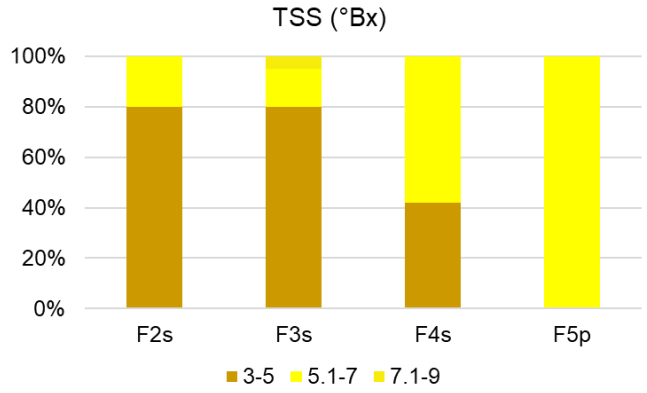

Figure 5.11. Total soluble solids (TSS) content, express as °Brix, in the selected plants (F_2s, F_3s and F_4s) and the final F_5 population (F_5p).

5.3.2 Orange population

The starting F_2 population for the orange field was obtained mixing F_2 seeds derived from the crosses and segregant populations listed in Table 5.3.

Table 5.3. Crosses that originate the F_2 orange population.

(F_1) Code	**Parent 1**		**Parent 2**		**Fixed or segregating loci**
	Code	**Name**	**Code**	**Name**	
269F	V710099	Caro Rich	V710028	Beta Bulgaria	BB Sp/sp
270F	V710030	High Beta	V710099	Caro Rich	BB Sp/sp
V710462-F2	V710462	Datterino type			BB Sp
V710313-F2	V710313	Susan			BB Sp
V710465-F2	V710465	Processing Soressi			BB sp

In the orange population, unlike the yellow one, the flesh color was due to a single mutation present in every parental line. *Beta* (*B*) is a gain-of-function mutation in the lycopene-β-cyclase (CYC-B) encoding gene. *CYC-B*, which catalyzes the conversion of lycopene into β-carotene, is down-regulated during tomato fruit ripening, leading to the accumulation of red pigment in the ripe fruit (Chattopadhyay et al., 2021). In the mutated lines, the *CYC-B* transcription is significantly increased, resulting in a high β-carotene content and consequently in an orange flesh (Ronen et al., 2000).

5.3.2.1 Qualitative traits

In the orange population the selection favored the uniparous inflorescence type, but a little variability was present at F_2p and F_3s, where the fishbone, the forked and the irregular inflorescence types were present as well (Figure 5.12).

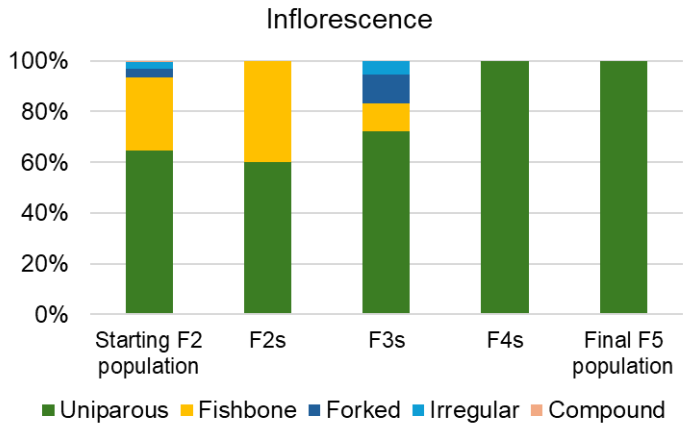

6

Figure 5.12. Dynamic of the inflorescence type trait under participatory selection from the original F_2 population to the final F_5 orange population. F_2s, F_3s, F_4s: selected plants for each generation.

For the green shoulder, all categories were present in the starting population (Figure 5.13). The uniform phenotype (absence of green shoulder) and the medium green shoulders were kept in every generation, being present in the 40% and 60% of the F_5 families, respectively. The light green category was under-represented in the starting population, and even if 16% and 30% of the selected F_3 and F_4 plants had it, it was not present in any of the F_5 families. The dark shoulder, counting for one third of the initial F_2p, peaked in F_2s (60%) but was eventually discarded.

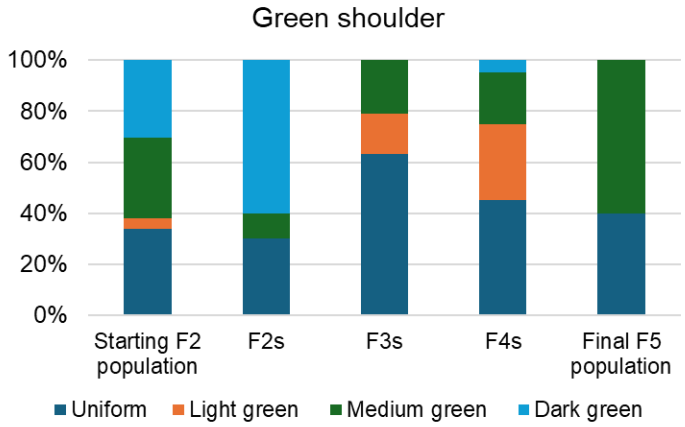

Figure 5.13. Dynamic of the green shoulder trait under participatory selection from the original F_2 orange population to the final F_5 population. F_2s, F_3s, F_4s: selected plants for each generation.

Similarly to the yellow population, the growth habit (Figure 5.14) variability was low. The indeterminate habitus was the most abundant one in all the generations, but in contrast to the yellow population, it was not the only type to be selected at the end of the experiment. The final

F_5p consisted of 60% of the families with indeterminate growth habit, 21% with determinate habitus and 19% with the semideterminate habitus.

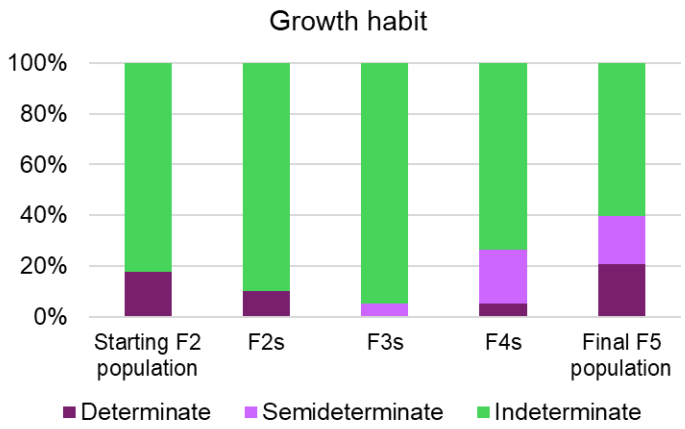

Figure 5.14. Dynamic of the growth habit trait under participatory selection from the original F_2 orange population to the final F_5 population. F_2s, F_3s, F_4s: selected plants for each generation.

For the fruit shape (Figure 5.15 A), there was less variability since the starting F_2p in comparison to the yellow population. The flat, heart and long rectangular shapes were not present at the beginning of the experiment. The long fruit type decreased from 40-50% in the F_2p and F_2s to 16% in the F_3s, until it disappeared during the final stages of the selection. The round fruits were the most stable during the selection and the prevalent category in the final F_5p (60%), indicating a preference of the participants for this shape. The ellipsoid type, which was present in low percentage during all the selection stages, eventually increased, representing 40% of the families in the final F_5p (Figure 5.15 B).

A

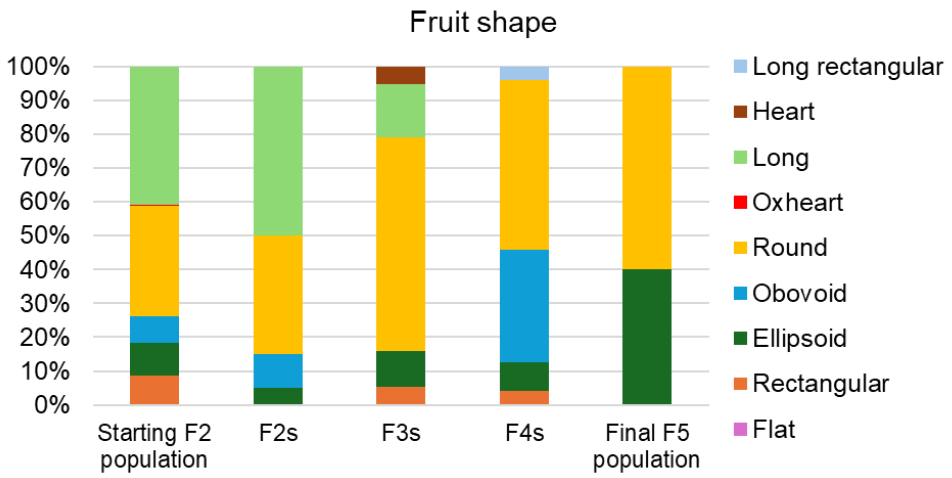

B

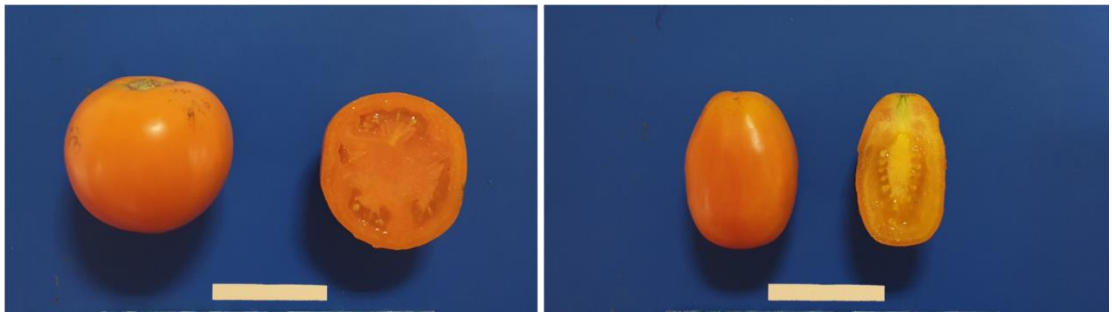

Figure 5.15. (A) Dynamic of the fruit shape trait under participatory selection from the original F_2 orange population to the final F_5 population. F_2s, F_3s, F_4s: selected plants for each generation. **(B)** Representative round and ellipsoid fruits from the selected plants.

5.3.2.2 Quantitative traits

For the earliness of flowering (Figure 5.16), as for the yellow population, earlier genotypes were preferred, even though the more tardive ones were always present throughout the experiment. The "21-30 d" was the prevalent category, representing the 80% of the F_5p families. The "0-20 d" peaked in the F_2s (65%) but did not exceed the 20 % in any other generation.

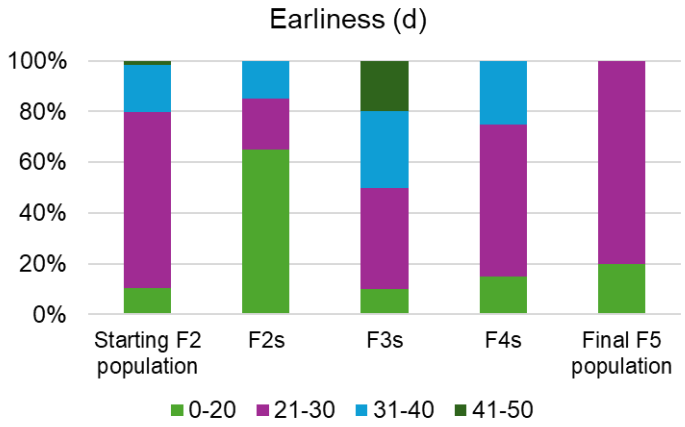

Figure 5.16. Dynamic of earliness of flowering, expressed in days (d), under participatory selection from the original F_2 orange population to the final F_5 population. F_2s, F_3s, F_4s: selected plants for each generation.

The fruit weight (Figure 5.17) trait was consistent throughout the selection process. Fruit of small size were preferred and always selected from the F_2s to the final F_5p (60%). Big fruits eventually disappeared, while medium sized fruits were kept in every generation, representing 40% of the F_5p families.

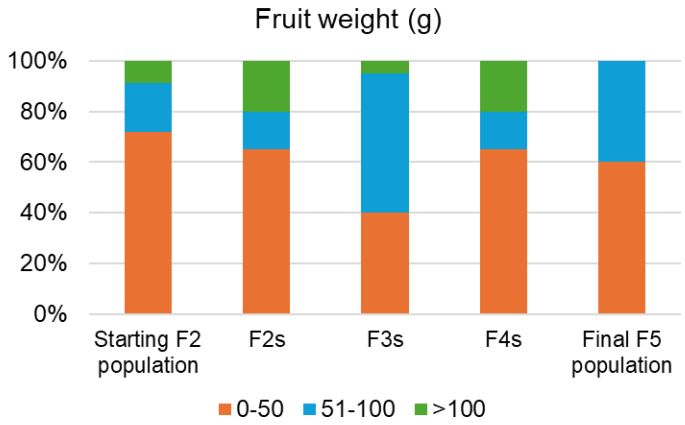

Figure 5.17. Dynamic of the fruit weight, expressed in grams (g), under participatory selection from the original F_2 orange population to the final F_5 population. F_2s, F_3s, F_4s: selected plants for each generation.

About the production-related traits, the few plants producing more than 60 fruits on the first three trusses present in the starting F_2p (Figure 5.18 A) were not selected, keeping the selection process balanced from the F_2s to the F_4s, with a reversal trend in the final F_5p, where the "21-40" category (60%) overcome the "0-20" (40%). For the yield (Figure 5.18 B), even though

plants that produced less fruits were selected, a positive selection towards an increased production occurred, with the plants producing up to 500g disappearing in the last year's field and the plants producing over 1 kg increasing to 60% in F5p.

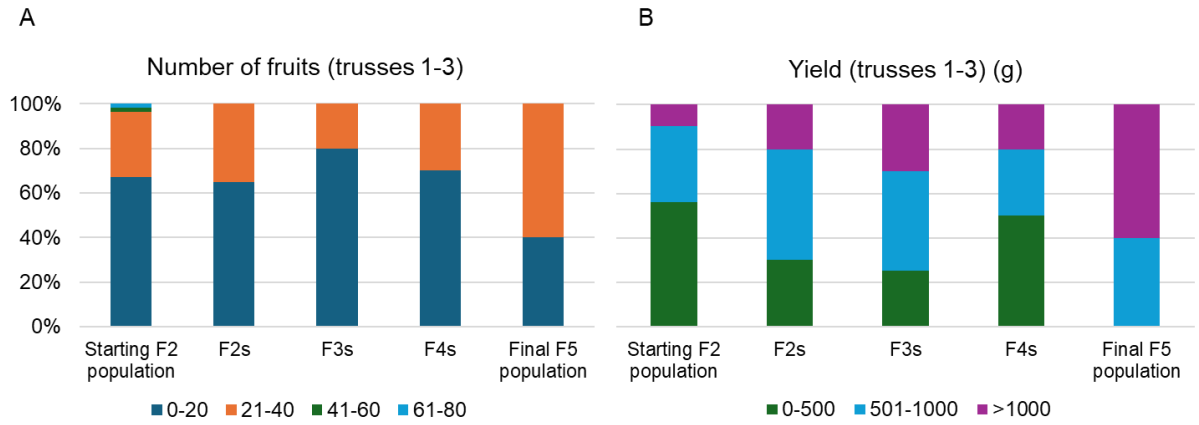

Figure 5.18. Dynamic of **(A)** number of fruits and **(B)** yields, expressed in grams (g), under participatory selection from the original F_2 orange population to the final F_5 population. F_2s, F_3s, F_4s: selected plants for each generation.

For the TSS content, unlike the yellow population in which during the first steps of selection plants with lower °Bx values were kept, the majority of the F_2s, F_3s, F_4s had TSS content ranging from 5.1 to 7 (Figure 5.19). Furthermore, in every generation, plants with °Bx values higher than 7 were selected, leading to a final F_5 population composed of families having > 5 TSS values, reflecting, analogously to the yellow counterpart, the selection of small and medium sized fruits.

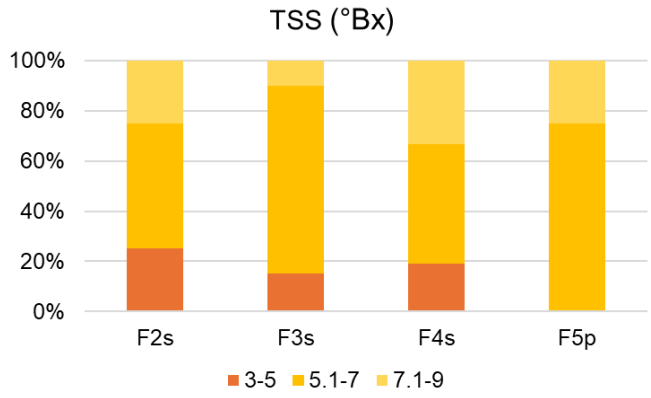

Figure 5.19. Total soluble solids (TSS) content, express as °Brix, in the selected plants (F_2s, F_3s and F_4s) and the final F_5 population (F_5p).

5.3.3 Fruit firmness increase was achieved by participatory selection

As for the TSS content, fruits were not touched by the participants during the selection process. Nevertheless, a positive selection of the texture occurred for some categories.

If considering all the selected plants together, no differences were detected among the F_2s and the final F_5p in the yellow population (Figure 5.20). The selected plants of the F_4 generation showed a lower firmness in comparison to the F_3s and the F_5p and the same trend, was found in the medium sized fruits, when the selections were separated according to the fruit size. For plants with smaller fruits, a positive selection for fruit firmness seems to have occurred during the four years, with fruits of F_5p firmer than the ones of the F_2s.

In comparison to the controls, the values of all the generations were distributed between the average firmness of Santy Yellow and TRVA0940.

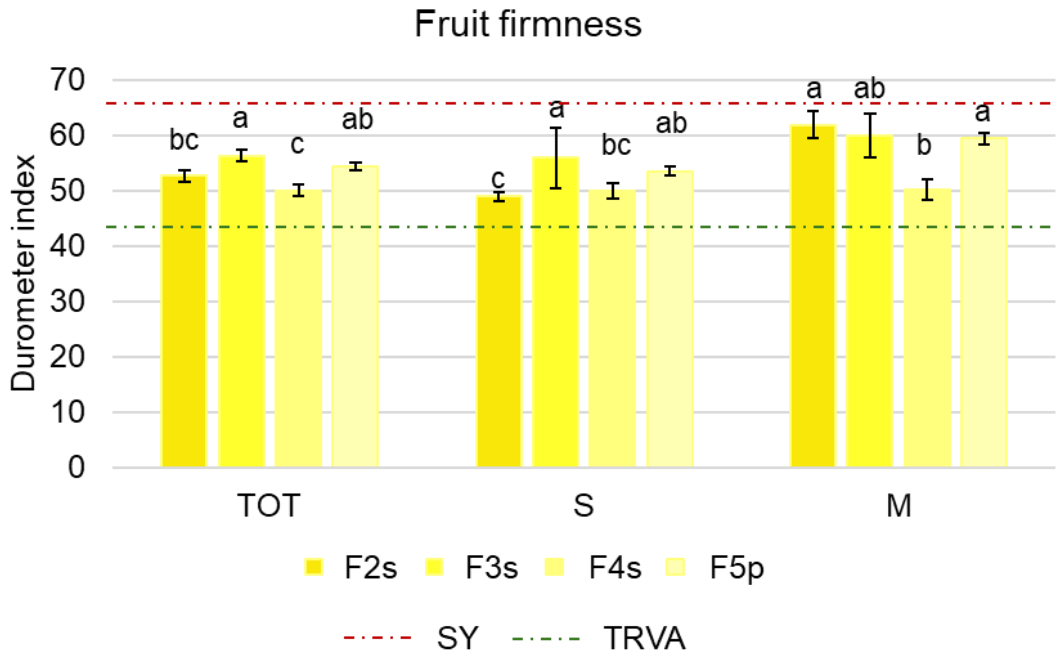

Figure 5.20. Dynamic of fruit firmness in the yellow F_2s, F_3s and F_4s selected plants and the final F_5 population (F_5p). TOT: totality of fruits in the corresponding population; S: small sized fruits; M: medium sized fruits. Controls: Santy yellow (SY) and TRVA0940 (TRVA). Letters indicate significant

difference among the samples calculated by Dunn's *post hoc* test ($p \leq 0.05$). Data are expressed as mean ± standard error.

No plants producing big fruits were present in the yellow population. Moreover, in the F_5 final population, firmness appeared significantly higher in the medium fruits (59.4 ± 5.1) than in the small ones (53.5 ± 8.9) (Supplementary Figure S5.2 A).

For the orange population, a tendency to increased fruit firmness can be observed in the total of the selected plants and in the S-sized fruit in the F_4s and F_5p, and in the B-sized fruits in the F_3s and F_4s (no big fruits were presents in the last orange field) (Figure 5.21). Additionally, the S fruits selected from the F_4 generation and grown in the final F5p trial, exhibited higher firmness values in comparison to both controls. For the M-sized fruits, genotypes homogeneous for the trait were chosen throughout the selection process, and in the F_5 final population, unlike the yellow population, firmness appeared significantly lower (46.2 ± 0.95) than the one of the smaller fruits (70.4 ± 1.2) (Supplementary Figure S5.2 B).

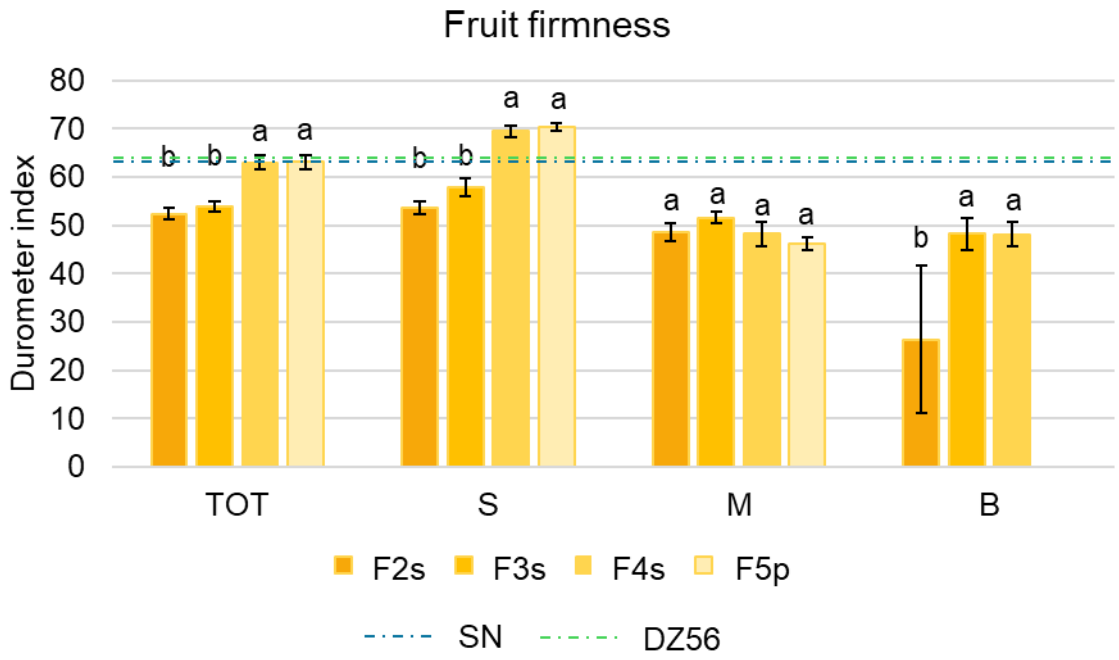

Figure 5.21. Dynamic of fruit firmness in the F_2s, F_3s and F_4s selected plants and the final F_5 population (F_5p). TOT: totality of fruits in the corresponding population; S: small sized fruits; M: medium sized, B: big sized fruits. Controls: Santy naranja (SN) and DZ56. Letters indicate significant difference among the samples calculated by Dunn's *post hoc* test ($p \leq 0.05$). Data are expressed as mean ± standard error.

By merging the data collected over the four-year experiment in both populations, it is clear that an overall texture improvement has been achieved (Figure 5.22), even if the selection process was not based on fruit quality attributes.

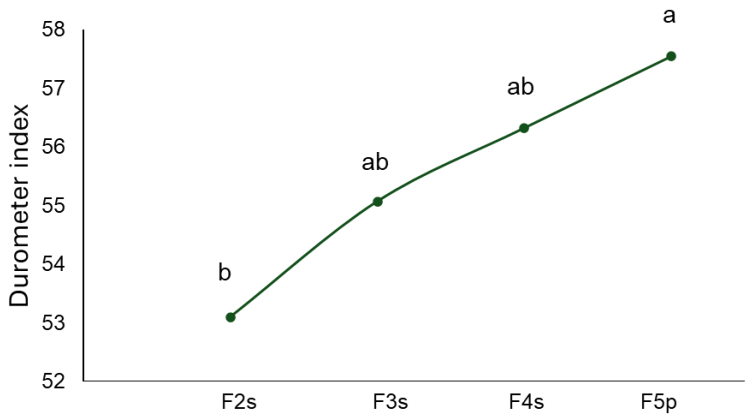

Figure 5.22. Comprehensive firmness values of the yellow and orange selected plants from the F_2 generation to the final F_5 population of breeding lines. Letters indicate significant difference among the samples calculated by Dunn's *post hoc* test ($p \leq 0.05$).

5.3.4 F5 Field: comparing Italian and Spanish genotypes

For the final stage of the participatory selection, the F_5 progenies of the top five F_4 plants selected in both Italy and Spain were grown in a single field (in both countries) to compare the genotypes, that have been selected under different farming managements (organic in Italy and conventional in Spain), and in different environments.

In the Italian field (Table 5.4), the main differences among the selections of the two countries were found in the green shoulder trait, for which the Spanish yellow genotypes presented all the categories; in the growth habit of the Italian orange genotypes, which were the most variable; and in the inflorescence and fruit shape traits for the Spanish orange material, that showed the forked inflorescence category and the long fruit class, which were absent in the other genotypes. For the quantitative traits, the main differences can be observed in the fruit weight of the Italian orange lines, reflected in a slightly higher yield in comparison to the Spanish genotypes, and in the fruit firmness of the Italian orange population, which was higher than the Spanish

counterpart. Additionally, both the yellow and the orange Spanish genotypes, had an important fluctuation in the firmness values of the samples, with a standard deviation of ± 12.74 and 14.7 respectively.

For all the other traits, the performance of the Italian and the Spanish plants was consistent, indicating that the selected material, even though was obtained under different farming methods and in two different environments, is resilient and able to adapt to different conditions.

Table 5.4. Comparison of Italian and Spanish genotypes grown in Italy in 2024. Quantitative traits are expressed as mean ± standard deviation.

Trait	ITA yellow	SPA yellow	ITA orange	SPA orange
Qualitative				
Inflorescence	Uniparous	Uniparous	Uniparous	Uniparous Forked
Green shoulder	Uniform Dark green	Uniform Light green Medium green Dark green	Uniform Medium green	Medium green Dark green
Growth habit	Indeterminate	Indeterminate	Determinate Semideterminate Indeterminate	Indeterminate
Fruit shape	Ellipsoid Obovoid Round	Obovoid Round	Ellipsoid Round	Ellipsoid Obovoid Long
Quantitative				
Earliness (d)	19 ± 2.7	18 ± 2.7	24 ± 2.8	23 ± 2.7
Fruit weight (g)	39 ± 13.9	35 ± 6.9	52 ± 31.5	38 ± 1.8
Number of fruits	24 ± 5.3	27 ± 4.5	24 ± 10.4	22 ± 5.7
Yield (g)	887 ± 123.6	908 ± 86.5	960 ± 285.5	799 ± 107
Firmness	54.4 ± 8.68	54.2 ± 12.74	63.1 ± 7.4	51.5 ± 14.7

Interestingly, when comparing the ranking obtained from the participants' scoring in the two countries, some lines were evaluated in similar way, i.e. 614P, which was the best line in both Italy and Spain, and 616P, 408P, ID84, ID19 and ID38, that had similar ranking. While for other lines, the assigned scores were contrasting, i.e. 604P, 392P, ID134 and 402P (Figure 5.23). Furthermore, seven lines selected in Italy and five lines selected in Spain ranked in the top ten of the opposite country, which comprised six yellow and four orange lines in both nations.

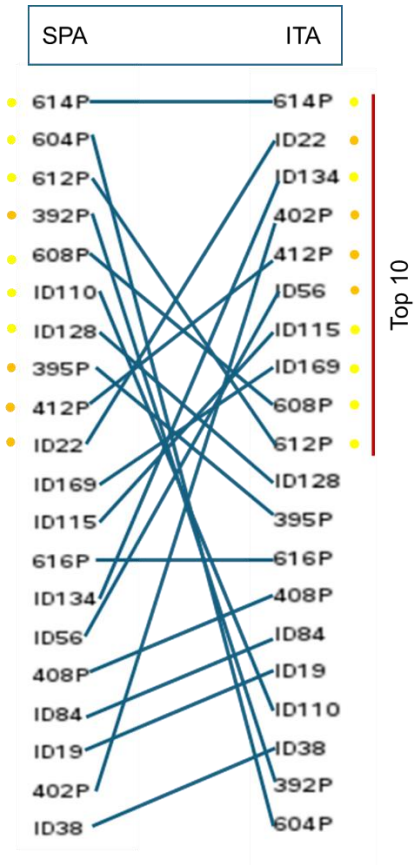

Figure 5.23. Ranking of the F_5 families, according to the participant scores, grown in Spain (SPA) and Italy (ITA) in 2024. Colored dots represent the population color.

5.4 Conclusions

Meeting farmer and consumer needs is the main objective of plant breeding. During the last decades the idea of involving the stakeholders in the selection of new varieties emerged and grew bigger to the present day (Ceccarelli et al., 2009). As people are demanding more transparency in every step of the agri-food chain, the inclusion of farmers and citizens in the research activity can be an efficient way to "open the laboratory doors", letting people know more about breeders' and researchers' work and to focus on their real needs, collaborating to achieve a common goal.

Most of the fresh tomato market is driven by red fruited varieties, however, a growing interest towards novel tomato genotypes with diversified flesh and skin color has emerged at the beginning of 21st century (Schouten et al., 2020). Thanks to the health promoting role of different pigments, tomato lines with improved pigmentation in fruits have been developed (Dono et al., 2022; Chattopadhyay et al., 2021). In the described participatory selection activity, two populations obtained by crossing different tomato genotypes with a yellow and orange fruit genetic background, were grown in conventional and organic fields, in Spain and Italy respectively, and evaluated in a four-year experiment by farmers and citizens. By the end of the project, it was possible to define common and differential preferences detected between countries and select yellow and orange-fruited lines suitable for organic farming, but also cultivable in conventional farming methods.

By scoring the plants according to their general appearance, the selection of material characterized by earlier flowering, higher productivity and higher TSS content has been achieved. Moreover, the participatory breeding allowed to fix firmness alleles in breeding lines with small sized fruits, and to some extent, to positively select plants with improved fruit firmness.

5.5 Supplementary material

Supplementary Table S1. Allelic arrangement of the parental genotypes used for the constitution of the yellow and orange populations.

Color	Name	Red + / r	High Beta + / B	Sherry color + / sh	Non ripening + / nor	Colorless fruit epidermis + / y	Uniform + / u	Self-pruning + / sp
Yellow	Taxi	r	+	+	+	+	u	sp
	Golden Jubilee	r	+	+	+	+	+	+
	White beauty	r	+	+	+	y	+	+
	Bell pepper	r	+	+	+	+	+	+
	Sherry color	R	+	sh	+	+	-	+
	Campanella dorata	r	+	+	+	+	+	+
	Invernale	R	+	+	nor	+	+	+
	Golden Boston	r	+	+	+	+	u	sp
Orange	Caro rich	+	B	+	+	+	+	+
	High beta	+	B	+	+	+	+	sp
	Datterino type	+	B	+	+	+	+	+
	Processing	+	B	+	+	+	u	sp
	Susan	+	B	+	+	+	+	+
	Beta Bulgaria	+	B	+	+	+	u	sp

A

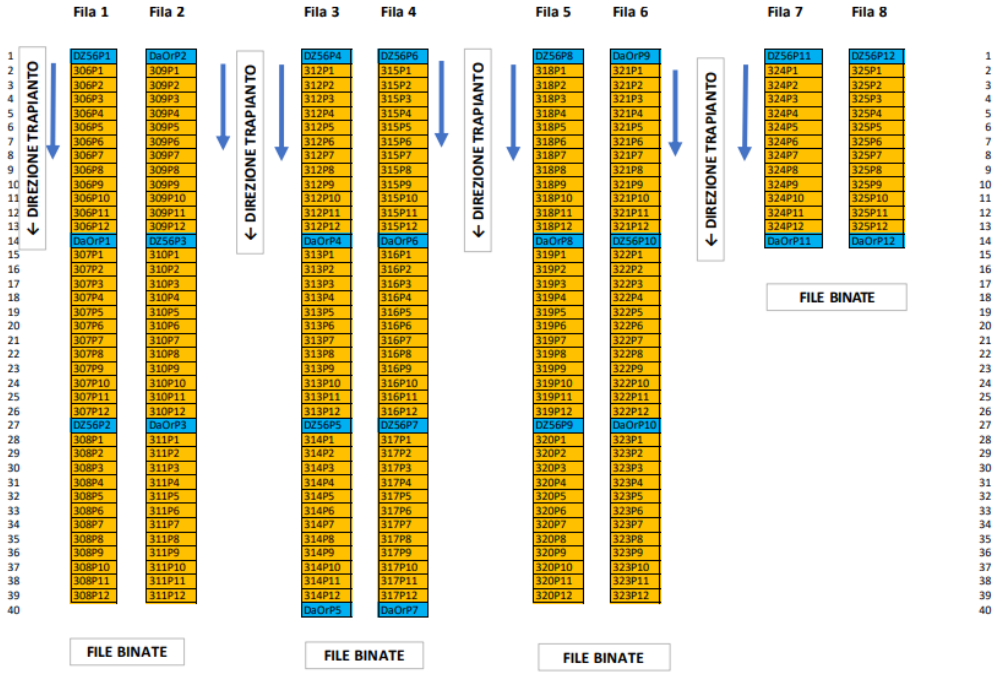

B

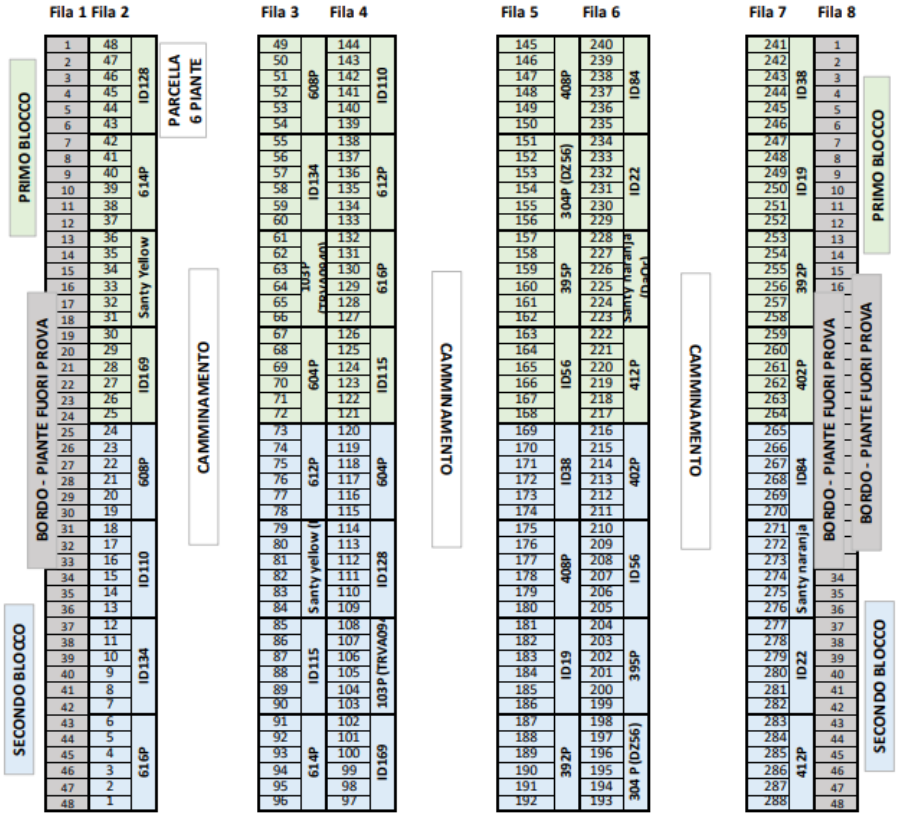

Supplementary Figure S5.1. Representative field maps of 2022 **(A)** and 2024 **(B)** selection years.

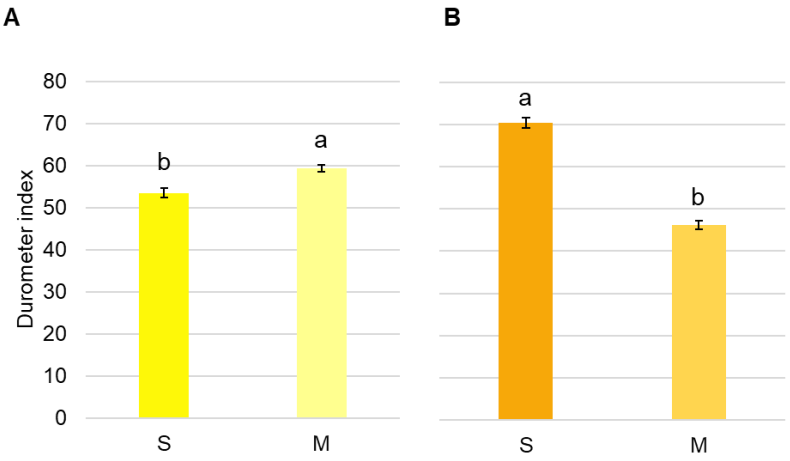

Supplementary Figure S5.2. Comparison of fruit firmness according to the small (S) and medium (M) fruit size of the yellow **(A)** and orange **(B)** F_5 populations. Letters indicate significant difference among the samples calculated by Dunn's *post hoc* test ($p \leq 0.05$). Data are expressed as mean ± standard error.

6. General conclusions

Over the years, different strategies and methods have been developed and integrated in the agricultural genetic and breeding fields. From the marker assisted selection (MAS) to the new breeding techniques, including the CRISPR/Cas system, the use of these technologies opened up new frontiers in the improvement of crops quality.

Nowadays, thanks to cutting-edge sequencing technologies, it is simpler to obtain wide datasets of markers, allowing the screening of large populations and the discovery of new genetic variants, making it easier to perform GWAS analysis to find candidate genes linked to traits of interest.

In this dissertation, different procedures have been adopted to find ways to improve tomato fruit firmness. The use of association analysis allowed the identification of QTLs and eventually candidate genes involved in fruit ripening and softening. By genome editing techniques, these genes can be validated in genotypes of interest and ultimately modified to induce precise mutations, leading to shorter breeding times and thus a prompter response to agricultural and market needs.

Moreover, populations where favorable alleles for traits of interest have been identified or populations consisting of *in-vitro* edited material (in a future perspective of allowing the cultivation of *New Genomic Techniques*-plants) can be grown in participatory selection‘s programs to be further selected in specific environments by farmers and growers, according to their specific needs.

7. Funding acknowledgements

This work received funding from the European Union's Horizon 2020 project HARNESSTOM (grant agreement No 101000716), from University of Tuscia, from Regione Lazio "Progetti di Gruppi di Ricerca 2020" - Progetto n. A0375-2020-36749 "Nuove varietà tipiche di pomodoro con migliorate caratteristiche agronomiche e di qualità (NOVIPOM)" and a mobility grant from Consorzio Interuniversitario per le Biotecnologie (CIB).

8. Bibliography

Adaskaveg, J. A., Silva, C. J., Huang, P., & Blanco-Ulate, B. (**2021**). Single and double mutations in tomato ripening transcription factors have distinct effects on fruit development and quality traits. *Frontiers in Plant Science*, *12*, 647035.

Adato, A., Mandel, T., Mintz-Oron, S., Venger, I., Levy, D., Yativ, M., ... & Aharoni, A. (**2009**). Fruit-surface flavonoid accumulation in tomato is controlled by a SlMYB12-regulated transcriptional network. *PLoS Genetics*, *5*(12), e1000777.

Ahmed, S., Wan Azizan, W. A. S., Akhond, M. A. Y., Juraimi, A. S., Ismail, S. I., Ahmed, R., & Md Hatta, M. A. (**2023**). Optimization of In Vitro Regeneration Protocol of Tomato cv. MT1 for Genetic Transformation. *Horticulturae*, *9*(7), 800.)

Aida, M., Ishida, T., Fukaki, H., Fujisawa, H., & Tasaka, M. (**1997**). Genes involved in organ separation in Arabidopsis: an analysis of the cup-shaped cotyledon mutant. *The plant cell*, *9*(6), 841-857.

Alexander, L., & Grierson, D. (**2002**). Ethylene biosynthesis and action in tomato: a model for climacteric fruit ripening. *Journal of experimental botany*, *53*(377), 2039-2055.

Almeida, J. L. F. (1961). Um novo aspecto de melhoramento do tomato. *Agricultura*, *10*, 43-44.

Arah, I. K., Ahorbo, G. K., Anku, E. K., Kumah, E. K., & Amaglo, H. (**2016**). Postharvest handling practices and treatment methods for tomato handlers in developing countries: A mini review. *Advances in Agriculture*, *2016*(1), 6436945.

Ashby, J. A. (**2009**). The impact of participatory plant breeding. *Plant breeding and farmer participation*, 649-671

Atanasova, V. K., & Gatseva, P. D. (**2019**). Natural Beverages and Their Role as Functional Foods. In Natural Beverages (pp. 37-71). Academic Press.

Aurand, R., Faurobert, M., Page, D., Maingonnat, J. F., Brunel, B., Causse, M., & Bertin, N. (**2012**). Anatomical and biochemical trait network underlying genetic variations in tomato fruit texture. *Euphytica*, *187*, 99-116.

Ayuso-Yuste, M. C., González-Cebrino, F., Lozano-Ruiz, M., Fernández-León, A. M., Bernalte-García, M. J. (**2022**). Influence of ripening stage on quality parameters of five traditional tomato varieties grown under organic conditions. *Horticulturae*, *8*(4), 313.

Balibrea, M. E., Martínez-Andújar, C., Cuartero, J., Bolarín, M. C., Pérez-Alfocea, F. (**2006**). The high fruit soluble sugar content in wild Lycopersicon species and their hybrids with cultivars depends on sucrose import during ripening rather than on sucrose metabolism. *Functional Plant Biology*, *33*(3), 279-288.

Barnes, W. J., Anderson, C. T. (**2018**). Release, recycle, rebuild: cell-wall remodeling, autodegradation, and sugar salvage for new wall biosynthesis during plant development. *Molecular Plant*, *11*(1), 31-46.

Barry, C. S., & Giovannoni, J. J. (**2006**). Ripening in the tomato Green-ripe mutant is inhibited by ectopic expression of a protein that disrupts ethylene signaling. *Proceedings of the National Academy of Sciences*, *103*(20), 7923-7928.

Barry, C. S., McQuinn, R. P., Thompson, A. J., Seymour, G. B., Grierson, D., & Giovannoni, J. J. (**2005**). Ethylene insensitivity conferred by the Green-ripe and Never-ripe 2 ripening mutants of tomato. *Plant Physiology*, *138*(1), 267-275.

Bauchet, G., Grenier, S., Samson, N., Bonnet, J., Grivet, L., & Causse, M. (**2017a**). Use of modern tomato breeding germplasm for deciphering the genetic control of agronomical traits by Genome Wide Association study. *Theoretical and applied genetics*, *130*, 875-889.

Bauchet, G., Grenier, S., Samson, N., Segura, V., Kende, A., Beekwilder, J., ... & Causse, M. (**2017b**). Identification of major loci and genomic regions controlling acid and volatile content in tomato fruit: implications for flavor improvement. New Phytologist, 215(2), 624-641.

Becker, A., & Theißen, G. (**2003**). The major clades of MADS-box genes and their role in the development and evolution of flowering plants. *Molecular phylogenetics and evolution*, *29*(3), 464-489.

Beckles, D. M. (**2012**). Factors affecting the postharvest soluble solids and sugar content of tomato (Solanum lycopersicum L.) fruit. *Postharvest biology and technology*, *63*(1), 129-140.

Bemer, M., Karlova, R., Ballester, A. R., Tikunov, Y. M., Bovy, A. G., Wolters-Arts, M., ... & de Maagd, R. A. (**2012**). The tomato FRUITFULL homologs TDR4/FUL1 and MBP7/FUL2 regulate ethylene-independent aspects of fruit ripening. *The Plant Cell*, *24*(11), 4437-4451.

Blanca, J., Pons, C., Montero-Pau, J., Sanchez-Matarredona, D., Ziarsolo, P., Fontanet, L., ... & Granell, A. (**2022**). European traditional tomatoes galore: a result of farmers' selection of a few diversity-rich loci. *Journal of experimental botany*, *73*(11), 3431-3445.

Borguini, R. G., & Ferraz Da Silva Torres, E. A. (**2009**). Tomatoes and tomato products as dietary sources of antioxidants. *Food Reviews International*, *25*(4), 313-325.

Bradbury, P. J., Zhang, Z., Kroon, D. E., Casstevens, T. M., Ramdoss, Y., & Buckler, E. S. (**2007**). TASSEL: software for association mapping of complex traits in diverse samples. *Bioinformatics*, *23*(19), 2633-2635.

Brouwer, B., Mensink, M., Woltering, E., & da Silva, F. P. (**2019**). *Predicting strawberry shelf life based on input quality: GreenCHAINge Fruit & Vegetables WP3* (No. 1912). Wageningen Food & Biobased Research.

Brummell, D. A., Bowen, J. K., & Gapper, N. E. (**2022**). Biotechnological approaches for controlling postharvest fruit softening. *Current Opinion in Biotechnology*, *78*, 102786.

Brummell, D. A., Harpster, M. H. (**2001**). Cell wall metabolism in fruit softening and quality and its manipulation in transgenic plants. *Plant molecular biology*, *47*, 311-339.

Brumos, J. (**2021**). Gene regulation in climacteric fruit ripening. *Current opinion in plant biology*, *63*, 102042.

Burns, J. K. (**1990**). α-and β-galactosidase activities in juice vesicles of stored Valencia oranges. *Phytochemistry*, *29*(8), 2425-2429.

Burstein, D., Sun, C. L., Brown, C. T., Sharon, I., Anantharaman, K., Probst, A. J., ... & Banfield, J. F. (**2016**). Major bacterial lineages are essentially devoid of CRISPR-Cas viral defence systems. *Nature communications*, *7*(1), 10613.

Camacho Villa, C., Maxted, N., Scholten, M., & Ford-Lloyd, B. (**2005**). Defining and identifying crop landraces. *Plant genetic resources*, *3*(3), 373-384.

Cao, K. E., Zhou, Z., Wang, Q. I., Guo, J., Zhao, P., Zhu, G., ... & Wang, L. (**2016**). Genome-wide association study of 12 agronomic traits in peach. *Nature Communications*, *7*(1), 13246.

Cao, X., Wei, C., Duan, W., Gao, Y., Kuang, J., Liu, M., ... & Zhang, B. (**2021**). Transcriptional and epigenetic analysis reveals that NAC transcription factors regulate fruit flavor ester biosynthesis. *The Plant Journal, 106*(3), 785-800.

Casals, J., del Castillo, R. R., Pons, C., Mazzucato, A., Tringovska, I., Pasev, G., ... & Granell, A. (**2024**). European fresh-market tomato sensory ideotypes based on consumer preferences. *Scientia Horticulturae*, *335*, 113351.

Castellarin, S. D., Gambetta, G. A., Wada, H., Shackel, K. A., & Matthews, M. A. (**2011**). Fruit ripening in Vitis vinifera: spatiotemporal relationships among turgor, sugar accumulation, and anthocyanin biosynthesis. *Journal of experimental botany*, *62*(12), 4345-4354.

Ceccarelli, S. and Grando, S. (**2022**). Return to agrobiodiversity: Participatory plant breeding. *Diversity*, *14*(2), 126.

Ceccarelli, S., Guimaraes, E. P., Weltzien, E. Plant Breeding and Farmer Participation. Rome: FAO (**2009**). ISBN 978-92-5-106382-8. doi:10.1017/S0014479710000268

Chaïb, J., Devaux, M. F., Grotte, M. G., Robini, K., Causse, M., Lahaye, M., & Marty, I. (**2007**). Physiological relationships among physical, sensory, and morphological attributes of texture in tomato fruits. *Journal of Experimental Botany*, *58*(8), 1915-1925.

Chang, C. C., Chow, C. C., Tellier, L. C., Vattikuti, S., Purcell, S. M., & Lee, J. J. (**2015**). Second-generation PLINK: rising to the challenge of larger and richer datasets. *Gigascience*, *4*(1), s13742-015.

Chattopadhyay, T., Hazra, P., Akhtar, S., Maurya, D., Mukherjee, A., & Roy, S. (**2021**). Skin colour, carotenogenesis and chlorophyll degradation mutant alleles: genetic orchestration behind the fruit colour variation in tomato. Plant Cell Reports, 40, 767-782.

Chebli, Y., & Geitmann, A. (**2018**). FRAP Experiments Show Pectate Lyases Promote Pollen Germination and Lubricate the Path of the Pollen Tube in Arabidopsis thaliana. *Microscopy and Microanalysis*, *24*(S1), 1376-1377.

Chen, Y. (**2013**). Dissection of agronomic traits in crops by association mapping. *Diagnostics in plant breeding*, 119-142.

Cheng, M., Fry, J. E., Pang, S., Zhou, H., Hironaka, C. M., Duncan, D. R., ... & Wan, Y. (**1997**). Genetic transformation of wheat mediated by Agrobacterium tumefaciens. *Plant physiology*, *115*(3), 971-980.

Cleveland, W. S. (**1979**). Robust locally weighted regression and smoothing scatterplots. *Journal of the American statistical association*, *74*(368), 829-836.

Clinton, S. K. (**1998**). Lycopene: chemistry, biology, and implications for human health and disease. *Nutrition reviews*,*56*(2), 35-51.

Concordet, J. P., & Haeussler, M. (**2018**). CRISPOR: intuitive guide selection for CRISPR/Cas9 genome editing experiments and screens. *Nucleic acids research*, *46*(W1), W242-W245.

Davuluri, G. R., van Tuinen, A., Mustilli, A. C., Manfredonia, A., Newman, R., Burgess, D., ... & Bowler, C. (**2004**). Manipulation of DET1 expression in tomato results in photomorphogenic phenotypes caused by post-transcriptional gene silencing. *The Plant Journal*, *40*(3), 344-354.

de Brito, A. A., Campos, F., dos Reis Nascimento, A., de Carvalho Corrêa, G., da Silva, F. A., de Almeida Teixeira, G. H., Júnior, L. C. C. (**2021**). Determination of soluble solid content in market tomatoes using near-infrared spectroscopy. *Food control*, *126*, 108068.

De Veau, E. I., Gross, K. C., Huber, D. J., Watada, A. E. (**1993**). Degradation and solubilization of pectin by β-galactosidases purified from avocado mesocarp. *Physiologia Plantarum*, *87*(3), 279-285.

Deltcheva, E., Chylinski, K., Sharma, C. M., Gonzales, K., Chao, Y., Pirzada, Z. A., ... & Charpentier, E. (**2011**). CRISPR RNA maturation by trans-encoded small RNA and host factor RNase III. *Nature*, *471*(7340), 602-607.

Deng, H., Pirrello, J., Chen, Y., Li, N., Zhu, S., Chirinos, X., ... & Liu, M. (**2018**). A novel tomato F-box protein, SlEBF3, is involved in tuning ethylene signaling during plant development and climacteric fruit ripening. The Plant Journal, 95(4), 648-658.

Diouf, I. A., Derivot, L., Bitton, F., Pascual, L., & Causse, M. (**2018**). Water deficit and salinity stress reveal many specific QTL for plant growth and fruit quality traits in tomato. *Frontiers in plant science*, *9*, 279.

Domínguez, E., Cuartero, J., & Heredia, A. (**2011**). An overview on plant cuticle biomechanics. *Plant Science*, *181*(2), 77-84.

Dong, T., Hu, Z., Deng, L., Wang, Y., Zhu, M., Zhang, J., & Chen, G. (**2013**). A tomato MADS-box transcription factor, SlMADS1, acts as a negative regulator of fruit ripening. *Plant physiology*, *163*(2), 1026-1036.

Dono, G. (**2020**). Characterization of a collection of tomato mutant lines in the San Marzano background.

Dono, G., Rambla, J. L., Frusciante, S., Fabene, E., Gómez-Cadenas, A., Granell, A., ... & Mazzucato, A. (**2022**). Pigment-related mutations greatly affect berry metabolome in san marzano tomatoes. *Horticulturae*, *8*(2), 120.

Doudna, J. A., & Charpentier, E. (**2014**). The new frontier of genome engineering with CRISPR-Cas9. *Science*, *346*(6213), 1258096.

Doyle, J. J. (**1987**) A rapid DNA isolation procedure for small quantities of fresh leaf tissue, Phytochem. Bull., 19, pp. 11–15. Available at: https://ci.nii.ac.jp/naid/10011287509/en/.

Earl, D. A., & VonHoldt, B. M. (**2012**). STRUCTURE HARVESTER: a website and program for visualizing STRUCTURE output and implementing the Evanno method. *Conservation genetics resources*, *4*, 359-361. DOI: 10.1007/s12686-011-9548-7. Version: v0.6.8 Oct 2011

El-Fatah, B. E. A., Imran, M., Abo-Elyousr, K. A., Mahmoud, A. F. (**2023**). Isolation of Pseudomonas syringae pv. Tomato strains causing bacterial speck disease of tomato and marker-based monitoring for their virulence. *Molecular Biology Reports*, *50*(6), 4917-4930.

Eriksson, O. (**2016**). Evolution of angiosperm seed disperser mutualisms: the timing of origins and their consequences for coevolutionary interactions between angiosperms and frugivores. *Biological Reviews*, *91*(1), 168-186.

Evanno, G., Regnaut, S., & Goudet, J. (**2005**). Detecting the number of clusters of individuals using the software STRUCTURE: a simulation study. *Molecular ecology*, *14*(8), 2611-2620.

Fang, W., Fasano, C., & Perrella, G. (**2023**). Unlocking the secret to higher crop yield: the potential for histone modifications. Plants, 12(8), 1712.

FAO "International Treaty on Plant Genetic Resources for Food and Agriculture", https://www.fao.org/plant-treaty/tools/toolbox-for-sustainable-use/details/en/c/1418424/#:~:text=Participatory%20plant%20breeding%20(PPB)%20is,Farmers%20know%20their%20needs%20best.

FAOSTAT https://www.fao.org/faostat/en/#data/QCL

Fils-Lycaon, B., & Buret, M. (**1991**). Changes in glycosidase activities during development and ripening of melon. *Postharvest Biology and Technology*, *1*(2), 143-151.

Forlani, S., Masiero, S., & Mizzotti, C. (**2019**). Fruit ripening: the role of hormones, cell wall modifications, and their relationship with pathogens. *Journal of Experimental Botany*, *70*(11), 2993-3006. https://doi.org/10.1093/jxb/erz112

Franssen, H. J., Vijn, I., Yang, W. C., & Bisseling, T. (**1992**). Developmental aspects of the Rhizobium-legume symbiosis. *Plant molecular biology*, *19*, 89-107.

Frusciante, L., Carli, P., Ercolano, M. R., Pernice, R., Di Matteo, A., Fogliano, V., & Pellegrini, N. (**2007**). Antioxidant nutritional quality of tomato. Molecular nutrition & food research, 51(5), 609-617.

Fulton, T. M., Beck-Bunn, T., Emmatty, D., Eshed, Y., Lopez, J., Petiard, V., ... & Tanksley, S. D. (**1997**). QTL analysis of an advanced backcross of Lycopersicon peruvianum to the cultivated tomato and comparisons with QTLs found in other wild species. *Theoretical and Applied Genetics*, *95*, 881-894.

Fulton, T. M., Grandillo, S., Beck-Bunn, T., Fridman, E., Frampton, A., Lopez, J., ... & Tanksley, S. D. (**2000**). Advanced backcross QTL analysis of a Lycopersicon esculentum× Lycopersicon parviflorum cross. *Theoretical and Applied Genetics*, *100*, 1025-1042.

Gao, Y., Wei, W., Zhao, X., Tan, X., Fan, Z., Zhang, Y., ... & Fu, D. Q. (**2018**). A NAC transcription factor, NOR-like1, is a new positive regulator of tomato fruit ripening. *Horticulture research*, *5*.

Gavrish, S. F., & Korol', V. G. (**1991**). Some biological features of F1 tomato hybrids carrying the *nor* gene.

Gianoglio, S. (**2018**). CRISPR/Cas9 gene editing for functional genomics in Solanaceae species.

Gianoglio, S., Comino, C., Moglia, A., Acquadro, A., García-Carpintero, V., Diretto, G., ... & Granell, A. (**2022**). In-depth characterization of greenflesh tomato mutants obtained by CRISPR/Cas9 editing: a case study with implications for breeding and regulation. *Frontiers in plant science*, *13*, 936089.

Giovannoni, J. (**2001**). Molecular biology of fruit maturation and ripening. *Annual review of plant biology*, *52*(1), 725-749.

Giovannoni, J. J., Noensie, E. N., Ruezinsky, D. M., Lu, X., Tracy, S. L., Ganal, M. W., ... & Tankslev, S. D. (**1995**). Molecular genetic analysis of the ripening-inhibitor and non-ripening loci of tomato: a first step in genetic map-based cloning of fruit ripening genes. *Molecular and General Genetics MGG*, *248*, 195-206.

Giovannoni, J., Nguyen, C., Ampofo, B., Zhong, S., & Fei, Z. (**2017**). The epigenome and transcriptional dynamics of fruit ripening. *Annual Review of Plant Biology*, *68*(1), 61-84.

Giovannoni, J.J., Tanskley, S., Vrebalov, J., Noensie, F., (**2004**). NOR gene compositions and methods for use thereof. Patent US 6. 762,347 B1.

Giovannucci, E., Ascherio, A., Rimm, E. B., Stampfer, M. J., Colditz, G. A., & Willett, W. C. (**1995**). Intake of carotenoids and retino in relation to risk of prostate cancer. *JNCI Journal of the National Cancer Institute*, *87*(23), 1767-1776.

Girard, A. L., Mounet, F., Lemaire-Chamley, M., Gaillard, C., Elmorjani, K., Vivancos, J., ... & Bakan, B. (**2012**). Tomato GDSL1 is required for cutin deposition in the fruit cuticle. *The Plant Cell*, *24*(7), 3119-3134.

Goodwin, S. M., & Jenks, M. A. (**2005**). Plant cuticle function as a barrier to water loss. *Plant abiotic stress*, 14-36.

Gramazio, P., Takayama, M., & Ezura, H. (**2020**). Challenges and prospects of new plant breeding techniques for GABA improvement in crops: tomato as an example. Frontiers in Plant Science, 11, 577980.

Guo, X., Zhang, Y., Tu, Y., Wang, Y., Cheng, W., & Yang, Y. (**2018**). Overexpression of an EIN3-binding F-box protein2-like gene caused elongated fruit shape and delayed fruit development and ripening in tomato. Plant Science, 272, 131-141.

Hagerman, A. E., Austin, P. J. (**1986**). Continuous spectrophotometric assay for plant pectin methyl esterase. *Journal of Agricultural and Food Chemistry*, *34*(3), 440-444.

Hall, D., Tegström, C., & Ingvarsson, P. K. (**2010**). Using association mapping to dissect the genetic basis of complex traits in plants. Briefings in functional genomics, 9(2), 157-165.

Han, Y., Chen, C., Yan, Z., Li, J., & Wang, Y. (**2019**). The methyl jasmonate accelerates the strawberry fruits ripening process. Scientia horticulturae, 249, 250-256.

Hattery, T. (**2022**). Characterization of genotypic and environmental influences on Zea mays cuticle deposition (Doctoral dissertation, Iowa State University).

Hirschhorn, J. N., & Daly, M. J. (**2005**). Genome-wide association studies for common diseases and complex traits. *Nature reviews genetics*, *6*(2), 95-108.

Hobson, G. E. (**1967**). The effects of alleles at the "Never ripe" locus on the ripening of tomato fruit. *Phytochemistry*, *6*(10), 1337-1341.

Hu, W., Phillips, G. C. (**2001**). A combination of overgrowth-control antibiotics improves *Agrobacterium tumefaciens*-mediated transformation efficiency for cultivated tomato (L. esculentum). *In Vitro Cellular & Developmental Biology-Plant*, *37*, 12-18.

Huang, M., Liu, X., Zhou, Y., Summers, R. M., & Zhang, Z. (**2019**). BLINK: a package for the next level of genome-wide association studies with both individuals and markers in the millions. *Gigascience*, *8*(2), giy154. https://doi.org/10.1093/gigascience/giy154.

Huang, X., Wei, X., Sang, T., Zhao, Q., Feng, Q. I., Zhao, Y., ... & Han, B. (**2010**). Genome-wide association studies of 14 agronomic traits in rice landraces. *Nature genetics*, *42*(11), 961-967.

Hwang, E. Y., Song, Q., Jia, G., Specht, J. E., Hyten, D. L., Costa, J., & Cregan, P. B. (**2014**). A genome-wide association study of seed protein and oil content in soybean. *BMC genomics*, *15*, 1-12

International Plant Genetic Resources Institute. (**1996**). *Descriptors for Tomato (Lycopersicon Spp.)* (Vol. 21). Bioversity International.

Ishino, Y., Shinagawa, H., Makino, K., Amemura, M., & Nakata, A. (**1987**). Nucleotide sequence of the iap gene, responsible for alkaline phosphatase isozyme conversion in Escherichia coli, and identification of the gene product. *Journal of bacteriology*, *169*(12), 5429-5433.

Itkin, M., Seybold, H., Breitel, D., Rogachev, I., Meir, S., & Aharoni, A. (**2009**). TOMATO AGAMOUS-LIKE 1 is a component of the fruit ripening regulatory network. *The Plant Journal*, *60*(6), 1081-1095.

Jansing, J., Bortesi, L., Zhu, C., Perez, L., Bassié, L., Nadi, R., ... Schillberg, S. (**2016**). Patterns of CRISPR/Cas9 activity in plants, animals and microbes. *Plant Biotechnology*.

Ji, Y., Xu, M., & Wang, A. (**2021**). Recent advances in the regulation of climacteric fruit ripening: Hormone, transcription factor and epigenetic modifications. *Front. Agric. Sci. Eng*, *8*(2), 314-334.

Jiang, J., Yao, L., Miao, Y., & Cao, J. (**2013**). Genome-wide characterization of the pectate lyase-like (PLL) genes in Brassica rapa. *Molecular genetics and genomics*, *288*, 601-614.

Jinek, M., Chylinski, K., Fonfara, I., Hauer, M., Doudna, J. A., & Charpentier, E. (**2012**). A programmable dual-RNA–guided DNA endonuclease in adaptive bacterial immunity. *science*, *337*(6096), 816-821.

Juan-Cabot, A., Galmés, J., & Conesa, M. À. (**2022**). The tomato long shelf-life fruit phenotype: Knowledge, uncertainties and prospects. *Scientia Horticulturae*, *291*, 110578.

Kachanovsky, D. E., Filler, S., Isaacson, T., & Hirschberg, J. (**2012**). Epistasis in tomato color mutations involves regulation of phytoene synthase 1 expression by cis-carotenoids. *Proceedings of the National Academy of Sciences*, *109*(46), 19021-19026.

Kader, A. A. (**2008**). Flavor quality of fruits and vegetables. *Journal of the Science of Food and Agriculture*, *88*(11), 1863-1868

Kang, M. Y., Yoo, S. C., Kwon, H. Y., Lee, B. D., Cho, J. N., Noh, Y. S., & Paek, N. C. (**2015**). Negative regulatory roles of DE-ETIOLATED1 in flowering time in Arabidopsis. *Scientific reports*, *5*(1), 9728.

Keller, F., Pharr, D. M. (**2017**). Metabolism of carbohydrates in sinks and sources: galactosyl-sucrose oligosaccharides. In *Photoassimilate Distribution Plants and Crops Source-Sink Relationships* (pp. 157-183). Routledge.

Kerr, E. A. (**1958**). Mutations of chlorophyll retention in ripe fruit. *Rep Tomato Genet Coop*, *8*, 22.

Kevany, B. M., Tieman, D. M., Taylor, M. G., Cin, V. D., & Klee, H. J. (**2007**). Ethylene receptor degradation controls the timing of ripening in tomato fruit. *The Plant Journal*, *51*(3), 458-467.

Khapte, P. S., & Jansirani, P. (**2014**). Correlation and path coefficient analysis in tomato (Solanum lycopersicum L.). *Electronic journal of plant breeding*, *5*(2), 300-304.

Kim, M., Nguyen, T. T. P., Ahn, J. H., Kim, G. J., & Sim, S. C. (**2021**). Genome-wide association study identifies QTL for eight fruit traits in cultivated tomato (Solanum lycopersicum L.). *Horticulture Research*, *8*.

Kombat, R. (**2023**, April). Agrobacterium-Mediated Transformation of Tomato CV Arka Vikas with Cry2ax1 Gene for Insect Resistance. < bound method Organization. get_name_with_acronym of< Organization: Forum for Agricultural Research in Africa>>.

Konozy, E. H., Causse, M., & Faurobert, M. (**2012**). Cell wall glycosidase activities and protein content variations during fruit development and ripening in three texture contrasted tomato cultivars. *Saudi journal of biological sciences*, *19*(3), 277-283.

Kopeliovitch, E., Mizrahi, Y., Rabinowitch, H. D., & Kedar, N. (**1980**). Physiology of the tomato mutant alcobaca. *Physiologia Plantarum*, *48*(2), 307-311.

Kopeliovitch, E., Rabinowitch, H. D., Mizrahi, Y., & Kedar, N. (**1981**). Mode of inheritance of Alcobaca, a tomato fruit-ripening mutant. *Euphytica*, *30*, 223-225.

Korte, A., & Farlow, A. (**2013**). The advantages and limitations of trait analysis with GWAS: a review. *Plant methods*, *9*, 1-9.

Kramer, M. G., & Redenbaugh, K. (**1994**). Commercialization of a tomato with an antisense polygalacturonase gene: The FLAVR SAVR™ tomato story. *Euphytica*, *79*, 293-297.

Krauss, S., Schnitzler, W. H., Grassmann, J., & Woitke, M. (**2006**). The influence of different electrical conductivity values in a simplified recirculating soilless system on inner and outer fruit quality characteristics of tomato. Journal of Agricultural and Food Chemistry, 54(2), 441-448.

Küster, H., Schröder, G., Frühling, M., Pich, U., Rieping, M., Schubert, I., ... & Pühler, A. (**1995**). The nodule-specific VfENOD-GRP3 gene encoding a glycine-rich early nodulin is located on chromosome I of Vicia faba L. and is predominantly expressed in the interzone II-III of root nodules. *Plant molecular biology*, *28*, 405-421.

Lamour, K. H., Stam, R., Jupe, J., Huitema, E. (**2012**). The oomycete broad-host-range pathogen Phytophthora capsici. *Molecular plant pathology*, *13*(4), 329-337.

Lanahan, M. B., Yen, H. C., Giovannoni, J. J., & Klee, H. J. (1994). The never ripe mutation blocks ethylene perception in tomato. *The Plant Cell*, *6*(4), 521-530.

Lara, I., Heredia, A., & Domínguez, E. (**2019**). Shelf life potential and the fruit cuticle: the unexpected player. *Frontiers in Plant Science*, *10*, 770.

Leamy, L. J., Zhang, H., Li, C., Chen, C. Y., & Song, B. H. (**2017**). A genome-wide association study of seed composition traits in wild soybean (Glycine soja). *BMC genomics*, *18*, 1-15.

Li, C., Hou, X., Qi, N., Liu, H., Li, Y., Huang, D., ... & Liao, W. (**2021**). Insight into ripening-associated transcription factors in tomato: A review. *Scientia Horticulturae*, *288*, 110363.

Li, M., Wang, L., Liu, Y., Lin, Y., Zhang, Y., Long, Y., ... & Luo, Y. (**2022c**). Characterization and regulation mechanism analysis of ubiquitin-conjugating family genes in strawberry reveals a potential role in fruit ripening. *BMC Plant Biology*, *22*(1), 39.

Li, R., Maioli, A., Yan, Z., Bai, Y., Valentino, D., Milani, A. M., ... & Acquadro, A. (**2022b**). CRISPR/Cas9-based knock-out of the PMR4 gene reduces susceptibility to late blight in two tomato cultivars. *International Journal of Molecular Sciences*, *23*(23), 14542.

Li, R., Sun, S., Wang, H., Wang, K., Yu, H., Zhou, Z., ... & Cui, X. (**2020**). FIS1 encodes a GA2-oxidase that regulates fruit firmness in tomato. *Nature Communications*, *11*(1), 5844.

Li, X., Wang, X., Zhang, Y., Zhang, A., & You, C. X. (**2022a**). Regulation of fleshy fruit ripening: from transcription factors to epigenetic modifications. *Horticulture Research*, *9*, uhac013.

Lian, J., Han, H., Zhao, J., Li, C. (**2018**). In-vitro and in-planta Botrytis cinerea Inoculation Assays for Tomato. *Bio-protocol*, *8*(8), e2810-e2810.

Lindstrom, E. W. (**1925**). Inheritance in tomatoes. Genetics, 10(4), 305.

Ling, Q., Sadali, N. M., Soufi, Z., Zhou, Y., Huang, B., Zeng, Y., ... & Jarvis, R. P. (**2021**). The chloroplast-associated protein degradation pathway controls chromoplast development and fruit ripening in tomato (May, 10.1038/s41477-021-00916-y, 2021). *Nature Plants*, *7*(10), 1433-1433.

Liu, H., Ding, Y., Zhou, Y., Jin, W., Xie, K., & Chen, L. L. (**2017**). CRISPR-P 2.0: an improved CRISPR-Cas9 tool for genome editing in plants. *Molecular plant*, *10*(3), 530-532.

Liu, J., Ma, Q., Liu, D., Meng, C., Hu, Z., & Ma, L. (**2022**). Identification of the cell wall proteins associated with the softening of Lycium barbarum L. fruit by using iTRAQ technology. *Food Chemistry: Molecular Sciences*, *4*, 100110.

Liu, X., Huang, M., Fan, B., Buckler, E. S., & Zhang, Z. (**2016**). Iterative usage of fixed and random effect models for powerful and efficient genome-wide association studies. *PLoS genetics*, *12*(2), e1005767. https://doi.org/10.1371/journal.pgen.1005767.

Liu, Z., Jiang, J., & Li, J. (**2023**). GWAS characterization of the genetic regions associated with nine important agronomic traits in tomato (*Solanum lycopersicum* L.). *Agronomy*, 13(5), 1191.

Lu YanLi, L. Y., Zhang ShiHuang, Z. S., Shah, T., Xie ChuanXiao, X. C., Hao ZhuanFang, H. Z., Li XinHai, L. X., ... & Xu YunBi, X. Y. (**2010**). Joint linkage-linkage disequilibrium mapping is a powerful approach to detecting quantitative trait loci underlying drought tolerance in maize.

Lu, CG., Xu, HL., Yian, RC., Yu, WG. (**1994**). Storage-linked physiological characters of tomato carrying fruit ripeningmutant genes and their implications in breeding. Jiangsu J. Agric. Sci. 10:5-10.

Luo, Y., Ge, C., Yang, M., Long, Y., Li, M., Zhang, Y., ... & Tang, H. (**2020**). Cytosolic/plastid glyceraldehyde-3-phosphate dehydrogenase is a negative regulator of strawberry fruit ripening. *Genes*, *11*(5), 580.

Ma, N., Feng, H., Meng, X., Li, D., Yang, D., Wu, C., & Meng, Q. (**2014**). Overexpression of tomato SlNAC1 transcription factor alters fruit pigmentation and softening. *BMC Plant Biology*, *14*, 1-14.

Ma, X., Zhang, Q., Zhu, Q., Liu, W., Chen, Y., Qiu, R., ... Liu, Y. G. (**2015**). A robust CRISPR/Cas9 system for convenient, high-efficiency multiplex genome editing in monocot and dicot plants. *Molecular plant*, *8*(8), 1274-1284.

Ma, Z., He, S., Wang, X., Sun, J., Zhang, Y., Zhang, G., ... & Du, X. (**2018**). Resequencing a core collection of upland cotton identifies genomic variation and loci influencing fiber quality and yield. *Nature genetics*, *50*(6), 803-813.

Makarova, K. S., Haft, D. H., Barrangou, R., Brouns, S. J., Charpentier, E., Horvath, P., ... & Koonin, E. V. (**2011**). Evolution and classification of the CRISPR–Cas systems. *Nature Reviews Microbiology*, *9*(6), 467-477.

Manning, K., Tör, M., Poole, M., Hong, Y., Thompson, A. J., King, G. J., ... & Seymour, G. B. (**2006**). A naturally occurring epigenetic mutation in a gene encoding an SBP-box transcription factor inhibits tomato fruit ripening. *Nature genetics*, *38*(8), 948-952.

Margossian, L. J., Federman, A. D., Giovannoni, J. J., & Fischer, R. L. (**1988**). Ethylene-regulated expression of a tomato fruit ripening gene encoding a proteinase inhibitor I with a glutamic residue at the reactive site. Proceedings of the National Academy of Sciences, 85(21), 8012-8016.

Marraccini, P., Rogers, W. J., Caillet, V., Deshayes, A., Granato, D., Lechat, S., ... & Pétiard, V. (**2005**). Biochemical and molecular characterization of α-D-galactosidase from coffee beans. *Plant Physiology and Biochemistry*, *43*(10-11), 909-920. https://doi.org/10.1016/j.plaphy.2005.08.010

Mazzucato, A., Cellini, F., Bouzayen, M., Zouine, M., Mila, I., Minoia, S., ... & Carriero, F. (**2015**). A TILLING allele of the tomato Aux/IAA9 gene offers new insights into fruit set mechanisms and perspectives for breeding seedless tomatoes. *Molecular Breeding*, *35*, 1-15.

McCormick, S., Niedermeyer, J., Fry, J., Barnason, A., Horsch, R., Fraley, R. (**1986**). Leaf disc transformation of cultivated tomato (L. esculentum) using Agrobacterium tumefaciens. *Plant cell reports*, *5*, 81-84.

Miricescu, A., Goslin, K., & Graciet, E. (**2018**). Ubiquitylation in plants: signaling hub for the integration of environmental signals. *Journal of Experimental Botany*, *69*(19), 4511-4527.

Mutschler, M. A., Wolfe, D. W., Cobb, E. D., & Yourstone, K. S. (**1992**). Tomato fruit quality and shelf life in hybrids heterozygous for the *alc* ripening mutant. *HortScience*, *27*(4), 352-355.

Nguyen, V. Q. (**1991**). Red Centre 'fresh-market tomato. *HortScience*, *26*(8), 1095-1096.

Nguyen, V. Q. (**1994**). Juliette 'Fresh-market Tomato. *HortScience*, *29*(4), 332-332.

Nie, H., Shi, Y., Geng, X., & Xing, G. (**2022**). CRISRP/Cas9-mediated targeted mutagenesis of tomato polygalacturonase gene (*SlPG*) delays fruit softening. *Frontiers in Plant Science*, *13*, 729128.

Nie, H., Yang, X., Zheng, S., & Hou, L. (**2024**). Gene-Based Developments in Improving Quality of Tomato: Focus on Firmness, Shelf Life, and Pre-and Post-Harvest Stress Adaptations. *Horticulturae*, *10*(6), 641.

Ogle DH, Doll JC, Wheeler AP, Dinno A (**2024**). *FSA: Simple Fisheries Stock Assessment Methods*. R package version 0.9.5, https://CRAN.R-project.org/package=FSA.

Olimpieri, I., Caccia, R., Picarella, M. E., Pucci, A., Santangelo, E., Soressi, G. P., & Mazzucato, A. (**2011**). Constitutive co-suppression of the GA 20-oxidase1 gene in tomato leads to severe defects in vegetative and reproductive development. *Plant Science*, *180*(3), 496-503.

Opabode, J. T. (**2006**). Agrobacterium-mediated transformation of plants: emerging factors that influence efficiency. *Biotechnol Mol Biol Rev*, *1*(1), 12-20.

Ortega-Salazar, I., Crum, D., Sbodio, A. O., Sugiyama, Y., Adaskaveg, A., Wang, D., ... & Blanco-Ulate, B. (**2024**). Double CRISPR knockout of pectin degrading enzymes improves tomato shelf-life while ensuring fruit quality. *Plants, People, Planet*, *6*(2), 330-340.

Osei, M. K., Danquah, A., Blay, E. T., Danquah, E., & Adu-Dapaah, H. (**2017**). An overview of tomato fruit-ripening mutants and their use in increasing shelf life of tomato fruits. *African Journal of Agricultural Research*, *12*(51), 3520-3528.

Pan, F., Zhang, Q., Zhu, H., Li, J., & Wen, Q. (**2023**). Transcriptome and metabolome provide insights into fruit ripening of cherry tomato (Solanum lycopersicum var. cerasiforme). Plants, 12(19), 3505.

Pasam, R. K., Sharma, R., Malosetti, M., van Eeuwijk, F. A., Haseneyer, G., Kilian, B., & Graner, A. (**2012**). Genome-wide association studies for agronomical traits in a world wide spring barley collection. *BMC plant biology*, *12*, 1-22.

Peng, Z. Z., Li, H. L., Liu, G. S., Su, X., Zhao, X., Grierson, D., ... & Fu, D. Q. (**2024**). Tomato NAC transcription factor NOR-like1 positively regulates tomato fruit softening. *Postharvest Biology and Technology*, *213*, 112923.

Peng, Z., Liu, G., Li, H., Wang, Y., Gao, H., Jemrić, T., & Fu, D. (**2022**). Molecular and genetic events determining the softening of fleshy fruits: a comprehensive review. *International Journal of Molecular Sciences*, *23*(20), 12482.

Peralta, I. E., & Spooner, D. M. (**2007**). History, origin and early cultivation of tomato (Solanaceae). *Genetic improvement of solanaceous crops*, *2*, 1-27.

Pérez-Llorca, M., Muñoz, P., Müller, M., & Munné-Bosch, S. (**2019**). Biosynthesis, metabolism and function of auxin, salicylic acid and melatonin in climacteric and non-climacteric fruits. *Frontiers in Plant Science*, *10*, 136.

Pons, C., Casals, J., Brower, M., Sacco, A., Riccini, A., Hendrickx, P., ... & Granell, A. (**2023**). Diversity and genetic architecture of agro-morphological traits in a core collection of European traditional tomato. *Journal of experimental botany*, *74*(18), 5896-5916.

Pons, C., Casals, J., Palombieri, S., Fontanet, L., Riccini, A., Rambla, J. L., ... & Granell, A. (**2022**). Atlas of phenotypic, genotypic and geographical diversity present in the European traditional tomato. *Horticulture research*, *9*, uhac112.

Posadinu, C. M., Rodriguez, M., Conte, P., Piga, A., & Attene, G. (**2023**). Fruit quality and shelf-life of Sardinian tomato (Solanum lycopersicum L.) landraces. *Plos one*, *18*(12), e0290166.

Posadinu, C. M., Rodriguez, M., Madau, F., & Attene, G. (**2022**). The value of agrobiodiversity: An analysis of consumers preference for tomatoes. *Renewable Agriculture and Food Systems*, *37*(3), 237-247.

Pritchard, J. K., Stephens, M., & Donnelly, P. (**2000**). Inference of population structure using multilocus genotype data. *Genetics*, *155*(2), 945-959.

Ranc, N., Muños, S., Xu, J., Le Paslier, M. C., Chauveau, A., Bounon, R., Rolland, S., Bouchet, J. P., Brunel, D., & Causse, M. (**2012**). Genome-wide association mapping in tomato (Solanum lycopersicum) is possible using genome admixture of Solanum lycopersicum var. cerasiforme. *G3 (Bethesda, Md.)*, *2*(8), 853–864. https://doi.org/10.1534/g3.112.002667

Ray, J., Moureau, P., Bird, C., Bird, A., Grierson, D., Maunders, M., ... & Schuch, W. (**1992**). Cloning and characterization of a gene involved in phytoene synthesis from tomato.

Rhouma, A., Hajji-Hedfi, L., Kouadri, M., Atallaoui, K., Matrood, A., Khrieba, M. (**2023**). *Botrytis cinerea*: The Cause of Tomatoes Gray Mold. *Egyptian Journal of Phytopathology*, *51*(2), 68-75. doi: 10.21608/ejp.2023.224842.1101

Rick, C. M., & Butler, L. (**1956**). Cytogenetics of the tomato. *Advances in genetics*, *8*, 267-382.

Rick, C.M. (**1991**). Tomato. Longman Scientific and Technical, Essex, England.

Robinson, R. (**1968**). Ripening inhibitor: a gene with multiple effects on ripening. *Rep Tomato Genet Coop*, *18*, 36-37.

Ronen, G., Carmel-Goren, L., Zamir, D., & Hirschberg, J. (**2000**). An alternative pathway to β-carotene formation in plant chromoplasts discovered by map-based cloning of Beta and old-gold color mutations in tomato. *Proceedings of the National Academy of Sciences*, *97*(20), 11102-11107.

Ruggieri, V., Francese, G., Sacco, A., D'Alessandro, A., Rigano, M. M., Parisi, M., ... & Barone, A. (**2014**). An association mapping approach to identify favourable alleles for tomato fruit quality breeding. *BMC plant biology*, *14*, 1-15.

Ruggieri, V., Francese, G., Sacco, A., D'Alessandro, A., Rigano, M. M., Parisi, M., ... & Barone, A. (**2014**). An association mapping approach to identify favourable alleles for tomato fruit quality breeding. BMC plant biology, 14, 1-15

Sacco, A., Ruggieri, V., Parisi, M., Festa, G., Rigano, M. M., Picarella, M. E., ... & Barone, A. (**2015**). Exploring a tomato landraces collection for fruit-related traits by the aid of a high-throughput genomic platform. PLoS One, 10(9), e0137139.

Saito, T., Ariizumi, T., Okabe, Y., Asamizu, E., Hiwasa-Tanase, K., Fukuda, N., ... & Ezura, H. (**2011**). TOMATOMA: a novel tomato mutant database distributing Micro-Tom mutant collections. *Plant and cell physiology*, *52*(2), 283-296.

Sarrion-Perdigones, A., Falconi, E. E., Zandalinas, S. I., Juárez, P., Fernández-del-Carmen, A., Granell, A., & Orzaez, D. (**2011**). GoldenBraid: an iterative cloning system for standardized assembly of reusable genetic modules. *PloS one*, *6*(7), e21622.

Sarrion-Perdigones, A., Falconi, E. E., Zandalinas, S. I., Juárez, P., Fernández-del-Carmen, A., Granell, A., & Orzaez, D. (**2011**). GoldenBraid: an iterative cloning system for standardized assembly of reusable genetic modules. *PloS one*, *6*(7), e21622.

Sauvage, C., Segura, V., Bauchet, G., Stevens, R., Do, P. T., Nikoloski, Z., ... & Causse, M. (**2014**). Genome-wide association in tomato reveals 44 candidate loci for fruit metabolic traits. *Plant physiology*, *165*(3), 1120-1132.

Schouten, H.J.; Tikunov, Yuri; Visser, R.G.F. Tomato diversified by modern plant Breeding. *Source Prophyta Annual 2020* (**2020**). - ISSN 1388-381X . p. 14 - 19

Schubert, R., Grunewald, S., von Sivers, L., & Hause, B. (**2019**). Effects of jasmonate on ethylene function during the development of tomato stamens. *Plants*, *8*(8), 277.

Segerson, N. A. (**2018**). Biochemical and functional characterization of CUTIN SYNTHASE 2 from tomato (*Solanum lycopersicum*).

Seroczyńska, A., Niemirowicz-Szczytt, K., & Korzeniewska, A. (**1998**). Utilization of three non-ripening mutants in tomato breeding for prolonged shelf life.

Shah, H. M. S., Singh, Z., Hasan, M. U., Woodward, A., & Afrifa-Yamoah, E. (**2025**). Preharvest methyl jasmonate application delays cell wall degradation and upregulates phenolic metabolism and antioxidant activities in cold stored raspberries. Food Chemistry, 462, 141020.

Shakir, M. S., Ejaz, S., Hussain, S., Ali, S., Sardar, H., Azam, M., ... & Canan, İ. (**2022**). Synergistic effect of gum Arabic and carboxymethyl cellulose as biocomposite coating delays senescence in stored tomatoes by regulating antioxidants and cell wall degradation. *International Journal of Biological Macromolecules*, *201*, 641-652.

Shi, Y., Vrebalov, J., Zheng, H., Xu, Y., Yin, X., Liu, W., ... & Giovannoni, J. J. (**2021**). A tomato LATERAL ORGAN BOUNDARIES transcription factor, *SlLOB1*, predominantly regulates cell wall and softening components of ripening. *Proceedings of the National Academy of Sciences*, *118*(33), e2102486118.

Signorell, A. (**2024**). DescTools: Tools for Descriptive Statistics. R package version 0.99.57, 694 https://github.com/AndriSignorell/DescTools/, https://andrisignorell.github.io/DescTools/.

Sim, S. C., Van Deynze, A., Stoffel, K., Douches, D. S., Zarka, D., Ganal, M. W., ... & Francis, D. M. (**2012**). High-density SNP genotyping of tomato (Solanum lycopersicum L.) reveals patterns of genetic variation due to breeding.

Smith, D. L., Abbott, J. A., & Gross, K. C. (**2002**). Down-regulation of tomato β-galactosidase 4 results in decreased fruit softening. *Plant physiology*, *129*(4), 1755-1762.

Soh, C. P., Ali, Z. M., Lazan, H. (**2006**). Characterisation of an α-galactosidase with potential relevance to ripening related texture changes. *Phytochemistry*, *67*(3), 242-254.

Solieman, T. H. I., El-Gabry, M. A. H., & Abido, A. I. (**2013**). Heterosis, potence ratio and correlation of some important characters in tomato (Solanum lycopersicum L.). *Scientia Horticulturae*, *150*, 25-30.

Starr, M. P., & Moran, F. (**1962**). Eliminative split of pectic substances by phytopathogenic soft-rot bacteria. *Science*, *135*(3507), 920-921.

Su, C., Cui, J., Liu, Y., & Luan, Y. (**2022**). Genome-wide identification and characterization of the tomato F-box associated (FBA) protein family and expression analysis of their responsiveness to Phytophthora infestans. Gene, 821, 146335.

Sun, H. J., Uchii, S., Watanabe, S., Ezura, H. (**2006**). A highly efficient transformation protocol for Micro-Tom, a model cultivar for tomato functional genomics. *Plant and Cell Physiology*, *47*(3), 426-431.

Sützl, L., Foley, G., Gillam, E. M., Bodén, M., & Haltrich, D. (**2019**). The GMC superfamily of oxidoreductases revisited: analysis and evolution of fungal GMC oxidoreductases. *Biotechnology for Biofuels*, *12*, 1-18.

Thompson, A. J., Tor, M., Barry, C. S., Vrebalov, J., Orfila, C., Jarvis, M. C., ... & Seymour, G. B. (**1999**). Molecular and genetic characterization of a novel pleiotropic tomato-ripening mutant. *Plant physiology*, *120*(2), 383-390.

Tieman, D., Zhu, G., Resende Jr, M. F., Lin, T., Nguyen, C., Bies, D., ... & Klee, H. (**2017**). A chemical genetic roadmap to improved tomato flavor. Science, 355(6323), 391-394.

Tigchelaar, E. C., M. L. Tomes, E. A.Kerr, and R. J. Barman. (**1973**). A new fruit ripening mutant, *non-ripening* (*nor*). Tomato Genetics Coop. 223:33-34.

Tripodi, P., Soler, S., Campanelli, G., Díez, M. J., Esposito, S., Sestili, S., ... & Cardi, T. (**2021**). Genome wide association mapping for agronomic, fruit quality, and root architectural traits in tomato under organic farming conditions. *BMC Plant Biology*, *21*, 1-22.

Turcich, M. P., Hamilton, D. A., & Mascarenhas, J. P. (**1993**). Isolation and characterization of pollen-specific maize genes with sequence homology to ragweed allergens and pectate lyases. *Plant molecular biology*, *23*, 1061-1065.

Uffelmann, E., Huang, Q. Q., Munung, N. S., De Vries, J., Okada, Y., Martin, A. R., ... & Posthuma, D. (**2021**). Genome-wide association studies. *Nature Reviews Methods Primers*, *1*(1), 59.

Uluisik, S., & Seymour, G. B. (**2020**). Pectate lyases: Their role in plants and importance in fruit ripening. *Food Chemistry*, *309*, 125559.

Uluisik, S., Chapman, N. H., Smith, R., Poole, M., Adams, G., Gillis, R. B., ... & Seymour, G. B. (**2016**). Genetic improvement of tomato by targeted control of fruit softening. *Nature biotechnology*, *34*(9), 950-952.

United Nations: https://www.un.org/en/global-issues

Van Eck, J., Keen, P., & Tjahjadi, M. (**2019**). Agrobacterium tumefaciens-mediated transformation of tomato. *Transgenic plants: methods and protocols*, 225-234.

Vohland, K., Land-Zandstra, A., Ceccaroni, L., Lemmens, R., Perelló, J., Ponti, M., ... & Wagenknecht, K. (**2021**). *The science of citizen science* (p. 529). Springer Nature.

Vouillot, L., Thélie, A., Pollet, N. (**2015**). Comparison of T7E1 and surveyor mismatch cleavage assays to detect mutations triggered by engineered nucleases. *G3: Genes, Genomes, Genetics*, *5*(3), 407-415.

Vrebalov, J., Pan, I. L., Arroyo, A. J. M., McQuinn, R., Chung, M., Poole, M., ... & Irish, V. F. (**2009**). Fleshy fruit expansion and ripening are regulated by the tomato SHATTERPROOF gene TAGL1. *The Plant Cell*, *21*(10), 3041-3062.

Vrebalov, J., Ruezinsky, D., Padmanabhan, V., White, R., Medrano, D., Drake, R., ... & Giovannoni, J. (**2002**). A MADS-box gene necessary for fruit ripening at the tomato ripening-inhibitor (rin) locus. *Science*, *296*(5566), 343-346.

Wang, D., & Seymour, G. B. (**2022**). Molecular and biochemical basis of softening in tomato. *Molecular Horticulture*, *2*(1), 5.

Wang, D., Lu, Q., Wang, X., Ling, H., & Huang, N. (**2023**). Elucidating the role of SlXTH5 in tomato fruit softening. *Horticultural Plant Journal*, *9*(4), 777-788.

Wang, D., Samsulrizal, N. H., Yan, C., Allcock, N. S., Craigon, J., Blanco-Ulate, B., ... & Seymour, G. B. (**2019**). Characterization of CRISPR mutants targeting genes modulating pectin degradation in ripening tomato. *Plant Physiology*, *179*(2), 544-557.

Wang, D., Yeats, T. H., Uluisik, S., Rose, J. K., & Seymour, G. B. (**2018**). Fruit softening: revisiting the role of pectin. *Trends in plant science*, *23*(4), 302-310.

Wang, J., & Zhang, Z. (2021). GAPIT version 3: boosting power and accuracy for genomic association and prediction. *Genomics, Proteomics and Bioinformatics*, *19*(4), 629-640.

Wang, Q., Tian, F., Pan, Y., Buckler, E. S., & Zhang, Z. (2014). A SUPER powerful method for genome wide association study. *PloS one*, *9*(9), e107684. https://doi.org/10.1371/journal.pone.0107684.

Wang, R., Angenent, G. C., Seymour, G., & de Maagd, R. A. (**2020b**). Revisiting the role of master regulators in tomato ripening. *Trends in plant science*, *25*(3), 291-301.

Wang, R., Lammers, M., Tikunov, Y., Bovy, A. G., Angenent, G. C., & de Maagd, R. A. (**2020a**). The *rin*, *nor* and *Cnr* spontaneous mutations inhibit tomato fruit ripening in additive and epistatic manners. *Plant science*, *294*, 110436.

Wang, W. Y., Barratt, B. J., Clayton, D. G., & Todd, J. A. (**2005**). Genome-wide association studies: theoretical and practical concerns. *Nature Reviews Genetics*, *6*(2), 109-118.

Wang, Y., He, Y., Zhang, M., Li, J., Xu, X., Shi, X., & Meng, L. (**2022**). Slltpg3, a non-specific lipid transfer protein, acts on the cuticle synthetic pathway to delay water loss and softening of tomato fruit. *Postharvest Biology and Technology*, *188*, 111899.

Wang, Y., Wang, W., Cai, J., Zhang, Y., Qin, G., & Tian, S. (**2014**). Tomato nuclear proteome reveals the involvement of specific E2 ubiquitin-conjugating enzymes in fruit ripening. Genome biology, 15, 1-19.

Wei, T. and Simko, V. (**2024**). *R package 'corrplot': Visualization of a Correlation Matrix*. (Version 0.95), https://github.com/taiyun/corrplot.

Wilkinson, J. Q., Lanahan, M. B., Yen, H. C., Giovannoni, J. J., & Klee, H. J. (**1995**). An ethylene-inducible component of signal transduction encoded by Never-ripe. *Science*, *270*(5243), 1807-1809.

Wing, R. A., Yamaguchi, J., Larabell, S. K., Ursin, V. M., & McCormick, S. (**1990**). Molecular and genetic characterization of two pollen-expressed genes that have sequence similarity to pectate lyases of the plant pathogen Erwinia. *Plant molecular biology*, *14*, 17-28.

Witcombe, J. R., Joshi, A., Joshi, K. D., & Sthapit, B. R. (**1996**). Farmer participatory crop improvement. I. Varietal selection and breeding methods and their impact on biodiversity. *Experimental agriculture*, *32*(4), 445-460.

Wu, B., Shen, F., Chen, C. J., Liu, L., Wang, X., Zheng, W. Y., ... & Zhang, X. Z. (**2021**). Natural variations in a pectin acetylesterase gene, MdPAE10, contribute to prolonged apple fruit shelf life. The Plant Genome, 14(1), e20084.

Xia, X., Cheng, X., Li, R., Yao, J., Li, Z., & Cheng, Y. (**2021**). Advances in application of genome editing in tomato and recent development of genome editing technology. *Theoretical and Applied Genetics*, *134*(9), 2727-2747.

Xie, Q., Hu, Z., Zhu, Z., Dong, T., Zhao, Z., Cui, B., & Chen, G. (**2014**). Overexpression of a novel MADS-box gene SlFYFL delays senescence, fruit ripening and abscission in tomato. *Scientific reports*, *4*(1), 4367.

Xu, C., Luo, F., & Hochholdinger, F. (**2016**). LOB domain proteins: beyond lateral organ boundaries. *Trends in plant science*, *21*(2), 159-167.

Yan, W., Cao, M., Shi, L., Wu, W., Xu, F., Chen, W., & Yang, Z. (**2024**). γ-Aminobutyric acid delays fruit softening in postharvest kiwifruit by inhibiting starch and cell wall degradation. Postharvest Biology and Technology, 213, 112916.

Yang, L., Huang, W., Xiong, F., Xian, Z., Su, D., Ren, M., & Li, Z. (**2017**). Silencing of SlPL, which encodes a pectate lyase in tomato, confers enhanced fruit firmness, prolonged shelf-life and reduced susceptibility to grey mould. *Plant Biotechnology Journal*, *15*(12), 1544-1555.

Yang, L., Huang, W., Xiong, F., Xian, Z., Su, D., Ren, M., & Li, Z. (**2017**). Silencing of SlPL, which encodes a pectate lyase in tomato, confers enhanced fruit firmness, prolonged shelf-life and reduced susceptibility to grey mould. *Plant Biotechnology Journal*, *15*(12), 1544-1555.

Yang, Y., Xu, R., Ma, C. J., Vlot, A. C., Klessig, D. F., & Pichersky, E. (**2008**). Inactive methyl indole-3-acetic acid ester can be hydrolyzed and activated by several esterases belonging to the At MES esterase family of Arabidopsis. *Plant physiology*, *147*(3), 1034-1045.

Yasmeen, A. (**2009**) 'An improved protocol for the regeneration and transformation of tomato (cv Rio Grande)', Acta Physiologiae Plantarum, 31(6), pp. 1271–1277. doi: 10.1007/s11738-009- 0364-6.

Yeats, T. H., Howe, K. J., Matas, A. J., Buda, G. J., Thannhauser, T. W., & Rose, J. K. (**2010**). Mining the surface proteome of tomato (Solanum lycopersicum) fruit for proteins associated with cuticle biogenesis. *Journal of Experimental Botany*, *61*(13), 3759-3771.

Yoder, M. D., Keen, N. T., & Jurnak, F. (**1993**). New domain motif: the structure of pectate lyase C, a secreted plant virulence factor. *Science*, *260*(5113), 1503-1507.

Yu, Q. H., Wang, B., Li, N., Tang, Y., Yang, S., Yang, T., ... & Asmutola, P. (**2017**). CRISPR/Cas9-induced targeted mutagenesis and gene replacement to generate long-shelf-life tomato lines. *Scientific reports*, *7*(1), 11874.

Zhang, J., Hu, Z., Yao, Q., Guo, X., Nguyen, V., Li, F., & Chen, G. (**2018a**). A tomato MADS-box protein, SlCMB1, regulates ethylene biosynthesis and carotenoid accumulation during fruit ripening. *Scientific reports*, *8*(1), 3413.

Zhang, L., Su, W., Tao, R., Zhang, W., Chen, J., Wu, P., ... & Kuang, H. (**2017**). RNA sequencing provides insights into the evolution of lettuce and the regulation of flavonoid biosynthesis. *Nature communications*, *8*(1), 2264.

Zhang, L., Zhu, M., Ren, L., Li, A., Chen, G., & Hu, Z. (**2018b**). The SlFSR gene controls fruit shelf-life in tomato. *Journal of Experimental Botany*, *69*(12), 2897-2909.

Zhang, S., Zhang, R., Gao, J., Song, G., Li, J., Li, W., ... Li, G. (**2021**). CRISPR/Cas9-mediated genome editing for wheat grain quality improvement. *Plant Biotechnology Journal*, *19*(9), 1684.

Zhang, Z., Mao, L., Chen, H., Bu, F., Li, G., Sun, J., ... & Huang, S. (**2015**). Genome-wide mapping of structural variations reveals a copy number variant that determines reproductive morphology in cucumber. *The Plant Cell*, *27*(6), 1595-1604.

Zhao, X., Li, F., Li, X., Ali, M., Ding, J., Song, Y., ... & Zhang, X. (**2024**). Integrated transcriptomic and metabolomic analyses revealed the role of SlMYC2 in tomato (Solanum lycopersicum L.) fruit development and ripening. *Scientia Horticulturae*, *325*, 112691.

Zhou, Y., Li, Z., Su, X., Hou, H., Jiang, Y., Duan, X., ... & Jiang, G. (**2024**). Histone deacetylase SlHDA7 impacts fruit ripening and shelf life in tomato. *Horticulture Research*, *11*(11), uhae234.

Zhu, M., Chen, G., Zhou, S., Tu, Y., Wang, Y., Dong, T., & Hu, Z. (**2014**). A new tomato NAC (N AM/A TAF1/2/C UC2) transcription factor, SlNAC4, functions as a positive regulator of fruit ripening and carotenoid accumulation. *Plant and Cell Physiology*, *55*(1), 119-135.

Zia, B., Zhang, H., Datsenka, T. U., Liu, W., Lang, Z., Zhu, J. K., & Handa, A. K. (**2018**). Use of Genome Editing to Characterize Gene Function of SlIAA9 in Plant Growth, Development and Fruit Quality in Tomato. Proc. Pak Soc. Hort. Sci, 84-93.

Zscheile, F. J., & Lesley, J. W. (**1967**). Pigment analysis of sherry: flesh color mutation resembling yellow in the tomato.

9. Ringraziamenti – Acknowledgements

Giunta alla fine di questo percorso il mio più sentito ringraziamento va al Prof. Andrea Mazzucato, senza il quale non avrei avuto questa opportunità e che mi ha guidata durante questi anni.

Ai miei compagni di laboratorio Maurizio, Fabrizio, Barbara, Lorenzo e Gabriella, del cui supporto e consiglio sono estremamente grata.

Alle persone conosciute grazie al progetto HARNESSTOM, per aver collaborato e lavorato insieme divertendoci.

Al Prof. Rinaldo Botondi e al Dott. Roberto Forniti (UniTus DIBAF) e al Dott. Muhammad Ilyas e alla Prof. Giulia De Lorenzo (Sapienza Università di Roma) per il loro contributo al raggiungimento di questi risultati.

A James Giovannoni, Julia Vrebalov e tutte le persone conosciute al BTI e alla Cornell University, per avermi accolta ed essersi presi cura di me, permettendomi di crescere sia come ricercatrice che come persona.

Infine alla mia famiglia e ai miei amici, per il loro costante sostegno ed incoraggiamento e la loro preziosa fiducia in me.

~

~

Having reached the end of this journey, my heartfelt thanks go to Prof. Andrea Mazzucato, without whom I would not have had this opportunity and who has guided me throughout these years.

To my lab mates Maurizio, Fabrizio, Barbara, Lorenzo and Gabriella, for whose support and advice I am extremely grateful.

To the people I met thanks to the HARNESSTOM project, for collaborating and working while having fun.

To Prof. Rinaldo Botondi and Dr. Roberto Forniti (UniTus DIBAF) and to Muhammad Ilyas and Prof. Giulia De Lorenzo (Sapienza University of Rome) for their contribution to the achievement of these results.

To James Giovannoni, Julia Vrebalov and all the people I met at BTI and Cornell University, for welcoming me and taking care of me, allowing me to grow as both a researcher and a person.

And finally, to my family and friends, for their constant support and encouragement and for trusting me.